Effects of evapotranspiration on leaf water and wax lipid D/H ratios in grasses collected along a relative humidity gradient in Argentina

seit 1558

BY

Jana Tischer

A thesis submitted in partial fulfillment of the requirements

for the degree of

Master of Science in

Biogeosciences

at

Friedrich-Schiller-University Jena

Jena, 3rd February 2014

Referees:

Prof. Gerd Gleixner

Prof. Kai Totsche

Table of Contents

List of abbreviations

ANPP	Aboveground net primary production
CI	Confidence interval
EA	Elemental analyzer
ET	Evapotranspiration
D	Deuterium
$\varepsilon_{root/p}$	soil water evaporative D-enrichment
$\varepsilon_{leaf/root}$	leaf water evaporative D-enrichment
ε_{app}	apparent fractionation
ε_{bio}	biosynthetic fractionation
IRMS	Isotope ratio mass spectrometry
GC	Gas chromatography
FID	Flame ionization detector
MAP	Mean annual precipitation
MAT	Mean annual temperature
RH	Relative humidity
SD	Standard deviation
SE	Standard error
SW	Short wave down-all sky
VSMOW	Vienna Standard Mean Ocean Water

List of figures

Appendix:

List of tables

Appendix:

1 Abstract

Isotopes are powerful tools for paleoclimatic reconstructions due to the fact that they record meteoric data. Increasingly established are hydrogen isotopic compositions (δD value) of leaf wax *n*-alkanes which are synthesized by terrestrial plants and persist in sediments for very long time periods. However, the interpreting of sedimentary records is challenging because the *n*-alkane δD values depend not only on source water isotopes but also on other factors such as life form or evapotranspiration (ET) processes. The relative importance of these parameters to the resulting sedimentary δD values remains unclear. In this study the effects of a temperature and relative humidity (RH) gradient, respectively, in a semi-arid area in Argentina on grass leaf wax *n*-alkane δD values are investigated. The hypothesis is that with increasing mean annual temperature (MAT) and decreasing RH, respectively, the soil and leaf water becomes more D-enriched due to enhanced ET and that this signal can be found in the leaf wax *n*-alkane δD values. The study revealed that the *n*-alkane D/H ratios reflect the D/H ratios of meteoric water but are also strongly affected by soil and leaf water D-enrichment. The impact of D-enrichment by ET increased with rising MAT whereat the influence of leaf water D-enrichment became stronger with increasing MAT than the soil water D-enrichment. The isotopic fractionation between leaf and root water was controlled by annual parameters as well as by daily conditions, especially by light intensity. The transpiration rates of the studied grasses confirmed that light intensity and temperature are important drivers of transpiration. For soil water D-enrichment light intensity and RH are important variables. Overall, MAT was identified as key driver of the apparent fractionation between *n*-alkane D/H ratios and meteoric water D/H ratios. A rise in temperature of one degree Celsius caused an increase in apparent fractionation of 6 ‰. This finding can improve the interpretation of sedimentary leaf wax *n*-alkane D/H ratios from semi-arid regions in order to reconstruct paleoclimate.

2 Introduction

2.1 Isotope definition and notation

Isotopes are elements that contain different numbers of neutrons in their atomic nuclei. Many elements form isotopes, about 300 stable and over 1200 unstable isotopes exist whereat isotopes with even numbers of protons or/and neutrons are in general more stable (Hoefs, 2009). The isotopes of one element differ in their weight. Molecules containing different isotopes differ slightly in their chemical and physical properties and concentrations. The absolute ratios of the elements of interest are defined as R (=abundance of rare isotope/abundance of abundant isotope). A superscript before the ratio symbol R refers to the isotope under consideration. Isotopic fractionations are the isotopic ratios of two compounds in a chemical equilibrium or before or after a physical or chemical transition process. The isotope fractionation factor α is defined as the ratio of the two isotope ratios:

$$\alpha_{B\text{-}A} = R_B/R_A \quad (1)$$

which expresses the isotope ratio R in the compound B divided by the corresponding ratio in compound A. Since isotope effects are in general small, $\alpha \approx 1$, the ε-value or separation factor is defined as:

$$\varepsilon_{B/A} = \alpha_{B/A} - 1 = R_B/R_A - 1 \ (\text{x } 10^3 \text{ ‰}) \quad (2)$$

ε shows either enrichment ($\varepsilon > 0$) or depletion ($\varepsilon < 0$) of the rare isotope in B with respect to A. ε is usually given in ‰ because it is mostly a small number. The isotopic compositions are commonly given in δ values that are calculated with an international standard:

$$\boldsymbol{\delta value} = \frac{R_{sample} - R_{standard}}{R_{standard}} \ (\text{x } 10^3 \text{ ‰}) \quad (3)$$

R_{sample} and $R_{standard}$ are the isotope ratios of the sample and the standard (e.g. $^2H/^1H$ and $^{18}O/^{16}O$). The international standard for the water isotopes is the Vienna Standard Mean Ocean Water (VSMOW) (Mook, 2006; Hoefs, 2009).

2.2 Environmental effects on water isotopes

Hydrogen has two stable isotopes: ^1H has an abundance of 99.9885 % and ^2H (D = deuterium) of 0.0115 %. Oxygen has three stable isotopes with the abundances ^{16}O: 99.757 %, ^{17}O: 0.038 % and ^{18}O: 0.205 % (Hoefs, 2009). The δD and $\delta^{18}O$ values of meteoric water correlate linearly whereat the global meteoric water line shows a D-excess ($\delta D = 8\ \delta^{18}O + 10$). The fractionation factor α of both isotopes decreases with increasing temperature. Liquid water is in general more enriched in heavy isotopes than the water vapor. Water vapor gets depleted in heavy isotopes during condensation and water gets enriched during evaporation. This effect is exponential and is called Rayleigh distillation or Rayleigh rainout effect. Diverse geographical settings cause depletion in the heavy water isotopes which is

related to the temperature and moisture losses of air masses. A drop in temperature causes cloud formation and rainout. Increasing latitude (latitude effect), altitude (altitude effect), distance to the coast (continental effect) and amounts of precipitation (amount effect) enhance the depletion in ^{18}O and ^{2}H of meteoric water. The estimated mean world-wide precipitation shows negative isotope composition of δD = -22 ‰ and $\delta^{18}O$ = -4 ‰. Due to these processes the isotope compositions of global and regional precipitation is predictable. The local precipitation isotope values give information about the origin of the water and the processes of the air masses (Clark and Fritz, 1997; Mook, 2006).

2.3 Isotopes in paleoclimate

Climate, biological and other environmental changes in the last century as well as the human influence therein are current issues of high significance. The ongoing anthropogenic processes, e.g. the production and the use of arable land or pollution caused by urbanization and industrialization have much negative impact on ecosystems and the environment. It is generally accepted that the climate is changing although the anthropogenic impact is discussed controversially. The climate change has predictable and unpredictable consequences. In this field of research, isotopes are a useful tool, because they are tracers, records and integrators of change in the terrestrial, aquatic, marine and atmospheric systems. Stable isotope data help to improve knowledge in various disciplines at different temporal and spatial scales, e.g. in paleohydrology, ecosystem sciences and forensic research. Data can be derived from diverse media and compounds, e.g. from plants, animals, sediments, soils, water as gas, liquid or solid phase, carbonates or gases. The isotope data are used to investigate environmental changes in the past and monitor ongoing changes. It can help to reveal how ecosystems responded to past climate changes. In addition, predictions and modeling of future transformations in ecosystems and climate including anthropogenic impacts might be improved (Dawson & Siegwolf, 2007; Kahmen et al., 2012b).

Hydrogen isotopes are suitable for paleoclimate research since the climate of the earth is strongly related to the hydrological cycle which is reflected by the water isotopes. Different climatic conditions cause different rates of evapotranspiration (ET). ET is the combined process of the transfer from liquid water to water vapor from open surfaces (evaporation) and through plants (transpiration) (Rosenberg et al., 1983). Fluctuating ET effects on plants or lake water are recorded in the hydrogen isotopes of biomass and sediments. Lacustrine sediments are increasingly used to gain paleoclimatic information since the influence of climate on the deposits is strong and the record is continuous with a high temporal and spatial resolution. Organic molecules that are specific to an organism or a plant type are called molecular fossils or biomarkers. Most of the biomarkers belong to the group of lipids. These molecules are stable over geological timescales and are rich in carbon-bound hydrogen that is non-exchangeable up to 150 °C (Gleixner & Mügler, 2007; Schimmelmann et al., 1999). The isotopic composition of biomarkers can be used to reconstruct environmental parameters and the water origin as they record the isotopic composition of the organism water source meaning the available meteoric

water (Hou et al., 2008), for instance water availability can be reconstructed via $\delta^{13}C$ values (Stewart et al., 1995).

In lake sediments, strong focus lies on the recalcitrant *n*-alkanes which are increasingly used as proxies across spatial and temporal scales where other plant materials like cellulose cannot be applied (Gleixner & Mügler, 2007). *N*-alkanes are produced by algae, bacteria, aquatic macrophytes and terrestrial vascular plants. They can be found in sediments, water particles, soils and atmospheric dust. Different groups of organisms produce *n*-alkanes with typical chain lengths (Hunt, 1996; Kahmen et al., 2012a). Algae and bacteria synthesize hydrocarbons with short chain lengths, for example with 17 to 19 carbon atoms (Hunt, 1996). Submerged and floating plants maximize at C_{23} or C_{25} *n*-alkanes (Ficken, 2000). Terrestrial and emerged plants have hydrocarbon chains with 21 up to 37 carbon atoms and maxima at 29 to 33 carbon atoms (Hunt, 1996). In terrestrial plants the *n*-alkanes are especially found in the waxy cuticles (Eglinton & Hamilton, 1967). The *n*-alkane δD isotopic composition is affected by many factors, especially by climate and the precipitation water isotopes, respectively. Additional factors are plant type and physiology, such as leaf architecture, photosynthetic pathway and growth form (Kahmen et al., 2012b; Smith & Freeman, 2006). The *n*-alkane δD values are determined by the δD values of the water used for their biosynthesis ("biosynthetic water pool") and the net biosynthetic fractionation (ε_{bio}) which is the fractionation between the isotope composition of *n*-alkanes and leaf water. The isotopic composition of the biosynthetic water pool varies because it depends on meteoric water and several positive fractionation processes (Kahmen et al., 2012a). The key drivers of leaf wax *n*-alkane D/H ratios are presented in Figure 1. During water uptake by roots no fractionation occurs (Hoefs, 2009) but surface soil water gets enriched in deuterium by evaporation ($\varepsilon_{soil/p}$), especially in arid regions, leading to an isotopic gradient with soil depth (Kahmen et al., 2012b). Different groups of plants use soil water from different depths and thus source water with different isotopic compositions, e.g. grasses use relatively more superficial water than shrubs and have relatively more D-enriched source water (Schulze et al., 1996). Leaf water evaporative D-enrichment ($\varepsilon_{leaf/root}$) and equilibrium exchange of hydrogen isotopes between the leaf and the surrounding water vapor (Kahmen et al., 2012b) have a strong effect on the biosynthetic water pool and cause D-enrichment of different extends. It has been simulated that leaf water D-enrichment changes substantially along climatic gradients. It is least pronounced in humid regions (0 - 20 ‰), intermediate in temperature regions (10 – 30 ‰) and highest in arid biomes (40 – 100 ‰) (Kahmen et al., 2012b). Decreasing relative humidity causes D-enrichment of leaf water due to the enhanced ET of soil and leaf water. Daily fluctuations in weather, atmospheric δD values and leaf physiology cause variations in the extent of leaf water D-enrichment (Kahmen et al., 2012b; Sachse et al., 2006). During biological reactions in which organic compounds are synthesized a large D-depletion occurs. It is considered to be constant for a given species even under different climatic conditions and independent on temperature (Hoefs, 2009; Kahmen et al., 2012a, Sachse et al., 2912). The net or apparent fractionation (ε_{app}) is defined as the fractionation that happens between the *n*-alkanes and the meteoric

water which includes the effects of soil evaporation, leaf water transpiration and biochemical hydrogen isotope fractionations during *n*-alkane biosynthesis (Sachse et al., 2006).

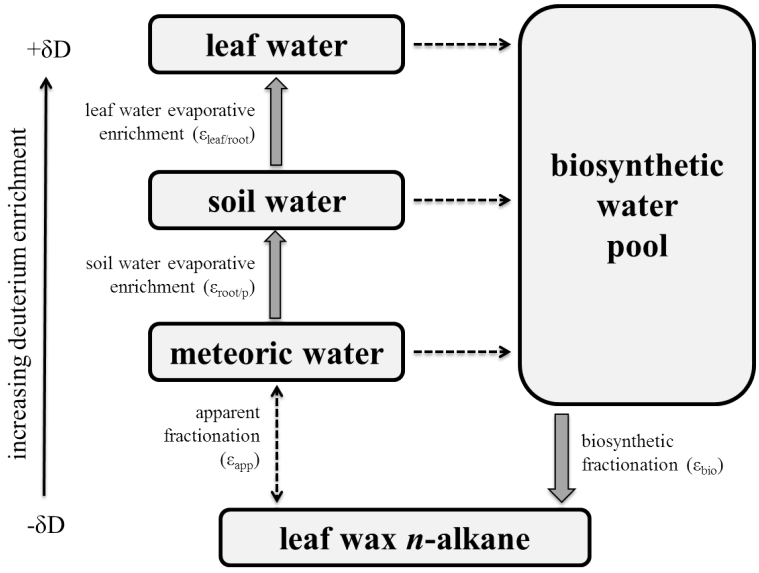

Figure 1. Conceptional model outlining the key drivers of leaf wax *n*-alkane δD values and apparent fractionation (ε_{app}), which are determined by the δD values of the biosynthetic water pool and the biosynthetic fractionation (ε_{bio}). The biosynthetic water pool δD values are controlled by the plant's source water (meteoric water), soil evaporative D-enrichment ($\varepsilon_{root/p}$) and leaf water D-evaporative enrichment ($\varepsilon_{leaf/root}$) (not to scale, modified from Sachse et al., 2006 and Kahmen et al., 2012a)

There is big potential in the interpretation of the δD values. However, the effects on the δD signature of *n*-alkanes are discussed controversially and results from studies are contradictory (e.g. Kahmen et al., 2012a; Kahmen et al., 2012b; McInerney et al., 2012; Sachse et al., 2006; Smith and Freeman, 2006). Different influencing factors and processes and the relative contributions of biosynthetic processes and ET are poorly understood. It is not known how strongly evaporation and D-enriched leaf water affect δD values of leaf wax *n*-alkanes. Hence, it is not clear whether conclusions from the leaf wax lipids δD values can be drawn to plant physiological processes and more particularly past precipitation δD values. To solve these questions, studies have to be done with analyses of leaf waxes of different plant types growing under different climatic condition (Gleixner & Mügler, 2007; Kahmen et al., 2012a). McInerney et al. (2010) state based on field and growth chamber experiments that transpiration in grass leaves does not affect the leaf water δD values and therefore neither the leaf wax δD values. They conclude that only soil evaporation contributes to the isotope enrichment effects. However, Kahmen et al. (2012a) showed in a greenhouse experiment that leaf water evaporative D-enrichment is strongly dependent on humidity conditions and plant transpiration. In addition, the isotopic enrichment was reflected in the leaf wax *n*-alkanes. Kahmen et al. (2012b) showed that the leaf wax *n*-alkanes D-enrichment increased in line with the leaf water D-enrichment along an aridity transect in Australia. Smith and Freeman (2006) provide evidence that *n*-alkane isotopic ratios reflect precipitation δD values. The apparent fractionation between *n*-alkanes and precipitation was dependent

on mean annual precipitation (MAP) and relative humidity (RH). The dry study sites exhibited smaller absolute apparent fractionations, which indicates that D-enrichment of source waters is controlled by leaf transpiration and soil evaporation. Hou et al. (2008) showed that the effect of RH on leaf wax D/H ratios is small. However, they found correlations between precipitation and leaf wax D/H ratios in experiments under both controlled and natural conditions. The correlation was more significant in drier regions. They suggest that sedimentary leaf wax D/H ratios are suitable as proxy for precipitation δD variations.

2.4 Response of plant activity to environmental factors

Transpiration of plants is the reason for leaf water evaporative D-enrichment and depends on some environmental parameters. Several universal correlations between plant biochemical processes and ambient conditions exist. Water availability is an important driver for plant growth and productivity. It is used for transport and translocations and hydration of cytoplasm and the maintenance of turgor (hydraulic pressure). But most of it passes through the plant and vaporizes and only 1 % is used involved in the metabolic activity. During one day plants can transport a multiple of the amount of water that it can hold at one time (Rosenberg et al., 1983). Plants need to take up carbon dioxide and release water to maintain their metabolic processes. The gas exchange between atmospheric air and plant occurs mainly through stomata. These are pores surrounded by a pair of specialized guard cells, mostly located on plant leaves. Their opening and closing controls the gas exchange. Sometimes the water is released from the plants through the cuticle as well (Willmer and Fricker, 1996). Transpiration rates are at the maximum as long as enough water/soil moisture is available (Rosenberg et al., 1983). Transpiration and photosynthesis are tightly connected with each other and the stomatal aperture. A rise in temperature elevates the metabolic activity of guard cells and the entire leaf which stimulates stomata opening. This increase reaches an optimum and decreases then because of increasing cell damages. There are also indirect effects of temperature which can change the temperature optimum. If respiration is dominating over photosynthesis, the internal CO_2 concentrations increase which causes a closure of stomata. In addition, temperature rises cause RH drops, meaning higher water vapour pressure gradient between leaf and air which is proportional to transpiration. Low RH leads eventually to stomatal closure and reduces transpiration, CO_2 exchange and photosynthesis whereat these processes are not necessarily linearly correlated. Temperature optima of stomatal aperture vary according to the surrounding conditions and the species. Optima can range between 20 and 40 °C, on average maximum apertures are observed at circa 30 °C (Rosenberg et al., 1983; Willmer and Fricker, 1996). Photosynthesis minimum lies between -2 and 0 °C, the optimum at 20 – 30 °C and the maximum between 40 and 50 °C (Lüttge et al., 2010). It increases with the strength of illumination until the saturation point is reached (Pisek et al., 1973) whereat transpiration increases without saturation at naturally occurring light intensities. The net radiation is the main driver of energy for ET. Transpiration is also dependent on wind speed, radiation, surface area, orientation and internal diffusive resistance (Gates, 1973). Wind speed increases ET from wet

surfaces and can be a dominating factor. However, when surfaces are dry, the effect of wind can be negative as well, depending on the plant resistance to diffusion of water vapour or on RH (Rosenberg et al., 1983).

2.5 Plant adaptations to dry climates

Plants species in general as well as individuals of the same species adapt to the prevailing environmental conditions such as temperature, light intensity or available water in their physiological, morphological, anatomic, metabolic and chemical traits (Moreno & Bertiller, 2012; Gates, 1973). Plants have genetic structural characteristics for drought resistance and also the ability to adapt in the short-term to dry conditions (Ristic & Cass, 1992; Klich et al., 1997). Plants with metabolically inactive parts that survive the drought are called arido-passive homoiohydrous plants. In contrast, arido-active homoiohydrous plants stay even in the driest and warmest times metabolically active, at least in parts. Their adaptations to the dry conditions include high amounts of root phytomass in relation to above-ground and photosynthesizing biomass, root growth in a big soil volume with a large horizontal and partly vertical extension, leaf movements to avoid heat loads, and in extreme drought years, suppression of flowering and fruiting (Evenari et al., 1985b). These plants have green leaves at all times of the year, fully expanded as well as incompletely expanded leaves that are ready to grow when water becomes available (Paruelo et al., 1998a; Soriano & Sala, 1984). The loss of water is kept low by adaptations that reduce the cuticular transpiration such as a reduced metabolically active surface (Evenari et al., 1985b) and enhanced microroughness that is ensured amongst others by stomatal depressions, triochomes, epidermal-cell surface contours or wax crystals (Klich et al., 1997). Leaf waxes provide protection against tranpiration losses, drought and heat stress and also against insects and diseases. They are complex mixtures and consist of different compounds, e.g. long-chain alkanes, alcohols, ketones, aldehydes, acetals, esters and acids (Eglinton and Hamilton, 1967). Plants under drought stress produce higher amounts of leaf waxes than with sufficient water. Also, younger leaves have usually higher wax concentrations than older leaves. The chemical composition of the leaf wax changes as the water conditions and the age of the leaves change (Lüttge et al., 2010; McWhorter, 1993). Adapted plants can tolerate high inorganic ion concentrations and can excrete salt by glands. In line with that the transpiration rates increase (Evenari et al., 1985b). In general, drought tolerant species show less phenotypic variations due to changing environmental conditions than less tolerant species. Species are more tolerant when stress has less impact on the performance (e.g. growth) (Couso and Fernández, 2012). Different photosynthetic pathways represent adaptions to climate as well. Three principal pathways are the C_3 cycle (Calvin cycle), the C_4 cycle (Hatch-Slack cycle) and the CAM cycle (Crassulacean acid metabolism). C_3 plants use the enzyme Rubisco for CO_2 fixation. They dominate in temperate and high latitude regions and in tropical forests. C_4 plants have a more efficient pathway where in an initial step the enzyme PEP carboxylase **(**Phosphoenolpyruvatcarboxylase) delivers more carbon to the Rubisco enzyme for fixation which increases the water use efficiency. Less than 5 % of plant species have the C_4 cycle but they dominate

in hot and dry ecosystems such as tropical and temperate grasslands. CAM plants use the C_3 cycle during the day but switch to the C4 cycle at night for carbon fixation. 10 % of plant species favour the CAM cycle. They dominate in desert ecosystems with species such as cacti. The type of pathway causes a typical bulk $\delta^{13}C$ value in the entire plant (C_3 plants: on average -27 ‰, C_4 plants: on average -12.5 ‰, CAM plants: intermediate) (Winkler and Schmidt, 1980; Clark and Fritz, 1998).

2.6 Purpose and hypothesis

Several studies investigated a RH gradient that was caused by changing MAP rates but had a similar temperature over the gradient (e.g. Hou et al., 2008; Kahmen et al., 2012b). However, experimental setups with RH gradients that are caused by varying MAT and not by varying precipitation rates, are missing. The purpose of this study is to investigate the effect of temperature and RH changes, respectively, on evaporative leaf and soil water enrichment (^{18}O and D) and in turn on leaf wax *n*-alkane D/H ratios. We aim to determine if temperature can be correlated to plant transpiration rates and if higher transpiration rates can be related to smaller leaf water *n*-alkanes fractionation. Leaf wax *n*-alkane δD values are compared with source water/precipitation δD values to investigate in which extend leaf wax *n*-alkane δD values record source water δD values, and to which extend they are controlled by soil and leaf evaporative D-enrichment and biosynthetic fractionation. The hypothesis is that with increasing temperature the plant transpiration increases and in line with that the leaf water and soil water evaporative D-enrichment. A further hypothesis is that enriched leaf water δD values are reflected in the leaf wax *n*-alkane δD values. The experimental design involves a temperature gradient in southern Argentina with similar MAP. On-site transpiration measurements and sampling of grass roots and leafs are included as well as δD analysis of root water, leaf water, leaf wax *n*-alkanes and meteoric water and the interpretation of the isotopic data in order to accept or reject the hypothesis.

2.7 Study area – Southern Argentina

2.7.1 Location of study area

The study country Argentina is elongated with a distance of about 3700 km from latitude 22° to 55°S and an area over 3 million km^2 (Mares et al., 1983). The diversity in biogeographical regions in this vast territory is big. However, in two third of the country arid and semi-arid rangelands are present. The study area includes different geographical provinces and ecosystems, respectively. Parts of the study area are the Argentinean provinces Santa Cruz, Chubut, Rio Negro, Neuquén, La Pampa and Mendoza. The southern part of the transect belongs to Patagonia and the northern part to the Monte steppe. Politically, Patagonia includes the Provinces of Tierra del Fuego, Santa Cruz, Chubut, Neuquén and Rio Negro (Paruelo et al., 1998b). However, the Monte ecoregion consists amongst others of parts of the provinces Mendoza, La Pampa and the Northeast of each Chubut, Rio Negro and

Neuquén. Different literature and maps show different borders between Patagonia and the Monte (Bisigato et al., 2009; Fernández & Busso, 1999; Guevara et al., 2009; Paruelo et al., 1998b).

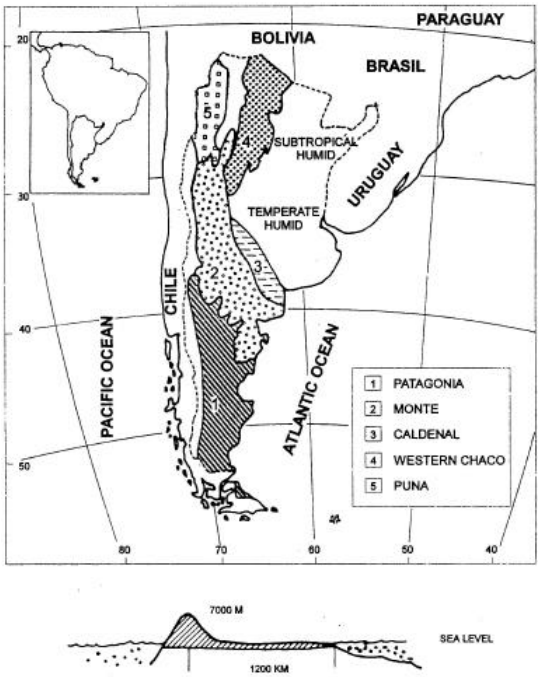

Figure 2. Major arid and semi-arid rangelands of Argentina (Fernández & Busso, 1999)

Patagonia extends approximately from 40-42° to 52-55° S from the Atlantic Ocean to an elevation in the inland about 1500 m with an area of 480 000 km² (Figure 2). The Monte desert extends in the north and northeast of Patagonia from north to south (24° to 44° S) in central and western Argentina with 500 000 km^2 (Figure 2) (Coopland, 1992; Labraga & Villalba, 2009).

2.7.2 Climate

The climate of Southern Argentina is largely controlled by the Andes which function as North-South distributed barrier. Furthermore, in the southern part of South America two high-pressure cells flank the continent whereas the pressure over the mainland is lower. This causes strong west winds in Patagonia. The cool and humid air masses coming from the Pacific Ocean lose most of their water in the Chilean/Andean area with extensive precipitation on windward slopes. In the east of the Andes the air gets hotter and drier through adiabatic warming. Towards the Atlantic Ocean the amount of precipitation decreases exponentially whereas the amount throughout the year remains relatively constant (Coupland, 1992; Soriano et al., 1983).

Patagonia has a temperate or cool-temperate climate, respectively. Most of the region has water deficits in spring and summer and is in the arid category with less than 200 mm MAP. During the coldest months from March to August the precipitation is highest (Soriano & Sala, 1984). This is related to the increasing frequency of Pacific synoptic perturbations during the winter months (Labraga & Villalba, 2009). The interannual variability of precipitation is highest in dry areas with

about 200 mm, e.g. in Pilcaniyeu with measured variations between 157 and 519 mm (Soriano et al., 1983). The characteristic of the temperature is like the precipitation NW-SE distributed due to the Andes and the latitude. The MAT ranges from 3 °C in the south to 12 °C in the northeastern part. Furthermore, the local topography and the wind influence the air temperature. The predominating strong winds from the west decrease the perception of the MAT by 4.2 °C (wind chill). The winds are persistent intense through the year with wind speeds between 15 km/h and 22 km/h in the center-west part with a minimum in the winter. In summer there is also a component from the south but both western and polar winds contain little air moisture. Humidity is higher in winter (> 70 %) than in summer (50 – 60 %) (Paruelo et al., 1998a; Soriano et al., 1983). Apart from precipitation and potential evapotranspiration, factors such as soil texture, percentage of stones, aspect, slope and leaf area index determine the distribution of water in the soil and its availability for the vegetation. Water losses of the soil are due to drainage and ET, which is for ET accounted for 34 % of the MAP (Paruelo et al., 1998a).

The Monte Region which is located north and northeast of Patagonia, differs from Patagonia regarding the climate. A transitional zone from summer to winter dominated rain regimes is observed south of 35°S. Therefore, the distribution of precipitation during the year is relatively uniform in the south. In the north the precipitation has its maximum during summer. The MAP is in general between 200 mm and 250 mm. The MAT lies between 13 and 17 °C and is greater than in Patagonia. In the entire Monte region there is a water deficit due to the low ratio between precipitation and potential evapotranspiration (Mares et al., 1985; Paruelo et al., 1998).

The main variables influencing the precipitation water isotopes in Argentina are the source water which comes mainly from the Pacific Ocean, and the Andes which function as barrier for free air flow and cause condensation of moisture and a depletion in heavy isotopes of rainfall. In the extra-Andean area in the south of South America the precipitation water isotopes are more uniform distributed. The changes are mainly caused by the seasonal variations in temperature. Summer shows a maximum in $\delta^{18}O$ and $\delta^{2}H$ and winter a minimum (Rozanski & Araguás-Araguás, 1995). Higher temperatures and lower latitudes, respectively, are connected with higher $\delta^{18}O$ and $\delta^{2}H$ values (Clark and Fritz, 1998).

2.7.3 Ecosystems in the study area

Worldwide many areas with low precipitation exist but they differ from each other in many factors and can often not be classified in the same ecosystem. No uniform definitions of terms like “desert”, “steppe”, “arid” and “semi-arid” exist. Variables that define different kinds of deserts and dry regions are precipitation, the seasonality of precipitation, temperature, air humidity, soil properties, wind, vegetation and geomorphologic and hydrological settings. “Arid” are by definition from Walter and Box (1976) regions with less than 200 mm average total precipitation per year. “Semi-arid“ regions range between 200 mm and 500 mm MAP. “Temperate zones” have considerable variations in temperature (West, 1985). “Semi-deserts”, especially deserts with winter rain, have precipitation

between 150 mm and 300 mm to 400 mm per year. True deserts have precipitation rates below 120 mm per year, and extreme deserts below 70 mm. Grasslands belong to the semi-deserts and are dominated by perennial grasses while trees and shrubs above 1 m are absent. Steppes are dominated by dwarf-shrubs which cover more than usually 10-30 % of the ground. Other growing plants are perennial grasses and cacti. Shrublands are dominated by shrubs that are more than 0.5 m and up to 2 m high and cover more than 30 % of the ground (Shmida, 1985). In general the dominance of shrubs decreases as effective soil moisture increases. The relative importance of grasses and fire increases along this gradient. There are different statuses of succession of grass-shrub-mixtures. Sometimes grasses would prevail if fires were frequent and livestock were removed. There are no hard borders between steppe (low grassland) and shrub steppe (West, 1985).

The cool semi-desert Patagonia is heterogeneous with different types of vegetation from real desert to semi-desert, perennial grassland, shrub steppe, shrub-grass-steppe, grass-shrub-steppe and grass steppe. Between the biozones species composition, plant functional relative abundance and ecosystem functioning changes. Approximately 45 % shrub desert, 30 % shrub-grass semi-desert, 20 % grass steppe and 5 % water surface and minor types such as meadows can be found (Coupland, 1992; Soriano et al., 1983). The vascular plants can be divided into three groups: shrubs, grasses and forbs. The shrubs are bigger than 0.5 m, don't have a main stem, are either evergreen or deciduous and use water mainly from lower soil layers. They cover up to 40 % of the soil surface. The grasses are tufted C_3 plants with stiff green leaves all year round. Their root system is mainly in the upper soil layer developed (Fernández & Busso, 1999). The bare soil surface is mostly 60 % or higher, seldom less (Soriano & Sala, 1984). Abundant genuses are *Festuca, Stipa* and *Poa* with the dominant grass species *Festuca pallescens*, *Stipa speciosa*, *Stipa humilis* and *Poa ligularis*. *Festuca* grasslands are in the south and west of Patagonia between richer grasslands and the desert grassland abundant and are associated with higher precipitation than *Stipa* grasslands (Coupland, 1992; Soriano & Sala, 1984). *S. speciosa* and *S. humilis* can occur together with varying dominance but there are also areas with only one of these species (Soriano et al., 1983). The mostly dicotyledonous forbs are annual and perennial evergreen or deciduous but their net biomass is much lesser than from shrubs or grasses (Fernández & Busso, 1999). Other species grow in valleys where more water is available (Soriano et al., 1983).

The Monte Region is the semiarid region west of the humid pampa in Argentina. The vegetation ranges from grass steppe in the east to xerophilous woodland, scrub woodland, semi-desert, scrub lands and shrub steppes (Coupland, 1992; Paruelo et al., 1998b). The most dominating plant communities are the evergreen shrubs, especially the group of Zygophyllaceae. In addition Cactaceae, herbaceous plants and grasses grow. Perennial grasses grow only in the protection of shrubs (Fernández & Busso, 1999). In the southern Monte the grass species *Stipa tenuis*, *S. speciosa* and *P. ligularis* grow (Guevara et al., 2009). The type of biozone is mainly dependent on the plant

available water and therefore on geomorphology and edaphic properties besides precipitation rates. In addition, factors such as grazing, fire, nutrient availability, microclimate or soil seed bank distribution can have effects on the vegetation (Bisigato et al., 2009).

The productivity and biomass in deserts is in general low with a linear positive correlation between MAP and aboveground net primary production (ANPP) in arid to subhumid regions. ANPP in Patagonia is strongly affected by precipitation. Additionally, ANPP has a peak at temperatures between 4 and 5.5 °C and lower values for colder or warmer temperatures (Paruelo et al., 1998a). However, plant productivity is mostly highly variable between years and places primarily because of differing precipitation rates. Species diversity is in general lower with less available water. The plant canopy cover is low but the root systems exploit most of the soil (Noy-Meir, 1985). Climate controls the distribution of plant species as well as functional groups. The relative abundance of shrubs increases with decreasing MAP. Grasses grow with higher precipitation rates. Hence, under conditions with high evaporation and low air and soil humidity shrubs predominate over grasses (Paruelo et al., 1998a). Forbs don't correspond to environmental gradients (Jobbágy et al., 1996). In the local scale climate is less important for ecosystem structure and functioning than edaphic characteristics or land use (Paruelo et al., 1998a). In addition, nutrients such as nitrogen and phosphorous sources can be limiting factors (Noy-Meir, 1985). Years of extreme drought reduce the ANPP, however, years with above average precipitation don't lead to an elevated ANPP. Hence, the relation between precipitation and ANPP is only linear until a certain precipitation value and a plateau is reached. It was suggested that excessive water cannot be taken up and be transpired by roots and leaves due to little surface areas (Fernández et al., 1991).

2.7.4 Geology and soils

The geology of Patagonia is formed by Late Paleozoic, Mesozoic and Cenozoic. Often the material at the surface is either sedimentary or volcanic. Most of the basins originated during the Late Jurassic or Early Cretaceous. Occurring morphology types are plateaus and hills, plains and dissected low plateaus. There are Triassic sediments in extra-Andean Patagonia with continental origin, Jurassic marine strata deposited in Chubut, Jurassic sediments in Santa Cruz with continental origin, mesosilicic and acidic effusive rocks in Chubut, Santa Cruz and Tierra del Fuego from the Middle Jurassic. Extra-Andean Patagonia is limited to the west by the Andean Cordillera with elevations between 2000 m and 2500 m or higher. To the north, extra-Andean Patagonia merges into the Pampa plains. To the east the area is limited by the South Atlantic Ocean. In the province of Rio Negro (north of Patagonia) the high plateaus begin at the sub-Andean foothills at elevations between 800 and 1200 m and descent towards the east. Often the plateaus are crowned by young volcanic forms such as Sierra de Somuncurá with levels up to 1200 m. (Soriano et al., 1983)

The soils of Patagonia are generally derived from glacial and volcanic materials and are mainly coarse with gravel and stones (Soriano & Sala, 1984). In the Monte desert the soils are dependent on slope

and elevation in a range from clayey to rocky (Mares et al., 1985). The soils are in general exposed to erosion, especially to wind erosion but also to water erosion which leads to low soil stability. High intensity of the west winds, evaporation in seasons with high wind intensity and the precipitation characteristics drive erosion. Low and sparse vegetation benefits soil erosion as well. Furthermore, human activities especially overgrazing and accidental fires enhance soil erosion to a big extend. The eroded material accumulates in macro- and micro-accumulations, barkans and fixed sand dunes (Soriano et al., 1983).

2.7.5 Grazing and land use management

When looking at the Patagonian vegetation and wildlife one has to take into consideration the huge human impact especially of the sheep industry. Since the beginning of the last century the entire region is used for sheep grazing. Sheep were first introduced to Rio Gallegos in 1885. In the following years the number of sheep increased enormously, from 369 264 in 1895 to 3 940 616 in 1914 (Soriano et al., 1985). An agricultural use of the arid and semi-arid areas was not possible and focussed to the humid regions (Fernández & Busso, 1999). It is most likely that during this time the biggest changes happened. There are only few detailed descriptions of the vegetation that was natural before the big human impact. There are no areas left where no sheep grazing was present and no documentations about the changes have been made. Hence, the changes made by sheep are not assessable. Today, in about 45 million hectares of arid Patagonia are about 10 000 ranches with around 12 million sheep that are kept on the range all year long continuously grazing, which leads to a huge grazing pressure. The sheep industry causes a desertification process in Patagonia. Changes due to overgrazing are reduction in diversity and in the relationship of live to dead tissue in the dominant grasses, increase in bare soil, soil erosion, soil water losses through evaporation and limited nutrient reserves and supplies. Related to the grazing history is also the increasing dominance of *S. humilis* and *S. speciosa* with their opportunistic strategies. Their life form is called opportunistic because they have active phenotypes even in the unfavorable dry summer-fall and cold winter season. They expand their leaves when resources become available (Golluscio et al., 2005; Soriano & Sala, 1984). The recovery of overgrazed areas is in general slow. With a rest of three or four years the best forage grass *P. ligularis* recovers. However, seed reserves in the soil recover really slowly (Soriano et al., 1983). Overgrazing is problematic in the Monte Steppe as well. It causes the disappearance of perennial forage grasses and the invasion of unpalatable shrubs, weedy forbs and annual grasses. Perennial grasses grow only under the protection of spiny shrubs. Livestock eats everything in dry years. In strongly affected regions sheep are replaced by goats which eat any kinds of plants (Fernández & Busso, 1999). The population density in Patagonia is very low with 0.6 people km^{-2}, nevertheless, the human impact is present, not only by the sheep grazing. In addition to that, the European hare spread all over the region as well, since it was introduced in 1911. In line with that development, the numbers of guanacos, pumas and lesser rhea was reduced. Apart from the changes in fauna, dam constructions, oil industry, wood cuttings and town and road buildings affect the vegetation and landscape (Soriano et al., 1983).

3 Samples and methods

3.1 The Argentinian transect

3.1.1 Selection of study sites

The area in South Argentina was selected for this study since the climatic settings are worldwide unique and particularly suitable for the aim of the study. Due to the NW-SE distributed temperature gradient and the relatively uniform precipitation range in extra-Andean Patagonia and the Monte a transect with MAT and RH, respectively, as main varying variables can be chosen. The MAT for the southern part of the study area is approximately 4 °C, for the northern part 14 °C. The range of precipitation lies between 150 mm and 300 mm per year. Therefore, the regions are arid and semi-arid. It is a region with a small number of plant species; a few perennial grasses are dominant or at least occurring over a wide range. Also, these species are similar in their morphology since they are concentrated in one exclusive phenological group (Golluscio et al., 2005). Hence, these species grow at most of the study sites and can be chosen as study plants. Furthermore, the landscape in Patagonia and the Monte consists of many plateaus of similar geological settings, mainly from two different time periods. These are ideal prerequisites for comparable study sites regarding underground, wind exposure, hydrological situation etc. The plateaus were selected according to their altitudes around 600 m, 800 m or 1200 m, except for the first site.

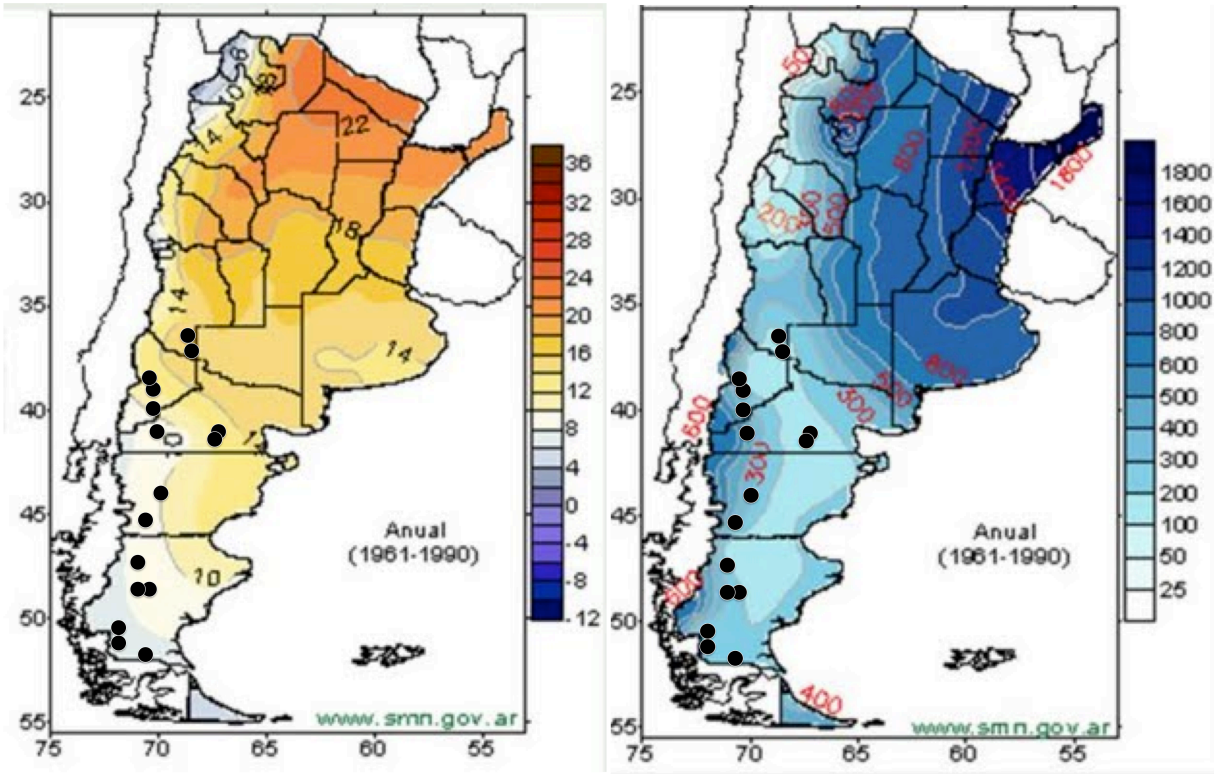

Figure 3. 16 Study sites in Argentina according to MAT and MAP (maps from http://geohistoricos.blogspot.de/)

3.1.2 Site descriptions

The locations of the study sites are shown in Figure 3. The coordinates and climate data of the investigated sites are listed in Table 1. The altitude ranges between 570 m and 1294 m with one exception, the site "pot" at 161 m. The distance between southernmost and northernmost site is approximately 1700 km. The MAT varies from 4.1 °C to 13.3 °C. The mean annual precipitation lies in a range between 139 m and 306 mm. The climate data are representative for 1950 – 2000 and are derived from the world climate database Worldclim (Hijmans et al., 2005) (www.worldclim.org). Data of shortwave down all sky (SW) radiation were used. These data were obtained from the NASA Langley Research Center Atmospheric Sciences Data Center NASA/GEWEX SRB Project (Global Energy and Water Cycle Experiment/ Surface Radiation Budget). Monthly data from daily averages were provided from 1983 to 2007 with a spatial resolution of 1° x 1° grid (unit: W m^{-2}). The monthly averages were added to calculate a yearly average.

Table 1. Site descriptions

Site code	Study date	Province	Coordinates		Altitude (m)	MAT[a] (°C)	MAP[a] (mm)	annual SW[b] (W m^{-2})
			Latitude	Longitude				
pot	08/03/2013	Santa Cruz	S 51°55.607'	W 070°24.399'	161	6.3	203	1250
tra	10/03/2013	Santa Cruz	S 51°19.985'	W 071°43.518'	570	4.5	266	1271
cer	11-12/3/13	Santa Cruz	S 50°37.641'	W 071°40.556'	821	4.1	219	1320
str	14/03/2013	Santa Cruz	S 48°37.210'	W 071°08.640'	871	5.7	181	1329
flo	16/03/2013	Santa Cruz	S 48°38.970'	W 070°29.991'	755	6.8	158	1329
hon	18/03/2013	Santa Cruz	S 47°02.968'	W 071°03.813	1294	4.5	193	1396
esc	20/03/2013	Chubut	S 45°08.510'	W 070°34.536'	665	8.2	238	1513
gps	22/03/2013	Chubut	S 44°04.190'	W 069°47.665'	1119	7	139	1563
so1	09/04/2013	Rio Negro	S 41°17.217'	W 066°49.501'	1220	8.8	203	1759
jac	25/03/2013	Rio Negro	S 41°03.466'	W 069°58.071'	1220	7.7	265	1759
so6	08/04/2013	Rio Negro	S 40°57.648'	W 066°42.612'	630	12	210	1759
est	27/03/2013	Neuquén	S 39°52.756'	W 070°11.018'	883	10.3	269	1872
zap	29/03/2013	Neuquén	S 39°06.685'	W 070°09.712'	1187	9.9	238	1956
laj	30/03/2013	Neuquén	S 38°36.768'	W 070°23.186	921	11.4	306	2016
but	02/04/2013	Mendoza	S 37°05.212'	W 068°26.743'	866	13.3	180	2103
win	05/04/2013	Mendoza	S 36°30.019	W 068°33.326'	1211	12.1	198	2164

[a] data from http://www.worldclim.org/, interpolations of observed data, representative of 1950 to 2000, [b] annual shortwave down all sky, data from NASA/SRB project, representative of 1983 to 2007.

The percentage of absolute vegetation cover and the composition of vegetation changed from site to site. Empirical estimations of the cover are shown in Table 2. In the south of the study area grasses are the dominant group of vegetation and no shrubs grow. The more in the north the less grasses and the more shrubs cover the soil. In addition, the percentage of bare ground increases. *P. ligularis* grows in the south of the study area and was found at ten study sites while *S. speciosa* grows in the north and was only found at four sites. At the site "but" it was the only growing grass species. The site was dominated by shrubs.

Table 2. Vegetation cover estimates

Site code	*% Poa ligularis*	*% Stipa humilis*	*% Stipa speciosa*	% all grasses	% shrubs	% forbs/ herbs/other	% bare ground
pot	75	0	0	85	0	0	15
tra	80	0	0	80	0	10	10
cer	80	0	0	80	0	10	10
str	35	15	0	50	0	15	35
flo	30	20	0	50	10	10	30
hon	55	25	0	80	0	0	20
esc	20	15	0	35	35	0	30
gps	35	15	0	50	20	0	30
so1	35	5	0	40	20	0	40
jac	15	10	10	35	25	0	40
so6	0	5	40	45	25	0	30
est	0	10	0	20	40	0	40
zap	0	10	0	20	15	5	60
laj	0	10	0	35	25	0	40
but	0	0	3	3	47	0	50
win	0	0	3	13	20	10	57

The grass plants growing were mainly small plants, mostly found in the shelter of shrubs. *S. humilis* was observed at eleven study sites in the middle of the transect. Other vegetation such as forbs appeared in some sites in low abundance. The soil was changing along the transect as well. The grain size distribution became gradually sandier in northern direction. The weather and soil conditions on the respective study day are presented in Table 3. The conditions varied a lot in between the sites. There were days without clouds and days with complete cloud cover, meaning varying light intensity. It was mostly dry, there was only one day with much rain ("pot") and two days with little rain ("tra" and "esc"). In addition, a strong rain event occurred before sampling at "but" and "win".

Table 3. Weather conditions at study sites, in order with increasing latitude.

Site code	Rain	Wind	Temperature (°C)	RH (%)	Soil moisture (%)	Mean light intensity ($\mu mol\ m^{-2}\ s^{-1}$)
pot	yes	strong	11	91.1	24.7	290
tra	little	strong	15	56.0	NA	850
cer	no	medium	9	56.8	26.7	570
str	no	little	14.4	35.2	14.0	775
flo	no	little	15	28.8	11.8	525
hon	no	little	20	38.0	17.9	1350
esc	little	strong	14.4	22.7	8.0	1080
gps	no	medium	10.5	69.0	16.7	253
so1	no	strong	18	43.7	18.1	1010
jac	no	little	18	24.9	12.6	1350
so6	no	medium	23	20.7	18.3	1300
est	no	little	36	12.7	10.3	1950
zap	no	medium	27	14.0	6.9	850
laj	no	little	23.4	22.0	9.5	1050
but	no	strong	20.5	60.2	30.2	1450
win	no	strong	17	33.2	23.7	895

NA: not available

The wind strength was empirically grouped into three categories (little, medium and high). Absolute temperatures were measured between 6 °C and 42 °C, RH between 12 and 91 % and soil moisture between ~7 % and 30 %. Soil moisture was measured with a ML 2x Theta probe (Delta-T Devices, Cambridge, UK) with 10 - 21 replicates around the study site with standard errors between 0.1 and 1.6. The other data were measured with the Li-Cor 6400 (Li-Cor Biosciences, Inc., Lincoln, NE, USA). Values measured between noon and 2 pm were used as estimates for the daily average. The daily light intensity is given as photosynthetically active radiation (µmol m^{-2} s^{-1}). It was used as general proxy for solar energy.

3.1.3 Investigated plants

3.1.3.1 Poa ligularis

P. ligularis (Figure 4) is a perennial, dioecious, greenish, turf grass, forming dense mats with intravaginal innovations. The thin and stiff reeds are (10-)20-50(-65)cm big with 2 – 4 nodes. The leaf sheaths are 5-15 (-20) cm long, smooth or rough, expanded and with cartilage in the base and margins, the basals are white-thatched. The ligules are ovate to acute, hyaline, sometimes lacerated and (0,5-) 2-1 (-15) mm long. The leaf blades foliate 5-20 (-35) cm x 1-2 (-3) mm, are folded convoluted, linear and filiform. The apex is acute to slightly navicular. The inflorescences are 4-12 (-16) x (0.5 -) 1-2.5 cm big, erect, contracted, dense, linear-oblong, green to purplish, with 10-15 (-20) nodes per panicle (Soreng, 2012). *P. ligularis* multiplies vegetatively by tillering and production of seedlings (Couso & Fernández, 2012). The subspecies *P. ligularis* var. *ligularis* is widespread. It belongs to the dominant perennial grasses in western and central Patagonia and the southern Monte, in steppes from La Rioja to the north of Santa Cruz, from sea level to nearly 4000 m asl in the Andes, and plains and mountains of the province of Buenos Aires (Soreng, 2012).

Figure 4. ***Poa ligularis***

3.1.3.2 *Stipa humilis*

S. humilis (Figure 5) is a perennial plant, densely caespitose, with short rhizomes or stolons until 2 cm long, rarely higher, with stems (10-) 25-30 cm high. It has cylindrical rods with 0.6-0.7 mm diameter that are erect, straight or geniculate and simple. *S. humilis* has few conspicuous knots which are

thickened, brown or straw-colored and glabrous. There are longitudinally striated internodes below the nodes that are glabrous or puberulous. The leaf sheaths are fluted and longer than the internodes, straw-colored or ivory, glabrous collar and hyaline margins. The leaf blades are linear, convoluted and 10 to 15 cm long x 0.3-0.4 mm diameter. The inflorescences is contracted, 3-10 cm long and its base covered by the upper leaf sheath. The most common subspecies *S. humilis* var. *humilis* is endemic to Argentina and lives from La Pampa and southern Mendoza to Patagonia. It is found from sea level to 1900 m asl. Flowering and fruiting happens between November and April (Cialdella, 2012).

Figure 5. ***Stipa humilis***

3.1.3.3 *Stipa speciosa*

S. speciosa (Figure 6) is a perennial grass, caespitose, usually robust, (7-) 30-60 cm high. It has cylindrical rods, 1.2-1.5 mm in diameter, straight to slightly geniculate erect and simple. The nodes are conspicuous, thickened, brown and glabrous to puberulous.

Figure 6. ***Stipa speciosa***

The internodes are longitudinally striated, glabrous and sometimes pubescent above the nodes. The fluted leaf sheaths are smaller than the internodes, the base is reddish or purplish-brown to blackish, the rest is straw-colored. The ligules are truncated, 0.8-1 mm long and membranous. The leaf blades are linear, convoluted or involuted, 3-25 cm long x circa 1 mm diameter, stiff and sometimes sharp or slightly curled and pubescent between the grooves. The inflorescences are contracted, (5-) 18-20 cm long, sticking out or included in the grass, partially covered by the superior leaf sheaths (Cialdella,

2012). *S. speciosa* multiplies mainly vegetatively by tillering while seedlings are rare (Couso and Fernández, 2012). It grows in North America, in the United States of America and Mexico, and in South America, Ecuador, Bolivia, Chile and Argentina, from Buenos Aires and south from Mendoza to Santa Cruz, between 400 m and 3800 m asl. It flowers from November to March (Cialdella, 2012).

3.1.3.4 Adaptations of study plants to the climate

The investigated species *S. speciosa, S. humilis* and *P. ligularis* belong to the dominant grass species in Patagonia and the Monte and to the group of arido-active perennials and the most drought tolerant species with opportunistic life form (Couso and Fernández, 2012; Soriano & Sala, 1984). Tussocks of these species keep old dead leaves as high proportions of biomass (Armas et al., 2008). The homogeneity in the group of perennial grasses is big; all species are concentrated in one exclusive phenological group. Hence, the competition between the species is big, especially the water competition (Golluscio et al., 2005). Perennial grasses can benefit from neighboring shrubs by protection from herbivores and enhanced microclimatic conditions such as more fertile soil and more available water. For instance, tiller height, blade length and blade area of *P. ligularis* increase as shrub cover and aridity increase (Moreno & Bertiller, 2012). The species composition in the vicinity of shrubs is different than in gaps between the shrubs. *S. humilis* appears more often beneath shrubs while *S. speciosa* grows more frequently in gaps between shrubs (Armas et al., 2008). *S. speciosa* can keep photosynthesis rates at a high level in a wide range of plant water potential (Fernández et al., 2002). Amongst others, *P. ligularis* and *S. speciosa* fold their foliar blades under water stress for protection from radiation and transpiration. They have bulliform cells along the main vein. When the water content decreases, the turgescence gets lost and the angle between the middle ridge and each of the two adjacent smaller ridges decreases (Klich et al., 1997).

3.2 Measuring of plant processes

Photosynthesis was measured with the Li-Cor 6400 open IRGA/Poratable Photosynthesis system (Li-Cor Biosciences, Inc., Lincoln, USA) with a 30 mm x 20 mm leaf chamber. The light source was provided by a red-blue LED light source (Li-6400-02B, Li-Cor Inc., Lincoln, NE, USA). The CO_2 source was either the reference air or a computer controlled CO_2 mixing system. Three grass leaves were measured at the same time in the leaf chamber. The system measured amongst others air temperature as well as each incoming and outgoing CO_2 concentration (ppm), air humidity (%) and light intensity (PAR – Photosynthetically Active Radiation, 400-700nm, µmol quanta m^{-2} s^{-1}). Gas flow through the leaf chamber was set to 500 µmol s^{-1} or the flow control was used to keep constant sample H_2O values. Plant processes were measured first under ambient conditions with ambient light and CO_2 conditions. Afterwards light intensity was set to 500 µmol quanta $m^{-2}s^{-1}$ and reference CO_2 to 385 ppm. For the statistical analysis, mostly the measurements under the actual conditions were used. When these measurements were not available (at sites “pot”, “tra”, “cer” and “str”), the data with controlled light and CO_2 were used. For each site three to six (mostly five) different leaf-triplets were

measured. Each time, three to six times was measured and a mean value was calculated. The standard deviation varied from < 0.01 to 2.9 µmol CO_2 m^{-2} s^{-1}, on average 0.8 µmol CO_2 m^{-2} s^{-1}. The SD of the transpiration measurements varied between < 0.01 and 0.43 H_2O m^{-2} $s^{-1}$with an average SD of 0.09.

In addition, light and CO_2 curves were made. The light curves were conducted using a CO_2 concentration set to 385 ppm. Light values were set to 0, (25), 50, 100, 200, 400, 800, 1200, 1800, 2500 µmol quanta $m^{-2}s^{-1}$. Each step was measured three times. Some light curves are measured with single measurements. The adjustment time between each measurement was 150 to 180 seconds. The standard deviation (SD) for each step for transpiration ranged between < 0.01 and 2.4 (average 0.27) µmol H_2O $m^{-2}s^{-1}$. The SD of photosynthesis ranged between 0.06 and 20.6 (average 1.6) µmol CO_2 m^{-2} s^{-1}. The CO_2 curves were made with a light value of 500 µmol $m^{-2}s^{-1}$. The reference CO_2 values were set to 400, 300, 200, 100, (75), 50, 400, 400, 600, 800, 1200, 1600, 2000, (2500) ppm. Each step was measured in triplicates with a waiting time between 60 and 90 seconds. Some CO_2 curves were measured with single measurements. The SD for each step for transpiration ranged between 0.01 and 2.1 (average 0.2) µmol H_2O m^{-2} s^{-1}. The STD ranged for photosynthesis between 0.2 and 22.7 (average 2.2) µmol CO_2 m^{-2} s^{-1}. From the light and CO_2 curve data the light and CO_2 compensation points were determined. For low light or CO_2 values the relation with photosynthesis rates is linear. A linear regression line was fitted to the linear part of the curve. The intercept with the x-axis where the net photosynthesis rate is zero represents the light and CO_2 compensation point, respectively. The water use efficiency (WUE) was calculated in form of the photosynthetic water use efficiency or instantaneous water use efficiency, respectively, as ratio of photosynthetic rate (A) and transpiration rate (E) as described in Nobel (1991):

$$\boldsymbol{WUE = \frac{A}{E}} \qquad \textbf{(4).}$$

3.3 Sampling

Samples were taken from green grass leaves. The lower pinkish part of the leaves was cut off. In addition, the top 2 cm roots from green parts of the plant were taken. The samples were taken in duplicates. The samples were stored in screw cap polypropylene vials, sealed tightly with electrical tape (30 ml volume). Water samples were taken along the transect, in the vicinity of the study sites from streams, lakes and precipitation from localized and sporadic rain events in 1.5 ml GC screw cap vials.

3.4 Plant selection and identification

The appearance of the study plants as well as the species used for Li-Cor measurements and leaf and root samples at each study site are shown in Table 4.

Table 4. Appearance of experimentally used grass species and conducted methods

Site code	*Poa ligularis*			*Stipa humilis*			*Stipa speciosa*		
	growth	samples	Li-Cor	growth	samples	Li-Cor	growth	samples	Li-Cor
pot	**x**	x	x						
tra	**x**	x	x						
cer	**x**	x	x						
str	**x**	x	x	**x**					
flo	**x**	x	x	**x**					
hon	**x**	x	x	**x**					
esc	**x**	x	x	**x**	x	x (am)			
gps	**x**	x	x	**x**	x	x			
so1	**x**	x	x	**x**	x	x (am)			
jac	**x**	x	x	**x**	x	x (am)			
so6				**x**	x	x	**x**	x	
est				**x**	x	x			
zap				**x**	x	x			
laj				**x**	x	x			
but							**x**	x	x
win							**x**	x	x (am)

am: only ambient conditions measured (no light and CO_2 curves)

3.5 Plant water extraction

Leaf and xylem water was cryogenically extracted at Paul-Scherrer-Intitute in Villigen, Switzerland, following the method described in West et al. (2006). The leaf and root samples were refilled in glass exetainers. Condensed water in the plastic bottles was soaked up with dry tissues and extracted as well. The exetainers were connected with an U-tube and a vacuum pump. The samples were submerged into a water bath with 80 °C. The U-tubes were submerged into a cold trap with liquid nitrogen at -191 °C. A vacuum of at least $5 \cdot 10^{-2}$ mbar was applied for at least 2 hours. After the vacuum was stopped the U-tubes were closed with stoppers. When the extracted water was melt and collected in the U-tube it was pipetted into 1.5 ml GC vials. 0.1 ml micro-Inlets were used when the amount of extracted water was not enough to fill the entire vial. Water was extracted from all samples.

3.6 Stable water isotope analysis

All water isotope analyses were conducted at Max-Planck-Institute for Biogeochemistry (MPI-BGC), Jena. The environmental water samples as well as the extracted root and leaf water were analyzed for δD and $\delta^{18}O$ values, measured by online high temperature reduction in the modified carbon reactor of a High Temperature Conversion/Elemental Analyzer system (TC/EA) coupled to an IRMS (Delta^{plus}XL, Finnigan MAT, Bremen, Germany). All samples were measured in three replicates. The SD for the environmental water samples varied between < 0.01 ‰ and 1.46 ‰ with an average of 0.34 ‰ for D and between < 0.01 ‰ and 0.15 ‰ with an average of 0.05 ‰ for ^{18}O, respectively. The SD for plant water samples was in a range between 0.01 ‰ and 1.02 ‰ with an average of 0.21 ‰.

For the ^{18}O isotopes the SD was between < 0.01 ‰ and 0.13 ‰ with an average of 0.04 ‰. The values were reported in delta notation in ‰ and were corrected to VSMOW.

3.7 *n*-alkane sampling, extraction, identification and quantification

The extraction, identification and quantification of *n*-alkanes were conducted at MPI-BGC, Jena. To determine the δD of leaf wax *n*-alkanes the same leaves that were used for leaf water extraction were collected and dried at 40 °C for 96 h. The dry leaf samples were ground to a fine powder using a ball mill (Retsch MM200, Düsseldorf, Germany). For the first step of *n*-alkane extractions, the ASE 200 (Accelerated Solvent Extractor; DIONEX, Idstein, Germany) was used. The ASE vials were filled with combusted sand, ground leaf material, 100 µl of an internal standard solution (250 ng *n*-C_{36}/µl isooctane) and more combusted sand. For extraction, a 9:1 dichlormethane (DCM)/methanol (MeOH) mixture was used at 110 °C and 103.4 bar. Three cycles were conducted with 1 min preheat, 6 min heat, 1 min static, 1 vol flush% and 100 sec purge. Afterwards, the extracts were dried. For the subsequent solid phase extraction (SPE) liquid chromatography (LC), glass columns were filled to three quarters with activated silica gel (0.04 – 0.063 mm, Merck KGaA, Darmstadt, Germany) and circa 0.5 cm combusted sand. The columns were rinsed with acetone, DCM and hexane and activated at 50 °C for 3-4 h. The dry extracts were solved in hexane and pipetted on top of the sand. Three fractions were extracted with each approximately 5 ml hexane (F1), 1:1 hexane/DCM (F2) and 1:1 DCM/MeOH (F3). The dried F1 and F2 fraction were transferred with DCM into GC vials with 350 µl inserts, the F3 fraction was transferred with a DCM/MeOH mixture. The extracts were dried before closing the GC vials.

The F1 fraction was used to identify and quantify the *n*-alkanes with gas chromatography with coupled flame ionization detector (GC-FID) (TRACE GC, CE Instruments, Thermo Quest, Rodano, Italy) with a HP5 column (30m, Agilent Technologies, Palo Alto). Helium was used as carrier gas. The GC oven was programmed to an initial temperature of 90 °C (held for 1 minute), a first heating rate of 10 °C/min up to a temperature of 300 °C (held for 17 minutes) and a second heating rate of 30 °C/min to a final temperature of 335 °C (held for 3 minutes). The Injector was used in PTV (Programmed Temperature Vaporization) splitless mode with an initial temperature of 45 °C (Split flow: 20ml/min, splitless time: 2 min, injection time: 0.1 min, transfer: 14.5 °C/s, 300 °C, 3 min, cleaning: 14.5 °C/s, 350 °C, 3 min). 1 µl of standard and sample solutions, respectively, were injected in single measurements and heated to 200 °C at a pressure of 101.3 kPa. For measuring the *n*-alkanes, the dry extracts of the F1 fraction were dissolved in 100 µl isooctane. The detection limit of the FID is ~1 ng/µl. For identification and quantification of the *n*-alkanes a standard mixture of *n*-C_{15} to *n*-C_{33} and additionally a *n*-C_{36} standard solution was used (concentrations 5, 25, 50, 75, 100, 150 and 200 ng/µl). The mean R^2 of the *n*-C_{15} to *n*-C_{33} calibration curves was 0.98366, the R^2 of the *n*-C_{36} calibration curve was 0.99986. The FID peak areas of the *n*-alkanes (*n*-C_{15} to *n*-C_{33}) were compared to the *n*-C_{15} to *n*-C_{33} calibration curves for quantification. The FID peak areas of the *n*-C_{36} were compared to the *n*-C_{36}

calibration curve. The absolute mass of *n*-alkanes in the extract ($m_{n\text{-}ALK}$) was calculated using measured *n*-alkane concentration in the extract (extract-$conc_{n\text{-}ALK}$) and the volume of solved extract ($V_{extract}$) which equals in all cases 100 µl:

$$\boldsymbol{m_{n-ALK} = extract - conc_{n-ALK} * V_{extract}} \quad [ng] \tag{5}$$

The amount of *n*-alkane per g of dry leaf (leaf-$conc_{n\text{-}ALK}$) was calculated using the weight of the measured extracted *n*-alkanes and the weight of leaves ($m_{dryleaf}$) used for the extraction:

$$\boldsymbol{leaf - conc_{n-ALK} = \frac{m_{n-ALK}}{m_{dry\ leaf}}} \quad \left[\frac{\mu g\ n-ALK}{g\ dry\ leaf}\right] \tag{6}$$

Between 0.26 and 0.59 g dry leaf were used. The percentage of remaining *n*-C_{36} in the extract after extraction (p) was calculated by means of the mass of measured *n*-C_{36} ($m_{n\text{-}C36}$) and the mass of added *n*-C_{36} before starting the extraction ($m_{n\text{-}C36\ IS}$ = 25000 ng):

$$\boldsymbol{p = \frac{m_{n-C36}}{m_{n-C36\ IS}}} \quad [-] \tag{7}$$

It was assumed that the loss of all *n*-alkanes is equally high. The percentage of *n*-C_{36} standard that remained in the extract varied between 12 and 83 %. On average 47 % of the added internal standard could be measured after the extraction process. The concentrations of the *n*-alkanes per g dry leaf were corrected with:

$$\boldsymbol{conc_{n-ALK} = \frac{leaf-conc_{n-ALK}}{p}} \quad \left[\frac{\mu g\ n-ALK}{g\ dry\ leaf}\right] \tag{8}$$

3.8 δD values of leaf wax *n*-alkanes

The δD value measurements of *n*-alkanes were performed at MPI-BGC, Jena. The deuterium isotopes of the *n*-C_{29} and *n*-C_{31} *n*-alkanes ($\delta D_{n\text{-}ALK}$) were measured with a GC-IRMS (GC: 7890A with Monitor FID, Agilent Technologies, Palo Alto, USA; IRMS: Delta V Plus Isotope Ratio MS, Thermo Fisher Scientific, Bremen, Germany). The Delta V Plus was coupled with a GC-Isolink and Conflo IV system. The *n*-alkane fraction was dissolved in isooctane dependent on their concentration and 1 µl was injected into the GC (HP5 column, 30m, Agilent Technologies, Palo Alto). The injector was operated at 280 °C in splitless mode. The oven temperature was maintained at 110 °C for 1 minute, heated to 220 °C with 10 °C/min (held for 1 minute), heated to 320 °C with 5 °C/min (held for 6 minutes) and finally heated to 350 °C with 30 °C/min (held for 2 minutes) with a total oven run time of 42 minutes. The stability of the ion-source conditions were ensured by the H_3 factor (Hilkert et al., 1999) that was measured once a day during the 9-days measurement period. The mean of the H_3 factor was at 4.5 (SD = 0.2) slightly decreasing over time. Additionally, a standard mixture of C_{15}-C_{33} *n*-alkanes was run at least once a day. The peaks had a clean baseline-separation which expresses good separation. H_2 gas of known isotopic composition was used as a working reference standard with three peaks in the beginning, one before the *n*-C_{26} peak and three in the end of the measurement (each 10 sec, ~2200 mV peak area). The samples were measured with two internal standards of known

δD values (n-C_{26} and n-C_{36} n-alkanes). Their concentrations were chosen to achieve peaks of similar peak areas at approximately 1200 mV. This was the case at circa 70 ng/µl for the n-C_{26} standard and at circa 140 ng/µl for the n-C_{36} standard. The δD values of the samples were corrected according to the internal standards, no drift correction was applied. The values were reported in delta notation in ‰ and were corrected to VSMOW. The δD values of the standard n-alkanes were calibrated against international reference substances (NBS-22; IAEA-OH22) using the offline high temperature pyrolysis technique (TC/EA; Gehre et al., 2004). Each sample and standard mixture was injected three times. Since the concentrations of the n-C_{29} and n-C_{31} n-alkane were varying for many on the samples, these samples were measured more than once with different dilutions and n-alkane concentrations, respectively, until a peak area between 800 and 2000 mV was achieved. Only in-between this interval the measurements have acceptable accuracy. A concentration weighted mean δD value between n-C_{29} and n-C_{31} was calculated as:

$$\delta D_{n-ALK} = \frac{\delta D_{C29} \cdot conc_{C29}}{conc_{C29-C31}} + \frac{\delta D_{C31} \cdot conc_{C31}}{conc_{C29-C31}} \text{ [‰]} \quad \textbf{(9)}$$

It is referred to as concentration-weighted n-alkane (CWA) δD values.

3.9 Calculation of fractionations

The fractionation between leaf water and root water ($\varepsilon_{leaf/root}$) was calculated with:

$$\boldsymbol{\varepsilon_{leaf/root}} = \left(\frac{\boldsymbol{\delta D_{leafwater}+1000}}{\boldsymbol{\delta D_{xylemwater}+1000}} - \mathbf{1}\right) * \mathbf{1000} \text{ [‰]} \quad \textbf{(10)}$$

Additionally to the measured water samples, annual precipitation (p) data from Bowen and Revenaugh (2003) by way of the Online Isotopes in Precipitation Calculator (OIPC) (www.waterisotopes.org) were used for fractionation calculation. The evaporative soil water enrichment ($\varepsilon_{soil/p}$) from precipitation δD values to soil water was calculated with:

$$\boldsymbol{\varepsilon_{soil/p}} = \left(\frac{\boldsymbol{\delta D_{xylemwater}+1000}}{\boldsymbol{\delta D_{precipitation}+1000}} - \mathbf{1}\right) * \mathbf{1000} \text{ [‰]} \quad \textbf{(11)}$$

Here, xylem water (root water) was used as proxy for soil water. The total evaporative fractionation between leaf water and annual precipitation water (ε_{ET}) was calculated as:

$$\boldsymbol{\varepsilon_{ET}} = \left(\frac{\boldsymbol{\delta D_{leafwater}+1000}}{\boldsymbol{\delta D_{precipitation}+1000}} - \mathbf{1}\right) * \mathbf{1000} \text{ [‰]} \quad \textbf{(12)}$$

The apparent fractionation (ε_{app}) between concentration-weighted n-alkanes δD values and plant source water δD values was determined as:

$$\boldsymbol{\varepsilon_{app}} = \left(\frac{\boldsymbol{\delta D_{n-ALK}+1000}}{\boldsymbol{\delta D_{precipitation}+1000}} - \mathbf{1}\right) * \mathbf{1000} \text{ [‰]} \quad \textbf{(13)}$$

The net biosynthetic fractionation (ε_{bio}) was calculated as fractionation between the concentration-weighted n-alkane δD values and the leaf water δD values:

$$\varepsilon_{bio} = \left(\frac{\delta D_{n-ALK}+1000}{\delta D_{leafwater}+1000} - 1\right) * 1000\ [‰] \quad (14)$$

3.10 Bulk $\delta^{13}C$ analysis

The bulk $\delta^{13}C$ in the leaves were measured with an EA-GC-IRMS (Elemental Analyzer-Gas Chromatograph-Isotope Ratio Mass Spectrometer) system at MPI-BGC, Jena. Weighted tin capsules with dried leaf samples were placed into an autosampler of the CHN combustion unit (EA 1100, CE, Mailand) with helium as carrier gas. With the additional flow of O_2 and a temperature of 1020 °C the sample carbon is quantitatively combusted to CO_2 and the sample gas is subsequently separated by a GC. Via a continuous flow (ConFlo III) interface the gas enters the Delta^{plus} IRMS (Finnigan MAT, Bremen, Germany) and is measured on-line (0.06 ‰ – 0.6 ‰ precision). Between 0.7 mg and 0.9 mg of dried and ground leaf samples have been weighted in tin capsules. In addition, 0.5 mg – 0.6 mg of standard ali-j3 and 0.7 mg – 0.8 mg of standard cat-j3 have been weighted in the capsules. Six out of 26 samples were measured in triplicates, the rest in single measurements. A mean value of the measured $\delta^{13}C$ values of the ali-j3 standard was calculated and subtracted from the set value (-30.06 ‰). The difference was added to the measured $\delta^{13}C$ values of the samples to correct them. The SD of the triplicates ranged between 0.03 ‰ and 0.18 ‰ $\delta^{13}C$ with an average of 0.09 ‰. The values were reported in delta notation in ‰ and were corrected to Pee Dee Belimnite standard (PDB).

3.11 Statistical Analysis

The statistical analysis was conducted with R (Version 0.97.551). Graphs were made with R or Microsoft Excel (Version 14.1.4). Missing values for soil moisture were replaced with mean values of all available data points. Statistics was used for identification of the most influencing variables and selection of the best model explaining the particular effect. In the beginning a multiple linear regression model with the design variables MAT and MAP was performed for some of the response variables. The chosen transect was supposed to have no variations in MAP but it was not possible to avoid variations between 150 and 300 mm. Therefore, besides MAT the MAP was used as design variable because MAP has been shown to be a significant variable on the studied parameters (e.g. Hou et al., 2008; Smith and Freeman, 2005). The other explaining variables were preselected with the method “random forest” (RF, R package: randomForest, Liaw and Wiener, 2002) which rates the variables according to their importance. The output “Mean Decrease in Accuracy” was used as RF value. The 1 – 6 variables with the highest ranks were selected for further analysis. In addition, the design variables MAT and MAP were used for further analysis when they were used in the design model independent on their significance. A stepwise backward regression with BIC (Bayesian Information Criterion) basis (Burnham and Anderson, 1998; Schwarz, 1978) was applied with the selected variables and the design variables. BIC is defined as:

$$\boldsymbol{BIC = -2\,log(L) + K * log(n)}. \quad (15)$$

L is the maximized value of the empirical likelihood function, K is the number of estimable parameters, n is the sample size. Low BICs mean that a model is more probable than models with higher BIC. In this procedure from an initial model the variable whose deletion from the model would cause the highest BIC was deleted from the model. Variables are removed from the model until deletion of variables doesn't cause an improvement of BIC anymore. The resulting variables were used for a final multiple linear regression (only continuous variables) or ANCOVA (analysis of covariance, categorical and continuous variables) model. Simple species effects without covariates were analyzed with ANOVA (Analysis of variances). The analysis parameters did not include latitude as it was highly correlated with the irradiation ($R^2 = 0.97$) and the effect of irradiation should be analyzed.

4 Results

4.1 Bulk $\delta^{13}C$ analysis

The bulk $\delta^{13}C$ values from the species *P. ligularis*, *S. humilis* and *S. speciosa* are in a range between -30 and -24 ‰ with mean values of -26.0 ± 0.4 ‰ (SE, *n* = 10), -27.1 ± 0.3 ‰ (SE, *n* = 8) and -26.0 ± 0.8 ‰ (SE, *n* = 3), respectively (Figure 7).

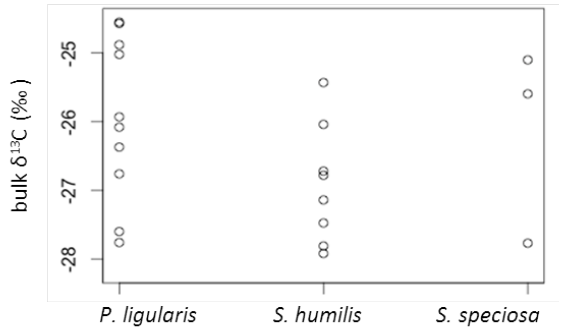

Figure 7. Bulk $\delta^{13}C$ values from plant samples for all species

4.2 Li-Cor measurements

4.2.1 Light response curves

Light response curves from 0 to 2500 µmol m^{-2} s^{-1} of *P. ligularis* (*n* = 11) and *S. humilis* (*n* = 4) were analysed. *S. speciosa* was not included (*n* = 1). All light response curves with photosynthesis and transpiration as response variables are shown in the appendix (Figure A1, Figure A2). Examples for *P. ligularis* at "so1" and *S. humilis* at "so6" are presented in Figure 8.

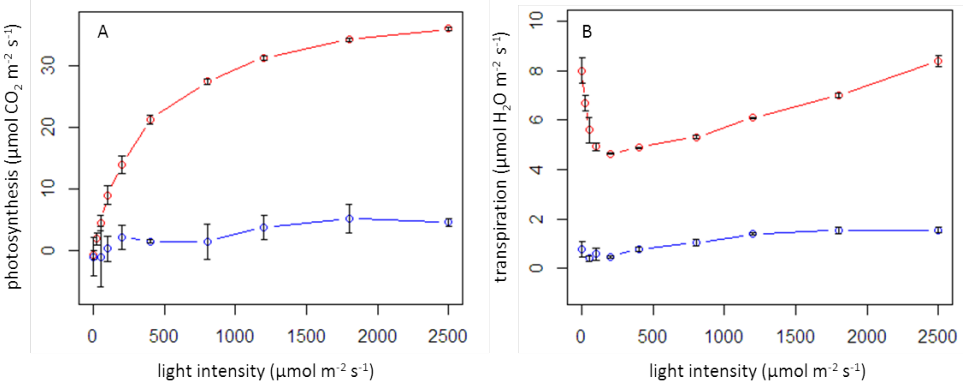

Figure 8. Examples for light response curves with A) photosynthesis and B) transpiration as response variable. Error bars indicate SD. Red: *P. ligularis* at "so1"; blue: *S. humilis* at "so6".

The photosynthesis rates increases with increasing light intensity as in Figure 8A. The relation between light and photosynthesis is linear in the beginning from 0 up to 25 – 200 µmol m^{-2} s^{-1}. After that the curves truncate. In most cases saturation is reached (between 200 and 2500 µmol m^{-2} s^{-1}). The

light response curve measured at the site "est" with a mean air temperature of 46.3 °C is an exception. The values for each light step are fluctuating a lot and barely reaching zero.

The light compensation points are varying between -31 and +147 µmol m^{-2} s^{-1}. The response curve at "est" is not used in the statistical analysis because the single measurements of *S. humilis* are too much fluctuating. The design variables MAT (P = 0.181) and MAP (P = 0.325) didn't have significant influence on the light compensation point in the design model. The variables with the highest RF importance ranks were RH, air temperature during the respective measurement and species (Appendix, Table A1). These three variables and MAT/MAP were included in the initial ANCOVA model. After the backward stepwise selection with BIC the only variable left was air temperature. The result of this analysis and the linear regression outputs with this variable are shown in Table 5. Leaf temperature is significantly (P < 0.001) influencing the light compensation point (Figure 9). The species effect is not important in this model.

Table 5. Explaining variables selected by a random forest (RF) approach to be of importance in predicting light compensation point.

variable	order		RF value	BIC	Beta	SE	t value	*P*
	importance	removal						
Intercept					-38.03	21.63	-1.76	0.102
air temperature	1		32.7		3.97	1.04	3.80	**0.002**
humidity (reference air)	2	a	31.6	111.0				
Species	3	d	16.9	107.1				
MAT		c		108.2				
MAP		b		109.0				

Notes: Order of importance (1-3) is the ordered importance of variables as given by the RF (random forest). Order of removal (letters a-d) is the order of traits in which the traits were removed in the backward stepwise selection. RF value is the importance score given by the RF for each trait. BIC (Bayesian Information Criterion) values are given for the model in the backward stepwise selection before the respective variable was removed. Beta, SE, t value and P values (statistical significance given for P < 0.05) are for the intercept and the remaining trait in the regression of light compensation point in the final model (R^2 = 0.53, P = 0.002, BIC = 107.0).

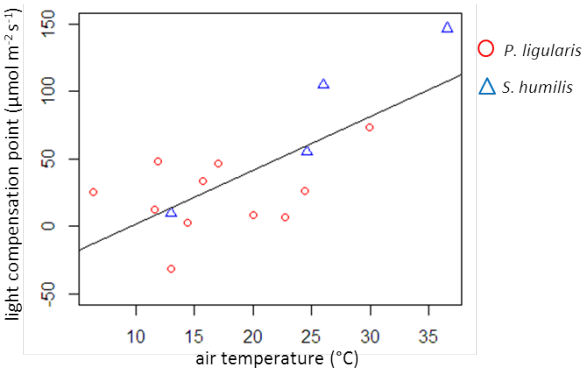

Figure 9. Light compensation point as a function of air temperature and species.

The transpiration decreases starting from dark conditions up to 50 – 200 µmol/$m^{-2}s^{-1}$. Then the transpiration increases. In most light response curves the transpiration reached no saturation (Figure 8B). Photosynthesis and transpiration are both increasing in the light response curves above light

intensities of 200 – 400 µmol m^{-2} s^{-1}. The resulting WUE increases for all light curves until light intensities of 200 – 400 µmol m^{-2} s^{-1}. With higher light intensities WUE stays at a constant level which ranged for the different light curves between 0 and 10 µmol CO_2/µmol H_2O. Photosynthesis, transpiration and WUE data of *P. ligularis* and *S. humilis* at the maximum light intensity of the light curves are shown in Figure 10.

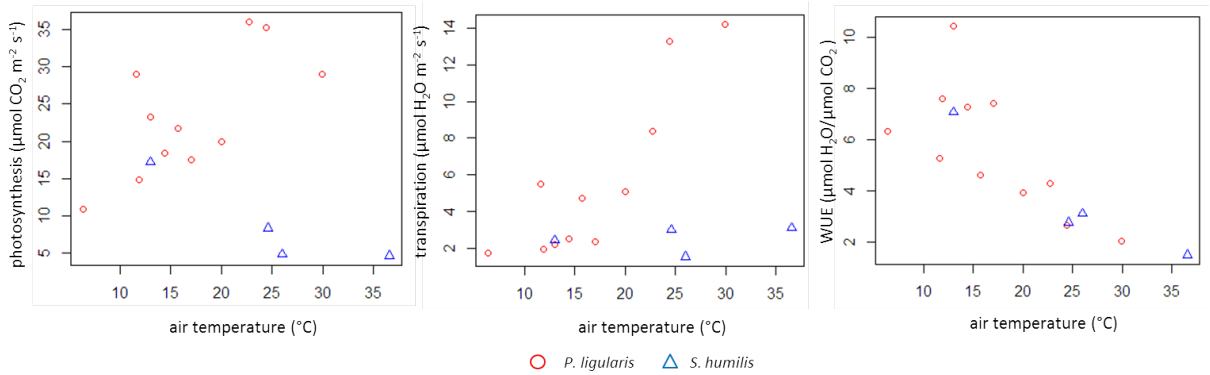

Figure 10. Photosynthesis, Transpiration and WUE of *P. ligularis* and *S. humilis* at maximum light intensity of light response curve (2500 µmol m^{-2} s^{-1}).

The photosynthesis and transpiration rates of *P. ligularis* are increasing with increasing temperature (between 5 and 30 °C) and decreasing RH, respectively. However, WUE declines with increasing temperature. The transpiration rates of *S. humilis* are at all temperatures low. Photosynthesis is low for temperatures of 25 °C and above but it was high at approximately 13 °C. WUE is declining with rising temperature as for *P. ligularis*. Here, WUE is not species dependent but the levels of photosynthesis and transpiration are higher for *P. ligularis* than for *S. humilis* at higher temperatures.

4.2.2 CO_2 response curves

The impact of increasing CO_2 concentrations on photosynthesis and transpiration are shown in Figure 11A+B in two CO_2 response curves, each one for *P. ligularis* and *S. humilis*.

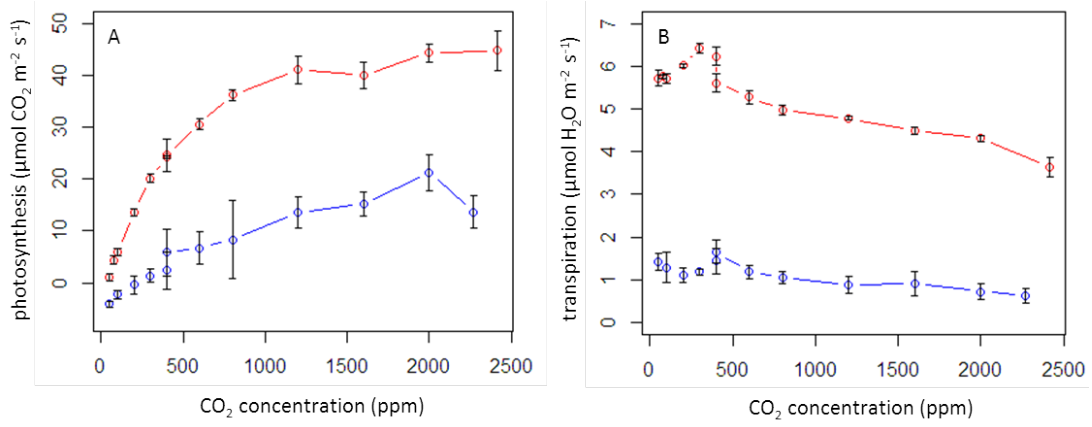

Figure 11. Example CO_2 curves with A) photosynthesis and B) transpiration. Error bars indicate SD. Red: *P. ligularis* at "so1"; blue: *S. humilis* at "so6".

All measured CO_2 response curves are presented in the appendix (Figure A3 and Figure A4). The photosynthesis rates increase with increasing CO_2 concentrations. The relation is linear in the beginning and truncates afterwards. The photosynthesis reaches saturation in approximately half of the CO_2 curves (between 1200 and 2400 ppm).

The CO_2 compensation points range between 23 and 343 ppm. The influencing variables on the CO_2 compensation point of 15 CO_2 response curves were analysed (from *P. ligularis* and *S. humilis*). The design variables were analysed in a multiple linear regression model. MAT is nearly significant ($P = 0.058$) with a positive effect whereat MAP is not significant ($P = 0.272$). In a random forest ranking species, air temperature and RH are most important (Appendix, Table A2). In the final model species and temperature remain. In an ANCOA species explains 60.6 % of the variance and air temperature 10.2 % (Table 6).

Table 6. Explaining variables selected by a random forest (RF) approach to be of importance in predicting CO_2 compensation point.

variable	order		RF value	BIC	df	*P*	SS (%)
	importance	removal					
Species	1		51.2		1	**< 0.001**	60.6
air temperature	2		18.5		1	0.063	10.2
humidity (reference air)	3	b	17.2	127.49			
MAT		a		130.15			
MAP		c		126.28			
Residuals					12		29.3

Notes: Order of importance (1-3) is the ordered importance of variables as given by the RF (random forest). Order of removal (letters a-c) is the order of traits in which the traits were removed in the backward stepwise selection. RF value is the importance score given by the RF for each trait. BIC (Bayesian Information Criterion) values are for the model in the backward stepwise selection before the respective variable was removed. *P* values (statistical significance given for $P < 0.05$), degrees of freedom (df) and sum of squares (SS) are for the remaining traits in the ANCOVA of CO_2 compensation point in the final model (BIC = 125.35).

The species is the dominant variable explaining the CO_2 compensation point. Higher temperatures as second influencing factor lead to a rise in CO_2 compensation points. CO_2 compensation points are higher for *S. humilis* than for *P. liguaris* even at the same temperature (Figure 12).

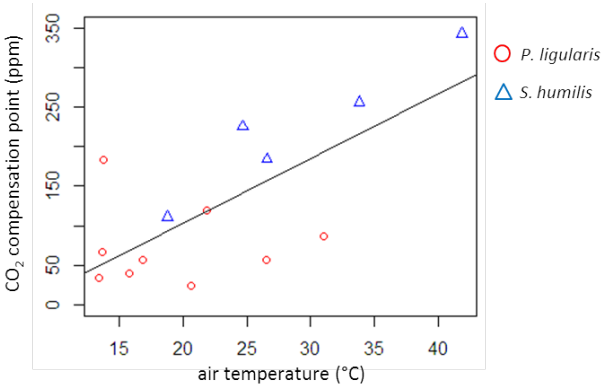

Figure 12. CO_2 compensation points as a function of air temperature and plant species.

The transpiration decreases in general with increasing CO_2 concentration with an approximately linear relation not counting the steps in the curves at about 400 ppm that are due to the settings. Some of the curves show high variations. The increasing photosynthesis rates and the decreasing transpiration rates cause a rise in WUE with increasing CO_2 in a linear relation.

4.2.3 Ambient measurements

4.2.3.1 Photosynthesis

Variations were highest for *S. humilis* under hot conditions. The dependency of photosynthesis on temperature can be seen in Figure 13A.

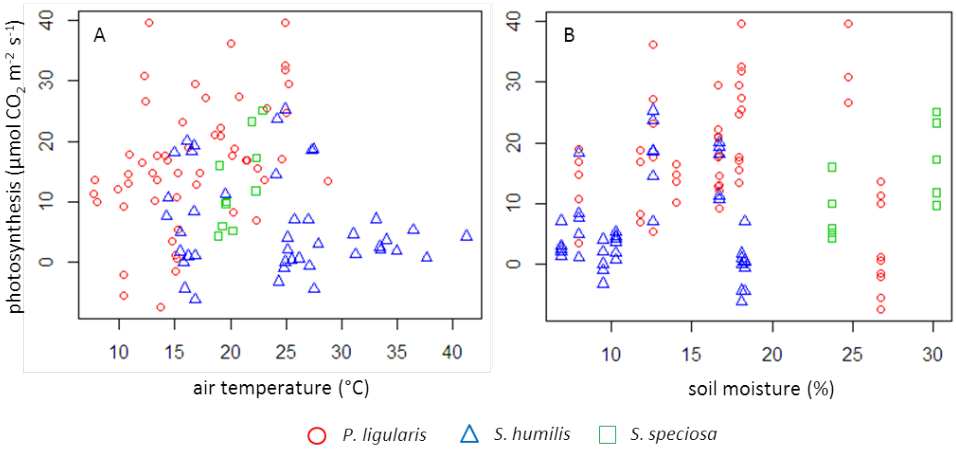

Figure 13. Photosynthesis as a function of A) air temperature and B) soil moisture.

For *P. ligularis* plant processes were measured between 8 and 28 °C. Photosynthesis rates are increasing with temperature from -5 to 40 µmol CO_2 m^{-2} s^{-1}. For *S. humilis* data with temperatures between 14 and 40 °C are available. For this species, no linear relation can be seen. Highest photosynthesis rates at circa 20 µmol CO_2 m^{-2} s^{-1} are measured between 15 and 25 °C but at the same range lower rates between -5 and 10 µmol CO_2 m^{-2} s^{-1} were measured as well. At very high temperatures (30 – 40 °C) little assimilation is happening (0 – 5 µmol CO_2 m^{-2} s^{-1}). The values for *S. speciosa* are all at approximately 20 °C and range between 4 and 25 µmol CO_2 m^{-2} s^{-1}. This species was left out of the analysis since it was only measured at two sites. Since for *S. humilis* no linear relation between photosynthesis and temperature as well as light intensity (not shown) was observed, only the data of *P. ligularis* were used for analysis of the most important explaining variables. The variables in the random forest analysis are ranked from soil moisture, air temperature, light intensity, relative humidity, leaf area to CO_2 concentration. All RF values are high (between 20 and 74), therefore all were used in the initial model. The model with the best BIC is with air temperature only. In the linear regression model it is significant (P = 0.002) (Figure 13A). However, the variations are high (R^2 = 0.166). The other variables as air humidity and CO_2 concentration had no significant effect. Light intensity is positively correlated with photosynthesis (R^2 = 0.164 and P = 0.003) and has a high RF value (RF = 55.6) but didn't stay in the final model after the backward stepwise selection.

Table 7. Explaining variables selected by a random forest (RF) approach to be of importance in predicting photosynthesis of *P. ligularis*.

variable	order		RF value	BIC	Beta	SE	t value	*P*
	importance	removal						
Intercept					28.56	44.16	0.65	0.521
soil moisture	1	a	83.7	264.2				
air temperature	2		56.3		0.82	0.25	3.25	**0.002**
light intensity	3	e	55.6	257.0				
RH (reference air)	4	d	29.2	258.2				
leaf area	5	b	28.0	262.5				
CO_2 concentration	6	c	21.3	260.7				

Notes: Order of importance (1-6) is the ordered importance of variables as given by the RF (random forest). Order of removal (letters a-e) is the order of traits in which the traits were removed in the backward stepwise selection. RF value is the importance score given by the RF for each trait. BIC (Bayesian Information Criterion) values are for the model in the backward stepwise selection before the respective variable was removed. Beta, SE, t value and *P* values (statistical significance given for $P < 0.05$), are for the remaining traits in the linear regression of photosynthesis in the final model (BIC = 156.6, $R^2 = 0.17$).

Soil moisture shows no effect on photosynthesis in the analysis. However, a positive trend for *P. ligularis* can be seen in Figure 13B. Only at the site "cer" the photosynthesis rates are low despite high soil moisture. Soil moisture shows for *S. humilis* a positive effect as well but only when excluding the sites "so6" and "so1" where despite high soil moisture photosynthesis rates were low. Additionally, the course of the day shows influence on photosynthesis (Figure 14A). For *P. ligularis* an optimum of photosynthesis is reached at about 2:30 pm. Very low and even some negative values are measured around noon and 6:30 pm.

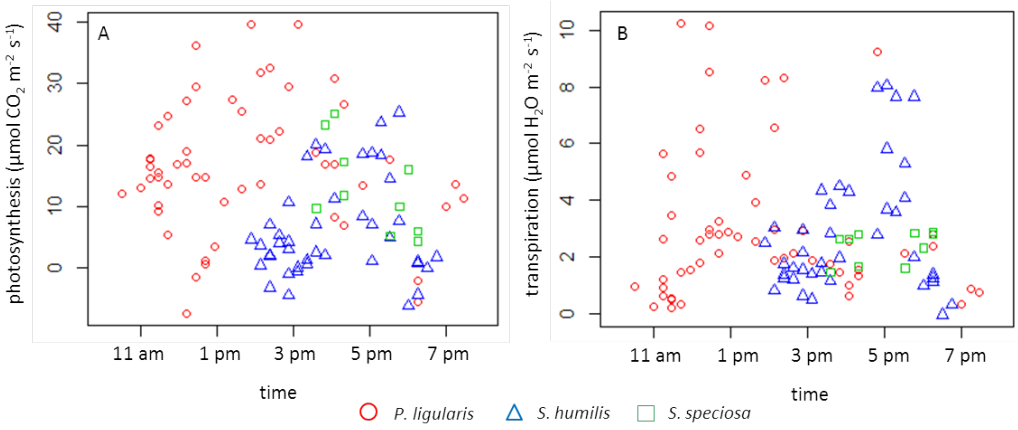

Figure 14. A) Photosynthesis and B) transpiration rates as a function of time.

S. humilis shows difference during the course of the day, too, but shifted to the afternoon with an maximum at about 5 pm and minima at 2:30 pm and 6:30 pm. However, no data before 2:30 pm are available. In addition, there is a trend that photosynthesis rates increase in line with leaf area with 19.0 µmol CO_2 m^{-2} s^{-1}/cm^2. *P. ligularis* (0.74 ± 0.03 cm, SE) has higher leaf area than *S. humilis* (0.41 ± 0.01 cm, SE) and *S. speciosa* (0.55 ± 0.02 cm, SE).

P. ligularis and *S. humilis* were compared by ANOVA in the temperature range where data for both species are available (14 – 29 °C), with the same light intensity setting (500 µmol m^{-2} s^{-1}). Photosynthesis of *P. ligularis* is significantly higher than of *S. humilis* (F value = 11.11 and $P = 0.001$).

4.2.3.2 Transpiration

As for photosynthesis, data for different temperature intervals for the different species are available. *P. ligularis* shows linear correlations with the ambient conditions whereat *S. humilis* shows non-linear relations (Figure 15).

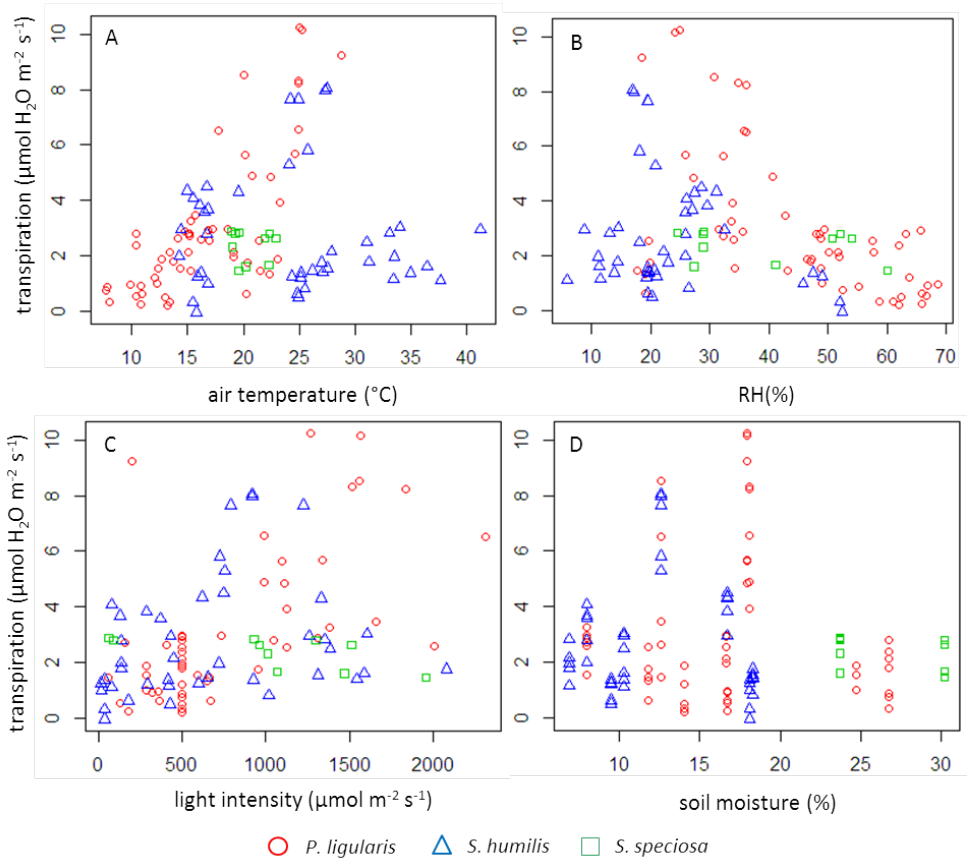

Figure 15. Transpiration rates as a function of A) air temperature, B) Relative humidity (RH), C) light intensity and D) soil moisture.

The transpiration rates of *S. humilis* show a similar pattern for the conditions especially temperature, humidity and light intensity. With intermediate conditions the transpiration is highest and it is decreasing toward extreme values. These conditions are correlated with each other (temperature and RH: $R^2 = 0.65$ and $P < 0.001$; temperature and light intensity, $R^2 = 0.29$ and $P < 0.001$). For instance, highest transpiration for *S. humilis* is observed for temperatures of approximately 25 °C with values up to 8 H_2O m^{-2} s^{-1}. At lower and higher temperatures lower transpiration is observed. At the highest temperatures between 30 °C and 40 °C transpiration rates are between 1 and 3 µmol H_2O m^{-2} s^{-1}. They are at a low level but not at zero. Here, fluctuations and SD, respectively, are very high. Even at

similar conditions the transpiration rates fluctuate for *S. humilis*, e.g. at temperatures of 25 °C and with low air humidity, the transpiration rates are between 0 and 8 µmol H_2O m^{-2} s^{-1}. At high RH the values are low (0 – 2 µmol H_2O m^{-2} s^{-1}).

P. ligularis shows mostly linear correlation with the environmental conditions (Figure 15). The transpiration rates are strongly increasing with increasing temperature with a linear relation from 0 up to 10 H_2O m^{-2} s^{-1}. Since temperature is correlated with air humidity (R^2 = 0.5728), transpiration decreases with increasing humidity. However, the correlation of transpiration is higher for temperature (R^2 = 0.55 and $P < 0.001$) than for humidity (R^2 = 0.30 and $P < 0.001$). There are some data points at low humidity (18 – 20 %) and moderate temperatures (20 °C – 22 °C) at the site "flo" were the transpiration rates are low and differ from the other data. In addition, light intensity shows a positive effect on transpiration (R^2 = 0.40 and $P < 0.001$). Light intensity is also correlated with temperature (R^2 = 0.22 and $P < 0.001$). The random forest analysis revealed that air temperature is most important, subsequently soil moisture, light intensity, air humidity, leaf area and CO_2 concentration. These variables were taken for the initial model. The subsequent stepwise backwards regression revealed temperature, soil moisture and light intensity as best variables for the final model. They all have a positive significant effect on transpiration of *P. ligularis* in the final multiple regression model.

Table 8. Explaining variables selected by a random forest (RF) approach to be of importance in predicting transpiration of *P. ligularis* under ambient conditions.

variable	order		RF value	BIC	Beta	SE	t value	*P*
	importance	removal						
Intercept					-58.7	10.567	-5.55	**< 0.001**
air temperature	1		83.5		0.316	0.044	7.21	**< 0.001**
soil moisture	2		63.2		0.119	0.037	3.26	**0.002**
light intensity	3		48.8		0.002	< 0.001	4.70	**< 0.001**
RH (reference air)	4	a	47.9	61.6				
leaf area	5	c	24.7	54.9				
CO_2 concentration	6	b	16.0	57.7				

Notes: Order of importance (1-6) is the ordered importance of variables as given by the RF (random forest). Order of removal (letters a-c) is the order of traits in which the traits were removed in the backward stepwise selection. RF value is the importance score given by the RF for each trait. BIC (Bayesian Information Criterion) values are for the model in the backward stepwise selection before the respective variable was removed. Beta, SE, t value and *P* values (statistical significance given for $P < 0.05$), are for the remaining traits in the multiple linear regression of transpiration in the final model (BIC = 53.91, R^2 = 0.71).

The transpiration during the course of the day was similar as for photosynthesis (Figure 14B). There is a maximum for *P. ligularis* at 1 pm and for *S. humilis* at 5 pm. The leaf area of the grass leaves was lower for *S. humilis* than for *P. ligularis*. Higher leaf area caused higher rates of transpiration (2.2 µmol H_2O m^{-2} s^{-1}/cm^2). When comparing the two species in the same temperature range (14 – 29 °C) and with the same light intensity (500 µmol m^{-2} s^{-1}) by ANOVA, no differences in transpiration can be seen (F value = 0.97 and P = 0.328).

4.2.3.3 Water use efficiency (WUE)

The similar rates of transpiration and the higher photosynthesis rates of *P. ligularis* compared to *S. humilis* result in a higher WUE of *P. ligularis.* The values for this species are especially high for low temperatures (8 – 15 °C) and high RH above 50 % with values up to 50 µmol CO_2/µmol H_2O (mean 10.9 ± 1.6 µmol CO_2/µmol H_2O, SE). WUE of *S. humilis* is rather constant for the different condition, on average 1.6 µmol ± 0.4 CO_2/µmol H_2O (SE). An ANOVA shows a significant difference for WUE measured in the same temperature range for both species (F value = 9.45 and $P = 0.003$).

4.2.4 Summary of Li-Cor measurements

The light compensation point was not affected by the species (Table 5). However, *S. humilis* showed a higher CO_2 compensation point than *P. ligularis* (Table 6) and in a temperature range between 14 °C and 29 °C similar transpiration rates but lower photosynthetic activity and a lower WUE. Besides the species effect, air temperature was the dominant variable on 1) light compensation point (Table 5), on 2) CO_2 compensation point (Table 6), on 3) photosynthetic activity (Table 7) and on 4) transpiration (Table 8).

4.3 Leaf wax *n*-alkanes identification and quantification

The identified and quantified leaf wax *n*-alkanes are shown in Table 9.

Table 9. Absolute and relative concentrations of *n*-alkanes

***n*-ALK**	***Poa ligularis* (*n*=10)**				***Stipa humilis* (*n*=8)**				***Stipa speciosa* (*n*=3)**			
	µg/g dry leaf	SE	r-conc (%)	SE	µg/g dry leaf	SE	r-conc (%)	SE	µg/g dry leaf	SE	r-conc (%)	SE
n-C_{15}	< 0.1				< 0.1				< 0.1			
n-C_{16}	< 0.1				< 0.1				0.7	0.7	0.1	0.1
n-C_{17}	0.1	0.1	< 0.1	< 0.1	< 0.1				0.7	0.7	0.1	0.1
n-C_{18}	0.2	0.1	0.1	< 0.1	0.3	0.1	< 0.1	< 0.1	1.3	1.0	0.1	0.1
n-C_{19}	0.3	0.1	0.1	< 0.1	0.2	0.1	< 0.1	< 0.1	0.8	0.5	0.1	0.1
n-C_{20}	0.3	0.1	0.1	< 0.1	0.2	0.1	< 0.1	< 0.1	0.8	0.5	0.1	0.1
n-C_{21}	1.8	0.5	0.5	0.2	1.9	0.2	0.1	< 0.1	5.0	1.8	0.4	0.2
n-C_{22}	0.8	0.2	0.2	0.1	0.7	0.1	< 0.1	< 0.1	4.0	2.5	0.3	0.3
n-C_{23}	2.1	0.5	0.6	0.2	4.3	0.5	0.3	< 0.1	10.3	3.6	0.7	0.4
n-C_{24}	1.1	0.2	0.3	0.1	1.4	0.2	0.1	< 0.1	2.0	1.1	0.2	0.1
n-C_{25}	15.4	2.5	3.2	0.4	12.9	5.5	0.6	0.1	16.5	7.4	1.1	0.8
n-C_{26}	1.3	0.2	0.3	0.1	3.0	1.0	0.1	< 0.1	5.4	2.0	0.3	0.1
***n*-C_{27}**	**36.5**	**6.0**	**7.8**	**1.3**	**163.1**	**80.4**	**7.0**	**2.1**	**78.4**	**38.2**	**3.8**	**0.9**
n-C_{28}	5.7	1.0	1.2	0.2	15.4	5.2	0.8	0.1	17.5	8.0	0.9	0.1
***n*-C_{29}**	**306.7**	**74.0**	**52.8**	**5.6**	**720.8**	**126.3**	**38.5**	**2.3**	**702.6**	**448.8**	**28.3**	**4.7**
n-C_{30}	4.2	0.7	0.9	0.1	24.3	4.0	1.3	0.1	32.4	8.2	1.9	0.4
***n*-C_{31}**	**121.8**	**36.6**	**23.9**	**3.7**	**800.9**	**84.7**	**44.7**	**3.1**	**1066.6**	**503.7**	**51.2**	**3.9**
n-C_{32}	2.4	0.7	0.7	0.3	8.4	1.4	0.5	0.1	15.3	1.6	1.1	0.4
***n*-C_{33}**	**35.5**	**13.8**	**7.1**	**1.4**	**108.7**	**16.8**	**6.0**	**0.8**	**167.0**	**48.1**	**9.5**	**1.8**
total	**536.1**	108.1			**1866.5**	288.0			**2127.3**	1053.8		

r-conc = relative concentration of *n*-alkane

The mean values for each grass species are shown with absolute and relative concentrations compared to the total amount including the standard error. Ten study sites with *P. ligularis* were analysed regarding the *n*-alkanes, eight with *S. humilis* and three with *S. Speciosa*. The analysis revealed that the *n*-alkane with the least number of carbon atoms in *P. ligularis* that could be detected is the *n*-C_{17}, in *S. humilis* it is the *n*-C_{18} and in *S. speciosa* the *n*-C_{16}. For all species all *n*-alkanes up to the *n*-C_{33} were abundant, the *n*-C_{29} and *n*-C_{31} were most concentrated besides the *n*-C_{27} and *n*-C_{33}. The other *n*-alkanes between *n*-C_{16} and *n*-C_{33} have much less concentrations whereat the odd *n*-alkanes have in general much higher concentrations than the even *n*-alkanes. The absolute and relative concentrations of these four *n*-alkanes are shown in Figure 16. *P. ligularis* has on average the lowest overall *n*-alkane concentration (536 µg/g leaf dry mass), *S. humilis* has 3.5-times higher concentrations (1867 µg/g leaf dry mass). *S. speciosa* has on average the highest *n*-alkane concentration (2127 µg/g leaf dry mass) but also the highest variations. The sample at "so6" showed extraordinary high *n*-alkane concentrations.

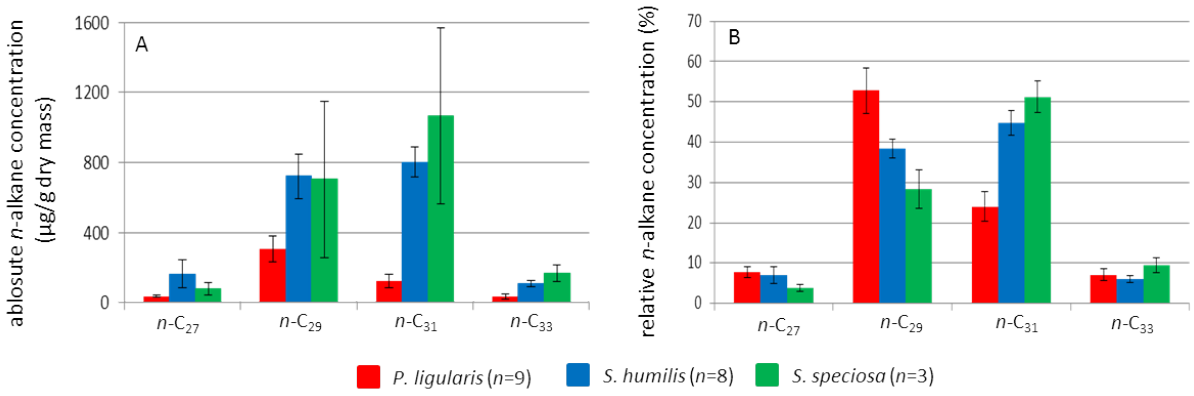

Figure 16. Absolute and relative concentrations of the four most abundant *n*-alkanes in the three studied grass species. Error bars indicate SE.

The most concentrated *n*-alkane of *P. ligularis* is the *n*-C_{29}, followed by *n*-C_{31} and *n*-C_{33}. The leaves of *S. humilis* show similar concentrations of *n*-C_{29} and *n*-C_{31} at high level. The next most concentrated *n*-alkanes are the *n*-C_{27} and the *n*-C_{33}. In *S. spesiosa* leaves the *n*-C31 is highest concentrated, followed by *n*-C_{29}, *n*-C_{33} and *n*-C_{29}. The distribution of the *n*-alkanes is different between the species. In *P. ligularis* the *n*-C_{29} is most abundant whereat in *S. humilis* the *n*-C_{29} and *n*-C_{31} are the *n*-alkanes with the highest concentrations. *S. speciosa* showed the highest concentrations for the *n*-C_{31} *n*-alkane. From *P. ligularis* to *S. humilis* to *S. speciosa* the total *n*-alkane concentrations increase as well as the relative contributions of long-chained *n*-alkanes. The total *n*-alkane concentration was analysed for explaining variables. In a model with the two design variables MAT is significant (P = 0.019) whereat MAP is non-significant (Table 10). A random forest analysis identified species, RH, daily temperature and annual irradiation radiation as most important (appendix, Table A3).

Table 10. Regression model for the total *n*-alkane concentration with design variables.

	Beta	Std. Error	t value	*P*
(Intercept)	-1368.8	1151.4	-1.189	0.250
MAT	199.8	77.5	2.579	**0.019**
MAP	4.4	4.8	0.933	0.363

$R^2 = 0.32$, $P = 0.032$

A stepwise backward selection with BIC with these four variables and the design variables removed MAT (first) and MAP (second) from the model. In the resulting ANCOVA model species is the most significant variable ($p < 0.001$) and explains 45.6 % of the variance. RH and annual irradiation are significant as well ($P = 0.016$, $P = 0.016$) with explaining power of 12.3 % and 12.2 %, respectively (Table 8).

Table 11. Explaining variables selected by a random forest (RF) approach to be of importance in predicting total *n*-alkane concentration.

	order						
variable	importance	removal	RF value	BIC	df	*P*	SS (%)
Species	1		47.6		2	**< 0.001**	45.6
day humidity	2		25.3		1	**0.016**	12.3
day temperature	3		18.9		1	0.105	4.9
annual light intensity	4		11.6		1	**0.016**	12.2
MAT		a		278.6			
MAP		b		276.6			
Residuals					15		24.9

Notes: Order of importance (1-4) is the ordered importance of variables as given by the RF (random forest). Order of removal (letters a-b) is the order of traits in which the traits were removed in the backward stepwise selection. RF value is the importance score given by the RF for each trait. BIC (Bayesian Information Criterion) values are for the model in the backward stepwise selection before the respective variable was removed. *P* values (statistical significance given for $P < 0.05$), degrees of freedom (df) and sum of squares (SS) are for the remaining traits in the ANCOVA of total *n*-alkane concentration in the final model (BIC = 274.7).

Increasing humidity shows a negative effect on the total *n*-alkane concentration. High annual irradiation values lead to elevated concentrations of *n*-alkanes (Figure 17).

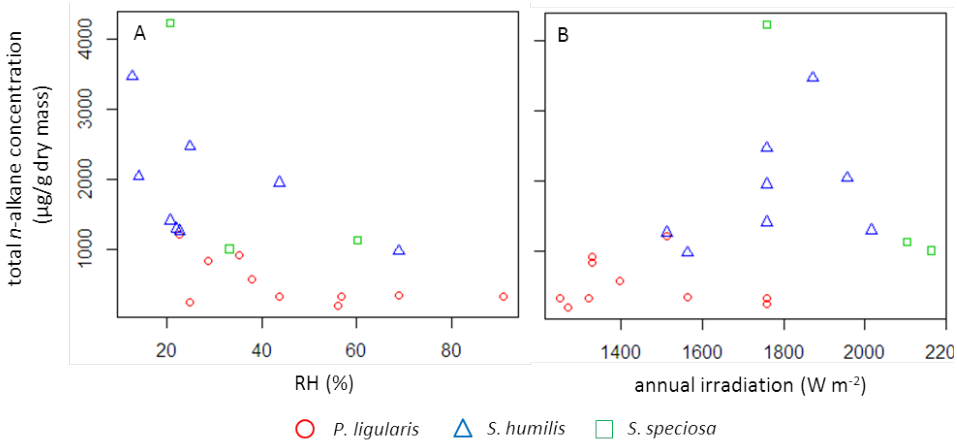

Figure 17. Total *n*-alkane concentration as a function of A) RH and B) annual irradiation.

4.4 Isotopes

4.4.1 Environmental water isotopes

The δD values of river, rain and lake water samples as well as the mean annual precipitation δD values from the 16 study sites as well as their regression line parameters (except for rain water samples) are shown in Figure 18.

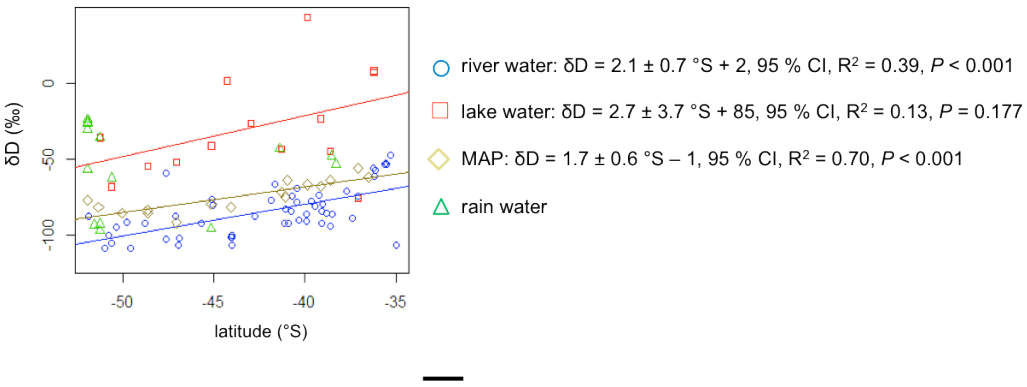

Figure 18. δD values of environmental water samples and MAP of study sites including regression lines, the slopes are given with 95 % confidence interval.

The MAP, river and lake water samples are getting enriched in D with low latitudes. The values of annual precipitation data are increasing with a similar slope but the river water samples have lower δD values (mean -84.1 ‰) than the annual precipitation (mean -74.8 ‰). In the mean they are 9.3 ‰ lower. Highest δD values are observed for the lake water samples (mean -30.6 ‰). Only 14 rain water samples were collected. Some are in the range of river and annual rain water values, but some are higher. The relation between δD and $\delta^{18}O$ values for river, rain and lake water as well as root and leaf water are shown in Figure 19. The black line is the global meteoric water line, a mean of the overall global precipitation.

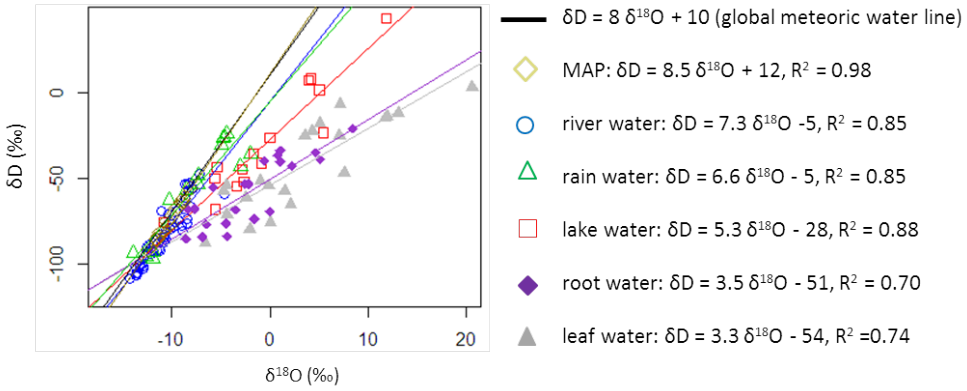

Figure 19. Relation of water δD and $\delta^{18}O$ values from water samples and annual precipitation

This line has a D excess of +10 ‰. The annual precipitation values for the 16 study sites have a bit higher D-excess than the global meteoric water line. River and rain water have lower slopes than the

global meteoric water line. Their slopes are very similar and show the same ^{18}O excess. Towards lake, root and leaf water the ^{18}O excess increases. The absolute D and ^{18}O values are also partially higher for these water samples compared to river and rain water.

4.4.2 δD values of water samples, plant waters and *n*-alkanes

The δD values of average annual precipitation, root water, leaf water and the *n*-alkanes for each study site and sampled species are shown in Table 12. The root water δD values range between -86 and -21 ‰, the leaf water δD values between -88 and +3 ‰, The hydrogen isotopes of the concentration weighted *n*-alkanes are much lighter than the hydrogen isotopes from river, root and leaves (between -258 ‰ and -163 ‰).

Table 12. δD values of average annual precipitation, root water, leaf water and individual *n*-alkanes and concentration weighted average leaf wax *n*-alkane (CWA) δD values of *P. ligularis*, *S. humilis* and *S. speciosa* along the Argentinian transect. SD values are the mean of three replicate measurements.

Species	Latitude (°S)	Site	MAP	root water		leaf water		n-C_{29}		n-C_{31}		CWA
			(‰)	mean (‰)	SD	mean (‰)	SD	mean (‰)	SD	mean (‰)	SD	(‰)
P. ligularis	-51.9	pot	-77	-54	0.0	-58	0.1	-208	2	-204	4	-206
P. ligularis	-51.3	tra	-82	-77	0.0	-71	0.3	-232	7	-223	6	-228
P. ligularis	-50.1	cer	-86	-69	0.9	-55	0.3	-260	3	-253	6	-258
P. ligularis	-48.6	flo	-84	-77	0.2	-80	0.2	-247	1	-232	1	-245
P. ligularis	-48.6	str	-86	-84	0.1	-88	0.1	-249	1	-231	7	-246
P. ligularis	-47.0	hon	-92	-86	0.3	-76	0.2	-247	1	-229	2	-245
P. ligularis	-45.1	esc	-80	-84	0.0	-58	0.0	-233	1	-227	5	-230
S. humilis	-45.1	esc	-80	-74	0.0	-66	0.2	-238	2	-236	2	-237
P. ligularis	-44.1	gps	-82	-68	0.1	-62	0.1	-236	3	-230	2	-234
S. humilis	-44.1	gps	-82	-43	0.4	-55	0.2	-234	2	-223	4	-230
P. ligularis	-41.3	so1	-72	-40	0.0	-25	0.3	-199	3	-186	2	-196
S. humilis	-41.3	so1	-72	-34	0.3	-23	0.3	-203	4	-191	3	-199
P. ligularis	-41.1	jac	-75	-37	0.2	-18	0.0	-183	4	-193	3	-189
S. humilis	-41.1	jac	-75	-54	0.3	-7	0.1	-208	2	-206	0	-207
S. humilis	-41.0	so6	-64	-35	0.1	3	0.1	-178	2	-180	2	-179
S. speciosa	-40.0	so6	-64	-41	0.1	-15	0.1	-167	5	-160	2	-163
S. humilis	-39.9	pie	-67	-39	0.2	-12	1.0	-178	7	-178	3	-178
S. humilis	-39.1	zap	-68	-21	0.2	-14	0.1	-191	1	-195	2	-193
S. humilis	-38.6	laj	-64	-69	0.4	-47	0.7	-210	1	-212	1	-211
S. speciosa	-37.1	but	-56	-68	0.1	-52	0.2	-157	5	-168	5	-165
S. speciosa	-36.5	win	-62	-56	0.3	-26	0.1	-194	1	-194	3	-194

The plant and river water δD values as a function of MAT are shown in Figure 20. Two outliers were removed. This concerns *S. speciosa* at the sites “but” and “win” which are the two northernmost sites. Here, two and five days, respectively, before sampling a rare and heavy rain event occurred. A comparison between measured root water δD values and annual average precipitation δD values shows much smaller differences to the other study sites. Therefore, the isotopic compositions especially of the plant water are not representative for normal conditions. For each site mean values for the plant

δD values were calculated when two species were sampled at one spot, to avoid a higher weight of these sites in the statistical analysis.

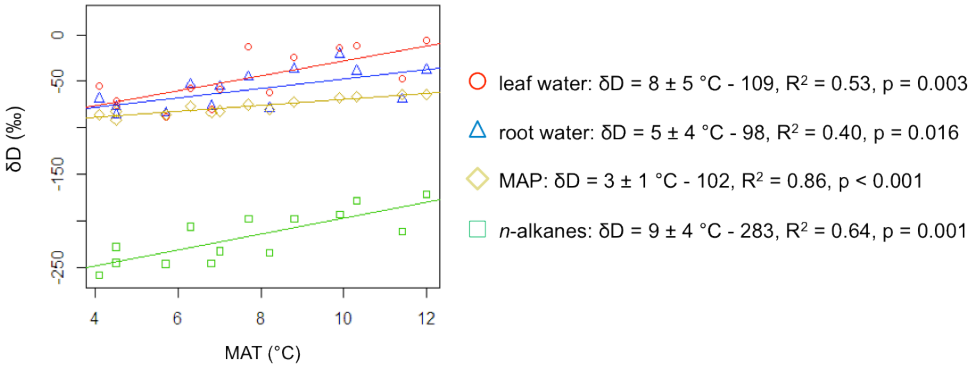

Figure 20. δD values of annual precipitation water, root water, leaf water and *n*-alkanes along a climatic gradient. Mean values for each study site were used, two outliers were removed (*n* = 14). The slopes are given with 95 % confidence interval.

MAT was used for the analysis of plant D/H ratios instead of latitude because it is the design variable. The isotopic water compositions are stronger affected by MAT than by latitude. This is indicated by the higher correlation between MAT and annual precipitation δD values (R^2 = 0.862 and $P < 0.001$) than between MAT and latitude (R^2 = 0.737 and $P < 0.001$). The δD values as a function of MAT including simple linear regression parameters are shown in Figure 20. All δD values are increasing with MAT towards the warmer regions (Figure 20), the annual precipitation δD values increases with a slope of 3 ± 1 ‰/°C (95 % CI). The root water δD values increase with a higher slope (5 ± 4 ‰/°C, 95 % CI). The slope of the leaf water δD values is with 8 ± 5 ‰/°C (95 % CI) higher than the slopes for precipitation water and xylem water δD values. The slope of the regression line of the *n*-alkane δD values against the latitude is highest of all with 9 ± 4 ‰/°C (95 % CI). The confidence intervals of the slopes of leaf water, root water and CWA D/H ratios over MAT are each overlapping indicating no statistical significance. The CI of MAP and leaf water, and MAP and root water, respectively, are overlapping as well. Only the CI of the slopes of MAP and CWA D/H ratios are not overlapping showing statistical significance. The relatively low R squares and the high 95 % CI especially for root and leaf water (Figure 20) point to high variations in the data. Regarding the measured plant D/H ratios, the *n*-alkane δD values have the lowest variation (R^2 = 0.64).

Table 13 shows the linear regression lines of the δD values and fractionations $\varepsilon_{soil/p}$, $\varepsilon_{leaf/soil}$, ε_{ET}, ε_{bio} and ε_{app} as a function of MAT. For analysis and exemplification of the change in D/H ratios and ε values with increasing MAT example values were calculated using the regression lines. In addition, the absolute and relative contributions of soil and leaf water enrichment to the total evaporative enrichment are shown. δD and fractionation values were calculated for the southernmost part of the transect (4 °C) and the northernmost part (12 °C). Furthermore, an average of the data was calculated.

Table 13. Analysis of changes in various δD values and fractionation processes along the MAT gradient and the contributions from soil and leaf water evaporative enrichment to total evaporative enrichment, with example values from the south, the north and the average of the transect. Two outliers were removed (*n* = 14).

	Regression parameters					Exemplification		Average
	Slope (‰/°C)	95 % CI	Intercept	R^2	*P*	MAT 4 °C	MAT 12 °C	MAT 8 °C (with SE)
precipitation δD (‰)	3	1	-102	0.86	<0.001	-89	-63	-77 ± 2
root water δD (‰)	5	4	-98	0.40	0.016	-78	-37	-59 ±6
leaf water δD (‰)	8	5	-109	0.53	0.003	-77	-13	-47 ± 8
CWA δD (‰)	9	4	-283	0.64	0.001	-249	-180	-217 ± 7
$\varepsilon_{soil/p}$ (‰)	2	4	4	0.10	0.296	12	28	19 ± 4
$\varepsilon_{leaf/soil}$ (‰)	3	3	-11	0.33	0.031	1	26	13 ± 4
ε_{ET} (‰)	5	5	-7	0.31	0.037	13	54	32 ± 6
ε_{bio} (‰)	2	3	-194	0.15	0.171	-186	-170	-178 ± 4
ε_{app} (‰)	6	4	-200	0.51	0.004	-185	-148	-152 ± 6
contribution of $\varepsilon_{soil/p}$ to ε_{ET} (%)						90	51	59
contribution of $\varepsilon_{leaf/soil}$ to ε_{ET} (%)						10	48	41

CWA: concentration-weighted n-alkanes, CI: Confidence Interval, SE: Standard error, statistical significance given for $P < 0.05$

The soil water evaporative enrichment as well as leaf water enrichment increases along the MAT gradient with 2 ± 4 ‰ and 3 ± 3‰/°C (95 % CI), respectively. For an increase of MAT from 4 °C to 12 °C this would mean a rise in δD values from -78 ‰ to -37 ‰ for root water and from -77 ‰ to -13 ‰ for leaf water. Hence, at 4 °C MAT leaf water D-enrichment plays a minor role for the *n*-alkane D/H ratios whereat soil water enrichment is almost alone responsible for isotopic enrichment of the *n*-alkanes. However, at 12 °C MAT soil and leaf water enrichment contributes both with circa 50 % to the total evaporative fractionation. ε_{ET} increases with 5 ± 5 ‰/°C (95 % CI) from 13 ‰ to 54 ‰. The net biosynthetic fractionation shows an increase of 2 ± 3 ‰/°C (95 % CI). These enrichment processes result in an increase of apparent fractionation of 6 ± 4 ‰/°C (95 % CI), in the example the *n*-alkane δD values rise from -249 ‰ to -180 ‰. This is a combination effect of the source water δD values, the evaporative D-enrichment and the biosynthetic fractionation.

4.4.3 Soil water enrichment ($\varepsilon_{soil/p}$)

Root water was used as proxy for soil water. However, at the four sites where two species were sampled, differences between them from 5 ‰ to 25 ‰ are observed (Table 12). The relation between precipitation and root water δD values (Figure 21) indicates with a slope of 2 ± 1 (95 % CI) that root or soil water, respectively, is higher D-enriched than the source water δD values and that the fractionation increases with elevated source water δD values. The two outliers were removed for this analysis and mean values for each study site were used after a RF showed that species don't affect soil water evaporative D-enrichment. Another value ("laj") is differing from the other values but this value was not removed because no rain event was observed before sampling and no reason for the fluctuation is known.

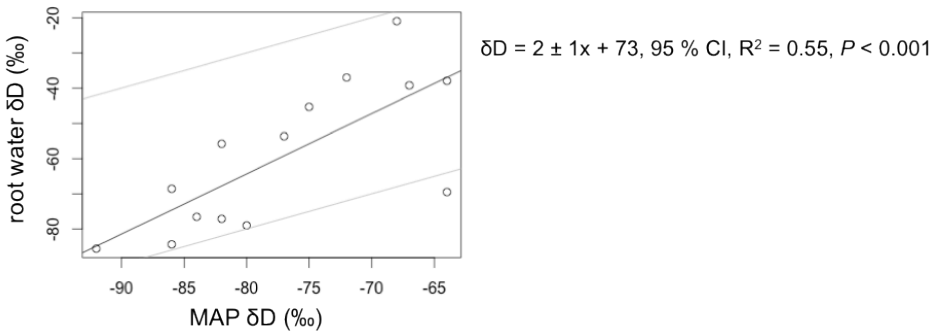

Figure 21. Relation between precipitation δD and root water δD. Grey lines indicate 1:1 lines.

The soil water enrichment fluctuates between -13 ‰ and 50 ‰ with a mean value of 19 ‰. The root water δD values are sometimes very close to the precipitation values but in other cases much higher D-enriched than the precipitation. This can be seen in Figure 20. A statistical analysis regarding influencing parameters has been conducted. The design variables don't affect the soil water enrichment significantly although there is a positive trend for MAT.

Table 14. Regression model for soil water enrichment ($\varepsilon_{soil/p}$) with design variables

	Beta	Std. Error	t value	*P*
(Intercept)	21.22	20.70	1.03	0.321
MAT	2.41	1.71	1.41	0.177
MAP	-0.09	0.09	-0.99	0.339

$R^2 = 0.13$, $P = 0.337$, df = 16

Table 15. Explaining variables selected by a random forest (RF) approach to be of importance in predicting soil water enrichment ($\varepsilon_{soil/p}$)

variable	order		RF value	BIC	Beta	SE	t value	*P*
	importance	removal						
Intercept					-73.40	33.83	-2.17	**0.046**
annual irradiation	1		29.0		0.05	0.02	2.80	**0.013**
day temperature	2	a	15.7	115.3				
daily RH	3		14.3		0.37	0.20	1.87	0.080
daily light intensity	4	c	9.0	110.3				
MAT		b		112.6				
MAP		d		108.6				

Notes: Order of importance (1-4) is the ordered importance of variables as given by the RF (random forest). Order of removal (letters a-d) is the order of traits in which the traits were removed in the backward stepwise selection. RF value is the importance score given by the RF for each trait. BIC (Bayesian Information Criterion) values are for the model in the backward stepwise selection before the respective variable was removed. Beta, SE, t value and *P* values (statistical significance given for $P < 0.05$) are for the intercept and the remaining traits in the multiple linear regression of soil water enrichment in the final model ($R^2 = 0.33$, $P = 0.040$, BIC = 107.5).

A random forest analysis revealed annual light intensity, daily temperature, daily air humidity and light intensity as most important factors (Appendix, Table A3). The backward regression showed that a model with annual irradiation and daily RH is best. In this multiple linear model, only annual radiation is significant. The model explains 33 % of variance and is weakly significant.

4.4.4 Leaf water evaporative enrichment ($\varepsilon_{leaf/root}$)

The leaf water evaporative enrichment has already been shown to increase with MAT in Figure 20. Here, the fractionation between xylem and leaf water was statistically analysed regarding the influencing factors. For the analysis of the impact of environmental parameters mean values for each site were calculated to avoid higher weight of the study sites with two sampled species. A random forest has revealed before that species does not influence $\varepsilon_{leaf/root}$ (not shown). The two outliers at "but" and "win" were not removed in this analysis because the source water D/H ratios were not assumed to affect $\varepsilon_{leaf/root}$, only the absolute δD values of root and leaf water. The linear model with the design variables shows higher significance of MAT than of MAP. $\varepsilon_{leaf/root}$ increases with increasing MAT as well as with increasing MAP, but with a lower slope.

Table 16. Regression model for $\varepsilon_{leaf/root}$ with design variables.

	Beta	Std. Error	t value	*P*
(Intercept)	-36.39	13.45	-2.71	**0.018**
MAT	2.43	0.86	2.84	**0.014**
MAP	0.14	0.06	2.46	**0.029**

$R^2 = 0.56$, $P = 0.005$, df = 13

Different abiotic and biotic parameters measured at the study day as well as annual data were used for a random forest analysis. For the initial model linear model the five highest RF ranked parameters daily light intensity, daily RH, annual irradiation, daily temperature and mean measured photosynthesis rates as well as the design variables (MAT and MAP) were used (Appendix, Table A5). The model after the stepwise backward selection with the best BIC included the variables daily light intensity, annual irradiation, daily temperature and MAP (Table 17, Figure 22).

Table 17. Explaining variables selected by a random forest (RF) approach to be of importance in predicting leaf water enrichment ($\varepsilon_{leaf/root}$).

variable	order		RF value	BIC	Beta	SE	t value	*P*
	importance	removal						
Intercept					-49.26	12.895	-3.82	**0.003**
day light intensity	1		41.1		0.02	0.007	3.33	**0.007**
annual light intensity	2		24.3		0.02	0.007	3.25	**0.008**
day temperature	3		14.6		-1.22	0.501	-2.44	**0.033**
day relative humidity	4	a	12.8	76.8				
measured photosynthesis	5	c	11.2	71.9				
MAT		b		74.3				
MAP					0.11	0.048	2.25	**0.046**

Notes: Order of importance (1-5) is the ordered importance of variables as given by the RF (random forest). Order of removal (letters a-c) is the order of traits in which the traits were removed in the backward stepwise selection. RF value is the importance score given by the RF for each trait. BIC (Bayesian Information Criterion) values are for the model in the backward stepwise selection before the respective variable was removed. Beta, SE, t value and *P* values (statistical significance given for $P < 0.05$) are for the intercept and the remaining traits in the multiple linear regression of leaf water enrichment $\varepsilon_{eaf/root}$ in the final model ($R^2 = 0.80$, $P < 0.001$, BIC = 71.1).

The daily and annual light intensity as well as MAP have positive influence on leaf water enrichment. The day temperature has weak positive correlation with leaf water D-enrichment in a single linear regression (R^2 = 0.25 and P = 0.051). Once daily and annual light intensity and MAP are taken into account in the multiple regression, daily temperature has a negative effect on leaf water enrichment in the model. This is a net suppression effect. All variables are positively correlated with the response variable as well as with each other. Still, one predictor variable has a negative regression coefficient. This means that the daily temperature has more in common with daily light intensity (R^2 = 0.63 and $P < 0.001$) and annual light intensity (R^2 = 0.37 and P = 0.013) than with leaf water. The purpose of day temperature in the model is rather to suppress the error variance in the other predictor variables than explaining leaf water enrichment. The effects of day light intensity, annual light intensity and MAP are presented in Figure 22.

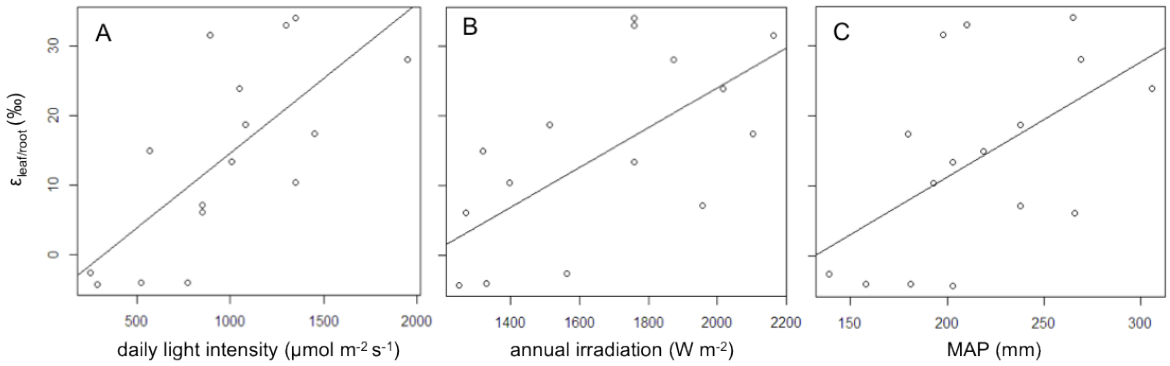

Figure 22. $\varepsilon_{leaf/root}$ as a function of A) daily light intensity, B) annual irradiation and C) MAP.

4.4.5 Biosynthetic fractionation (ε_{bio})

The two *S. speciosa* outliers were removed in this analysis because the rain event lowered the leaf water D/H ratios which are not representative for average annual D/H ratios any more. No mean values for each site were calculated because the effect of species on biosynthetic fractionation was to be investigated. The slope between leaf water δD and CWA δD values is below one (0.8 ± 0.2, 95 % CI) (Figure 23) meaning not the entire isotopic information from leaf water δD values is recorded in the *n*-alkanes 1:1. They are on average higher enriched than the leaf water. The variations are comparatively low (R^2 = 0.75 and $P < 0.001$).

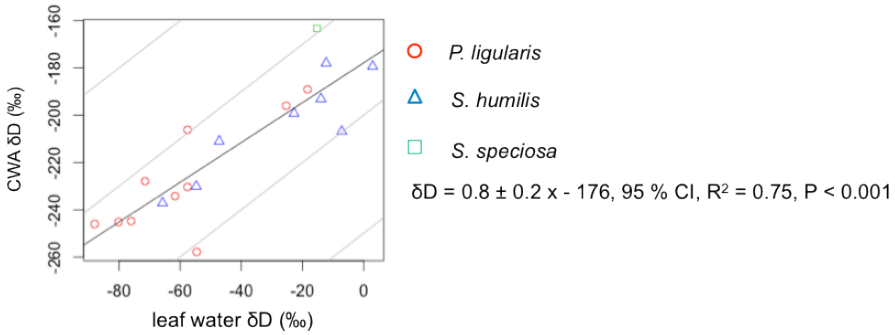

Figure 23. Relation between leaf water δD and leaf wax *n*-alkane δD values. Grey lines indicate 1:1 relations.

The variations in net biosynthetic fractionation (ε_{bio}) were analyzed regarding explaining variables. The model with design variables showed that neither MAT (P = 0.123) nor MAP (P = 0.860) are significant (Table 18).

Table 18. Regression model for ε_{bio} with design variables.

	Beta	Std. Error	t value	*P*
(Intercept)	-194,08	17,07	-11,37	< 0.001
MAT	2,29	1,41	1,63	0.123
MAP	-0,01	0,08	-0,18	0.860

R^2 = 0.15, df = 16

Most random forest values for environmental parameters were below zero meaning they have no importance (Appendix, Table A6). The highest value showed the daily temperature and was analyzed in a stepwise backward selection together with the design variables (Table 19). MAT remained as explaining variable but without significance (P = 0.107).

Table 19. Explaining variables selected by a random forest (RF) approach to be of importance in predicting biosynthetic fractionation (ε_{bio})

variable	order		RF value	BIC	Beta	SE	t value	*P*
	importance	removal						
Intercept					-196.40	10.80	-18.19	< 0.001
daily temperature	1	b	4.6	104.91				
MAT					2.22	1300	1.70	**0.107**
MAP		a		107.6				

Notes: Order of importance (1) is the ordered importance of variables as given by the RF (random forest). Order of removal (letters a – b) is the order of traits in which the traits were removed in the backward stepwise selection. RF value is the importance score given by the RF for each trait. BIC (Bayesian Information Criterion) values are for the model in the backward stepwise selection before the respective variable was removed. Beta, SE, t value and *P* values (statistical significance given for $P < 0.05$) are for the intercept and the remaining traits in the multiple linear regression off biosynthetic fractionation in the final model (R^2 = 0.15, P = 0.107, BIC = 102.3).

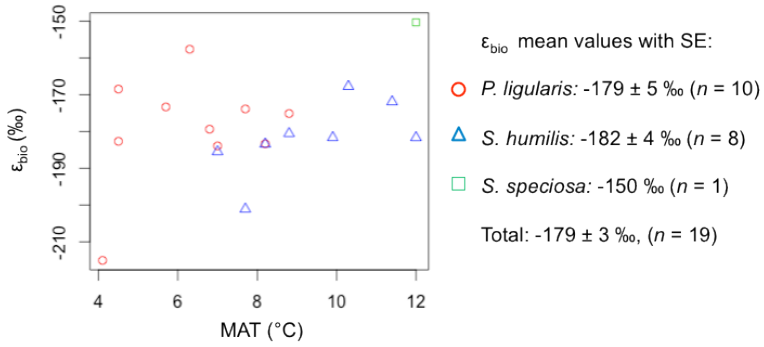

Figure 24. Biosynthetic fractionation as a function of MAT

The biosynthetic fractionation (ε_{bio}) as a function of MAT and different species is shown in Figure 24. The values of *P. ligularis* vary between -158 ‰ and -183 ‰ with one low value at -215 ‰ (mean -179 ± 5 ‰, SE). *S. humilis* shows values between -168 ‰ and -201 ‰ (mean -182 ± 4 ‰, SE). *S. speciosa* shows the highest biosynthetic fractionation -150 ‰ (n = 1). However, the species have no significant effect.

4.4.6 Apparent fractionation (ε_{app})

Here, the apparent fractionation was analyzed with mean values of each spot without outlier removal because the outliers were not assumed to influence the *n*-alkane D/H ratios or ε_{app}. The outliers were only changed in their root water isotopic composition and not in the annual average. The *n*-alkane δD values as a function of precipitation δD values are shown in Figure 25. They are highly correlated ($R^2 = 0.82$ and $P < 0.001$) showing that the *n*-alkane δD values reflect the precipitation δD values.

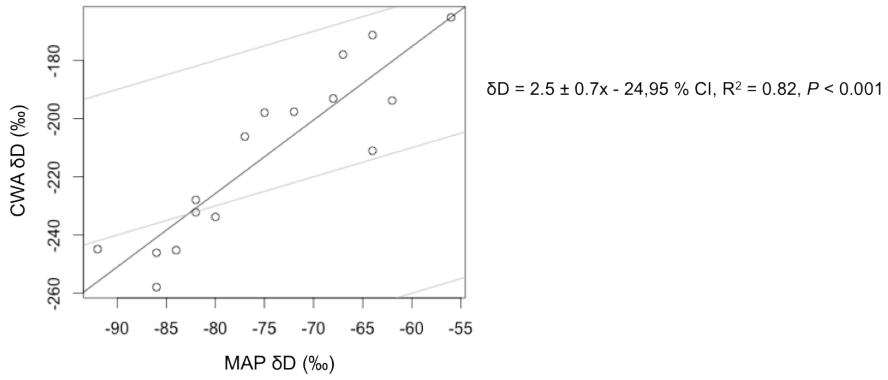

Figure 25. Relation between δD values of annual precipiation and *n*-alkanes. Grey lines indicate 1:1 lines.

The slope of 2.5 ± 0.7 (95 % CI) demonstrates that the *n*-alkane δD values are D-enriched compared to the precipitation. Apart from the source water δD values the influences of climate/weather conditions were analysed. A multiple linear regression with the design variables MAT and MAP reveals that MAT is highly significant and MAP has very little influence (Table 20).

Table 20. Regression model for ε_{app} with design variables

	Beta	Std. Error	t value	*P*
(Intercept)	-207.20	22.64	-9.15	0.000
MAT	5.75	1.44	3.99	0.002
MAP	0.05	0.10	0.50	0.624

$R^2 = 0.570$, $P = 0.004$, df = 13

A random forest analysis shows that annual irradiation, day temperature and daily light intensity have highest importance (Appendix, Table A7). However, after the backward stepwise regression including the design variables only MAT remains as main driver (Table 21). The apparent fractionation as a function of MAT is presented in Figure 26.

Table 21. Explaining variables selected by a random forest (RF) approach to be of importance in predicting apparent fractionation (ε_{app}).

variable	order		RF value	BIC	Beta	SE	t value	*P*
	importance	removal						
Intercept					-197.71	12.15	-16.27	**< 0.001**
annual irradiation	1	c	57.8	94.6				
day temperature	2	d	26.1	92.2				
day light intensity	3	b	11.6	97				
MAT					5.86	1.39	4.23	**0.001**
MAP		a		99.7				

Notes: Order of importance (1-3) is the ordered importance of variables as given by the RF (random forest). Order of removal (letters a-d) is the order of traits in which the traits were removed in the backward stepwise selection. RF value is the importance score given by the RF for each trait. BIC (Bayesian Information Criterion) values are for the model in the backward stepwise selection before the respective variable was removed. Beta, SE, t value and *P* values (statistical significance given for $P < 0.05$) are for the intercept and the remaining traits in the multiple linear regression of leaf water enrichment ε_{eapp} in the final model ($R^2 = 0.56$, $P < 0.001$, BIC = 91.9).

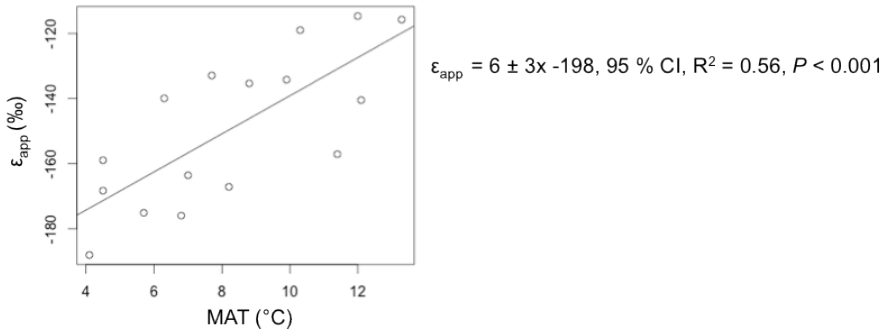

Figure 26. Apparent fractionation (ε_{app}) as a function of MAT.

5 Discussion

5.1 Bulk $\delta^{13}C$ analysis

P. ligularis, *S. humilis* and *S. speciosa* can be identified as C_3 grasses since their $\delta^{13}C$ value are with -26.0, -27.1 and -26.0 ‰ in the typical range of C_3 plants due to the fractionation processes during metabolism. This is accordant to the literature where a lack of C_4 plant in Patagonia is stated (Golluscio et al., 2005). Furthermore, species of the genus *Stipa* and *Poa* have already been identified as C_3 plants (Smith and Brown, 1973). However, not all appearing grass species at the study sites have been sampled and analysed regarding their metabolism. At the northernmost site of the transect ("win") *A. mendozina*, which is a C_4 plant, was observed (Cavagnaro, 1988; Smith and Brown, 1973). It can be concluded that in the biggest part of the transect the dominant grass species are C_3 plants. The climatic conditions are warm and dry but the temperatures and the aridity are not high enough for C_4 plants to have an advantage over the C_3 metabolism and to compete with C_3 plants. Only in the northernmost part where temperatures are highest and least water is available C_4 species become dominant due to their higher WUE (Winkler and Schmidt, 1980).

5.2 Li-Cor measurements

5.2.1 Light response curves

Light is the essential condition for photosynthesis and the light compensation point where respiration and photosynthesis are equally high is an important trait of plants. They can only survive when the light compensation point can be exceeded and thus a net carbon gain by photosynthesis is achieved. The linear part of the curve at low light quantity is in the photochemical area. Photosynthesis is limited by quantum flux density. The saturation range of the curve is in a biochemical area. Here, photosynthesis depends on the performance of CO_2 assimilation which is limited by enzyme activity, CO_2 uptake, number and aperture of stomata and temperature. Temperature rises increase the light compensation point because respiration is increasing as well and more CO_2 has to be fixed before a net carbon gain happens (Lüttge et al., 2010). This strong temperature effect was also found in the measured light response curves. Light compensation points were increasing from about zero to 150 µmol m^{-2} s^{-1} from 9 to 35 °C (Figure 9). Saturation was observed for most but not for all light response curves meaning the plants still had free capacities. They are adapted to the hot environment and are able to use very high light intensities that could not have been used by other plants such as shadow plants (Lüttge et al., 2012).

In general, transpiration enhances as well when light intensity increases because the stomata are opening. This was shown by all light curves. The highest light intensity in the response curves was 2500 µmol m^{-2} s^{-1}. Highest possible natural values under full sunshine are between 1500 and 1800 µmol m^{-2} s^{-1}. Light had a strong positive effect on transpiration whereat even with light

intensities above the natural maximum no saturation or maximum of transpiration was observed. This effect can be important for the leaf water evaporative D-enrichment. Besides RH and temperature as key drivers for transpiration the light might contribute to the isotopic fractionation with a similar extend.

A decrease of transpiration in the beginning of the curves was observed what has not been observed in other studies (Agata et al., 1985; Habermann et al., 2003; Welander and Ottoson, 1999). The Li-Cor method might have had influence on this effect. Stomata close rapidly in the dark but the opening takes longer, sometimes up to 60 minutes (Willmer and Fricker, 1996). The stomata might not have had enough time to open again after the closing in the dark.

The WUE of *P. ligularis* and *S. humilis* at highest light intensity was dependent on temperature. Both transpiration and photosynthesis increased with higher temperatures but the photosynthesis more compared to transpiration, resulting in a decreasing WUE. The high absolute amounts of photosynthesis and transpiration indicate that soil moisture was sufficient for plant activity even with low measured soil moisture values. The plants can use the soil water efficiently. *S. humilis* showed very low rates of photosynthesis and transpiration at highest light intensity even at moderate temperatures (about 25 °C) where *P. ligularis* was still far more active. The optimum of activity seems to be lower for *S. humilis* whereat it is less efficient than *P. ligularis* at these temperatures. Very arid conditions are generally adverse for plants and only less activity and productivity is possible due to the high energy needed for respiration (Fernández et al., 1991).

5.2.2 CO_2 response curves

The net photosynthesis increased with elevated CO_2 concentrations whereat transpiration losses decreased with high CO_2 concentrations. The increase of photosynthesis rates due to higher CO_2 concentrations is a well-known effect since it is a precursor of the net photosynthetic reaction (Lüttge et al., 2012). Furthermore, the effect of lowered transpiration has been shown in different studies (e.g. Dugas et al., 2001; Lewis et al., 2002; Pospíšilová and Čatský, 1999; Wullschleger et al., 2002). High CO_2 concentrations cause narrowing of stomata and thus reduction of stomatal conductance and transpiration. With less gas exchange more CO_2 is available for photosynthesis and WUE rises. The bend in the photosynthesis and transpiration – CO_2 response curves is due to the settings. It was started with CO_2 concentrations of 400 ppm decreasing to 50 ppm and then going back directly to 400 ppm before increasing to over 2000 ppm. The time for the stomata to adjust to the new conditions after the step back to 400 ppm was too low (1-3 minutes).

The atmospheric CO_2 is increasing since over 150 years, from 270 ppm to currently around 394 ppm in 2013 (Dlugokencky and Tans, NOAA/ESRL). Only slight changes happen in the short-term, in Argentina values between 380 and 390 ppm were measured. However, the CO_2 concentrations are known to fluctuate during the history of earth (Royer, 2005). It has been shown that elevated CO_2

concentrations lead to a higher WUE and thus to lower transpiration rates. This, in turn, might lead to a decrease in leaf water evaporative enrichment and a change in apparent fractionation. Hence, when interpreting paleoclimate records such as sediments one has to take into consideration the CO_2 conditions at the time the *n*-alkanes were produced. More CO_2 might have led to less transpiration and a higher ε_{app} meaning lighter leaf wax *n*-alkane δD values. The effect has to be quantified.

In the same way temperature is known to increase the light compensation point, it is known to increase the CO_2 compensation point since the respiration raises are higher compared to the raise in assimilation. CO_2 compensation points of C_3 plants are usually in a range between 40 and 100 ppm at 25 °C (Lüttge et al., 2012). Approximately half of the CO_2 compensation points were in this range. Higher values were due to temperatures above 25 °C. The CO_2 compensation point analysis showed in addition that *S. humilis* had higher CO_2 compensation points than *P. ligularis*, independent from the temperature effect. This points to a higher general metabolic efficiency of *P. ligularis*, as result of more beneficial conditions at lower MAT. The hot temperatures in the region where *S. humilis* grows are less favourable. Hence, not only the current temperature matters but also long-term adaptions.

5.2.3 Ambient measurements

The ambient measurements revealed some differences between the species and between the environmental effects on photosynthesis and transpiration. For *S. humilis* an optimum at approximately 25 °C was observed which is in a typical range of optimal temperature for sun plants (between 20 and 30 °C). Photosynthesis minimum lies between -2 and 0 °C and the maximum between 40 and 50 °C. Above the optimum denaturation of enzymes starts or losses via transpiration get too high and at lower temperatures kinetic energy limits processes (Lüttge et al., 2010; Rosenberg et al., 1983). However, in the same temperature range the photosynthesis and transpiration rates of *S. humilis* varied a lot. Hence, the temperature optimum changes according to the conditions. Apart from temperature many other factors control biological optima. For instance, when not enough water in the soil is available, even optimal temperatures can't enhance assimilation processes. Other drivers are irradiation, RH or nutrient availability, amongst others (Rosenberg et al., 1983). At temperatures above 30 °C *S. humilis* lowered its photosynthesis and transpiration rates to a minimum compared to better conditions. This species is adapted to conditions with low soil moisture and air humidity and high temperatures. Under these conditions like at the sites "est" and "zap", high transpiration water losses are avoided without closing the stomata completely. Small rates of transpiration as well as a positive net photosynthesis can be maintained. At these sites the measured soil moisture was low. Hence, even little available soil water can be used by the plants. *P. ligularis* showed linear correlation up to the highest temperatures of about 25 – 30 °C. Most likely the optimum is reached approximately in this range since temperature optima for C_3 plants are usually not higher than 30 °C (Lüttge and Kluge, 2012). The statistical analysis of *P. ligularis* showed that temperature is the main driver of transpiration, even more than RH. Temperature affects transpiration in different ways. It decreases RH

because warm air can hold more water than cold air and the vapour pressure deficit between leaf surface and air increases. Warm air supplies energy to the surface and the temperature gradient between air and surface, respectively, which increases ET. Additionally, at higher temperatures less energy is required to evaporate warm water than cool water and the stomatal openings increase with temperature (Rosenberg et al., 1983). Photosynthesis had only temperature as main driver in the statistical analysis but with little explaining power. It depends on temperature according to the van't Hoff rule that the velocity of chemical reaction increases twofold or more with each 10 °C rise in temperature. RH can have an indirect effect via stomatal closure at low RH which causes less gas exchange and photosynthesis. This effect could not be observed, likely because the stomata of *P. ligularis* were at all conditions open. At every site positive transpiration was measured and thus, always enough CO_2 could enter the leaves for assimilation. A light effect could be seen but it was not part of the best explaining model. Temperature was correlated with light intensity and thus overlying the light effect. Photosynthesis rates of *P. ligularis* showed on average an increase with soil moisture except for the site "cer". Hence, there is possibly an effect of soil moisture and only "cer" is an exception because other unfavourable conditions lead to low plant activity. This positive effect could be seen for *S. speciosa* and *S. humilis* as well. Just at the site "so6" and "so1" the photosynthesis of *S. humilis* was low despite high soil moisture. Both *P. ligularis* and *S. humilis* have been measured between 14 and 30 °C with a constant light intensity. In this range the absolute transpiration rates were not significantly different but then photosynthesis was significantly higher for *P. ligularis,* which results in a higher WUE compared to *S. humilis.* This shows that *P. ligularis* is in general a higher efficient plant. For the same assimilation rates less water passage through the plant is required. More water has to be transpired. This is accordant to the finding that *S. humilis* has higher CO_2 compensation points than *P. ligularis*.

A lot of variation remained in the statistical models that could not be explained by the daily conditions. Photosynthesis and transpiration depend on many other factors that have not been investigated such as leaf water pressure/turgor, leaf orientation, internal diffusive resistance or availability of nutrients as potassium, nitrogen or phosphorous (Rosenberg et al., 1983). Since the measurements were done in a closed chamber wind could not be taken into consideration either. In addition, the plant age was not known. The age can have effects on plant activity because young plants have in general faster stomatal reactions and larger apertures whereas the responses of older leaves become more sluggish and aperture maxima become smaller (Willmer and Fricker, 1996). In the statistics disregarded was also the effect of daytime. The data showed a dependency on the daytime that indicates different adaptions of *S. humilis* and *P. ligularis*. There was a minimum of photosynthesis and transpiration at 2:30 pm and a maximum at 5 pm for *S. humilis*. No data for the morning are available. However, it is possible that there was another maximum in the morning and the stomata were only closed at the hottest time of the day which is a typical behaviour of plants growing in hot and arid regions (Rosenberg et al., 1983; Wang et al., 2013). *P. ligularis* showed a shifted

maximum that was at 2:30 pm and thus earlier than for *S. humilis*. Transpiration and photosynthesis were lower in the morning and afternoon/evening without a depression in the middle of the day. Hence, *P. ligularis* does not need to drop activity at the hottest time of the day to reduce water losses at least not at temperatures below 30 °C. The time of the day explains, therefore, also a part of the variation but could not be included in the model because it is not a linear relation. Other influencing parameters are the plant size and leaf width. Both taller plants and broader leaves transpire in general more due to the higher surface (Rosenberg et al., 1983). The increase in transpiration is linked to an increase in photosynthesis. A trend of rising photosynthesis and transpiration caused by increasing leaf areas was observed for all available data with all species. However, the statistics were only done for *P. ligularis*. Since this species showed only small differences in their leaf area, this effect was less important than the environmental parameters and not significant in the analysis. Uncertainties in all Li-Cor measurements could have been derived due to small leaf areas of the grass leaves that were mostly below 1 cm^2 in total. The Li-Cor leaf chamber is intended for leaf areas up to 6 cm^2 and small leaf surfaces can lead to higher variations and lower precision and accuracy, respectively.

5.2.4 Summary of Li-Cor measurements

In general it has been shown that the environmental/weather conditions have higher impact on transpiration than on photosynthesis indicated by higher correlations and slopes for transpiration. Especially temperature, RH and light intensity had higher influence on transpiration than on photosynthesis. This results in a worse WUE at higher temperatures. With increasing temperature and light intensity as it is the case in low latitude regions of the transect plants transpire more amounts of water whereat assimilation increases to a smaller extend. Therefore, life forms and plant morphologies change along climatic gradients. *P. ligularis* as study species in the colder part of the transect is a plant that has longer and broader leaves than *S. humilis* in the warmer part. *S. humilis* has shorter and smaller leaves und produces in general less biomass. Due to the higher temperatures it needs to respire more and it uses possibly more energy for transpiration protection measures. The aboveground net primary production is according to Paruelo et al. (1998a) highest between 4 and 5.5 °C and decreases with higher MAT. This can be linked to WUE of *P. ligularis* which was particularly high at low temperatures.

Regarding to transpiration and the isotopic leaf water composition, temperature was identified as the main driver. The effect of RH was inferior to the temperature effect. Besides temperature, soil moisture and light intensity had a positive effect on transpiration. At a specific latitude, the light intensity is constant in the annual average. Hence, the isotopic signal in sediments of one lake does not reflect different light intensities through the time. However, when comparing different locations around the world with similar MAT and RH, respectively, but with different latitudes, light could be a factor that changes the apparent fractionation due to different leaf water evaporative D-enrichment.

5.3 Leaf wax *n*-alkanes identification and quantification

The long-chain *n*-alkanes are typical components of terrestrial plants. They are part of the leaf wax and have amongst others the function as protector against transpiration through the cuticle (Eglinton and Hamilton, 1967). Since different plant species and organisms grow under different climatic conditions their *n*-alkane absolute and relative concentrations are adapted to the climate. *P. ligularis*, which grows in the colder part of the transect has the lowest *n*-alkane absolute concentration of all investigated grass species. This species does not need higher protection against transpiration. *S. humilis* need more transpiration protection due to higher temperatures and has accordingly higher *n*-alkane absolute concentration. *S. speciosa*, the species found in the northern part of the transect has on average the highest values but also the highest variations. The total *n*-alkane concentration is mainly affected by species but apart from that environmental conditions control the production of leaf wax as well. The statistical analysis showed that the grasses had high amounts of *n*-alkanes at sites with low air humidity (Table 11). The humidity was measured at the respective study day in March or April. However, it can be assumed that the daily values are at least partially representative for the whole year. An indication for that is the correlation of the measured humidity with the mean annual temperature ($R^2 = 0.14$ and $P = 0.147$) and latitude ($R^2 = 0.25$ and $P = 0.046$). The high variations are caused by the current weather conditions at the study day. Low humidity in arid regions causes in general higher transpiration which is adverse for the plants due to the high water losses through the cuticle. Hence, plants adapt by developing transpiration protection mechanisms. One is the leaf wax which consists amongst others of *n*-alkanes with different chain lengths. More carbon atoms in the compound are supposed to provide higher protection (Eglinton and Hamilton, 1967). Therefore, plants under water stress produce better protecting leaf waxes with higher *n*-alkane concentrations. In this connection, the purpose of leaf wax is mainly to avoid water losses through the cuticle. The stomatal aperture is independent from that. The same principle applies for the radiation. Higher light intensity means higher transpiration through the cuticle and the plants need higher protection against it. In the model with the design variables MAT is significant. In the final model with the best BIC it is not significant any more, but humidity and annual irradiation are. These are indirect effects of the temperature and explain the *n*-alkane concentrations better than temperature itself. Since the precipitation rates along the transect are not differing too much they don't have significant influence on the total *n*-alkane concentration. The partly high variations of *n*-alkanes within one species are probably caused by varying climate and weather and possibly different availabilities of resources. The weather within the time when a plant started growing does not necessarily reflect the annual averages over decades. The conditions that a plant during life time experiences are important. High concentrations of *n*-alkanes are particularly produced when the plant is under water stress (McWhorter, 1993). The investigated plants have been shown to have a positive net photosynthesis under all found condition, even when it was hot and dry and soil moisture was low. This indicates that they are well adapted and unwanted transpiration losses are small. Variations within species could also

be explained with missing nutrients such as phosphorous or nitrogen. The grazing management in Argentina with a lot of sheep and other livestock caused a decrease in grass cover, an increase in shrub cover and a change in species distribution which has adverse effects on soil properties and nutrients (Soriano et al., 1983). The nutrient availability might be different at the different study sites which can cause different production rates of leaf waxes.

The high concentrations of *S. speciosa* at "so6" could be due to local weather. It is possible that here no or only little rain fell during the last years so the plants had to react and produce more *n*-alkanes. The plants at "but" and "win" might have been growing since the rain event but didn't synthesize *n*-alkanes because there was no need due to the missing drought stress. When plants grow and produce biomass but no *n*-alkanes the concentrations per g dry leaf sink.

Because the quantification was conducted with single measurements only the precision of the GC-FID cannot be estimated. Therefore some of the variance is probably caused by the missing replicate measurements. In addition, the concentrations were determined with an internal standard (n-C_{36}) whereat it was assumed that the percentage loss of the internal standard and the *n*-alkanes in the sample were equally. However, they have different chain-lengths and properties as solubility in different solvents and the loss might have been different for different *n*-alkanes.

5.4 Isotopes

5.4.1 Environmental water isotopes

The precipitation δD values decreased with higher latitudes. This is an effect of decreasing temperature that causes more condensation and depletion in δD and $\delta^{18}O$ (Clark and Fritz, 1998). The river water δD values were on average lower than the annual precipitation δD values. Both were increasing with a similar slope over latitude. This suggests that the river water does not consist of the local precipitation δD values. Instead, the river water came mostly from western direction where the Andes are located and the altitude effect causes depletion in heavy isotopes. The lake water δD values were much higher D-enriched compared to river or precipitation water due to evaporation from the lake surface. This enrichment increased as latitude and MAT increased. The rain water sample δD values were on average higher than the annual average. This is partly a seasonal effect, the δD values are in March higher than the annual average (Bowen et al., 2005).

The annual precipitation water line of δD and $\delta^{18}O$ is very close to the global meteoric water line with a slight D excess (**Figure 19**). River and precipitation water show similar ^{18}O excess and lake water a strong excess ^{18}O. D and ^{18}O are fractionated in a similar way but with slight differences. Rainout is an equilibrium process but evaporation is a kinetic process (non-equilibrium) which is stronger for ^{18}O than for D and causes excess ^{18}O (Clark and Fritz, 1998). This effect induced the high excess ^{18}O of lake water compared to precipitation and river water.

The ^{18}O excess of root and leaf water was higher compared to the lake water meaning they were higher influenced by evaporation. The direct source of root water is precipitation water from soil that is evaporative D and ^{18}O enriched, whereat lakes gain water from groundwater aquifers, too, which is less affected by ET. The variations of the $\delta D/\delta^{18}O$ lines are highest for root and leaf water indicating that the extend of evaporation effect varied the most. Some samples reflect more the source water and some were more affected by ET and show higher excess ^{18}O, e.g. because of fluctuating time durations of the soil water from precipitation event to sampling and different climate.

5.4.2 δD values of water samples, plant waters and *n*-alkanes

All measured plant δD values and the annual precipitation δD values increased significantly with MAT (Figure 20). The two northernmost sites "but" and "win", where *S. speciosa* was sampled were removed from the analysis because the root and leaf water showed extremely light isotopic composition compared to the other sites, due to a strong rain event prior to the sampling. At the site "laj" the difference between precipitation water and root water of *S. humilis* is also very small but this site was kept in the data because no rain event was observed. When analysing specific *n*-alkanes from lake sediments it is not known from which species it is derived. Probably it is a mix of several species. Only the chain-length of the *n*-alkane can tell from which group of organisms the *n*-alkanes are derived, e.g. algae, higher aquatic plants or higher terrestrial plants. Therefore, it is important to regard several plant species at once. For this reason, mean values for each site has been used when two species were analysed. Anyhow, no significant differences in $\varepsilon_{leaf/root}$ and transpiration rates among the species have been observed. The annual precipitation D/H ratios are stable values with little variations along the gradient ($R^2 = 0.86$ and $P < 0.001$). The *n*-alkane D/H ratios show a bit higher variations ($R^2 = 0.64$ and $P < 0.001$). Since the perennial grasses in Argentina can grow during the whole year the *n*-alkanes reflect probably an average leaf water isotopic composition. The variations were higher for leaf water ($R^2 = 0.53$ and $P < 0.001$) and highest for root water ($R^2 = 0.40$ and $P < 0.001$) because these D/H ratios are much more controlled by the daily conditions than the *n*-alkanes are. Nevertheless, these data are used as proxies for an annual average and for an estimation of absolute and relative amounts of different fractionation processes. It can be assumed that the variations are moderate. The sampling took place in March and April, in autumn and the end of summer, respectively, where weather conditions are rather moderate and without extreme values. Better estimates were not possible.

The δD values of precipitation are relatively constant over the year at one location and depend on different global, regional and local atmospheric streams and processes (Clark and Fritz, 1998). During uptake of soil water by plant roots no fractionation occurs. Therefore, the δD values of root water are used as proxy for soil water. The values are higher compared to the MAP δD values, probably caused by soil evaporation. The annual precipitation δD values increase with circa 3 ± 1 ‰/°C (95 % CI) and the root δD values increased with circa 5 ± 4 ‰/°C (95 % CI). Hence, the average difference between

precipitation regression line and root water regression line increased over the transect, meaning rises in MAT lead to higher soil evaporation which is in line with the literature (e.g. Rosenberg et al., 1983). In total, $\varepsilon_{root/p}$ increased with 2 ± 4 ‰/°C (95 % CI). However, the effect is statistically not significant due to the overlapping CI which are caused by the high fluctuations in the data.

The water is taken up by roots and transported through the leaves until it transpires through the stomata. This process is also known to cause an enrichment of heavy isotopes. The data show that in average the δD values of the leaf water are higher than the δD values of the root water. As a function of MAT they also have a higher slope (8 ± 5 ‰/°C, 95 % CI) than root water δD values (5 ± 4‰/°C, 95 % CI) which implies that leaf water enrichment increases with increasing MAT, supporting the hypothesis that leaf water D-enrichment by transpiration is temperature dependent. $\varepsilon_{leaf/root}$ increased with 3 ± 3 ‰/°C (95 % CI) and thus has a larger magnitude than $\varepsilon_{root/p}$. MAT affects leaf water enrichment more than soil water D-enrichment. However, statistical significance is not given either. The δD values of the leaf water can be found in the δD values of the *n*-alkanes since their slope is similar with circa 9 ± 4 ‰/°C (95 % CI). It can be concluded that *n*-alkanes are synthesized when temperatures are high and the leaf water is D-enriched. The *n*-alkanes are known to be synthetized especially under water stress (McWhorter, 1993). The slightly higher slope of n-alkane D/H ratios compared to leaf water D/H ratios implies that the biological fractionation is slightly increasing with MAT (2 ± 3 ‰/°C, 95 % CI). However, this increase is not significant and might be an effect of the high variations in leaf water δD values.

The *n*-alkanes record highly D-enriched leaf water compared to the precipitation (Figure 20). The slope of the *n*-alkane D/H ratios is with 9 ± 4 ‰/°C MAT (95 % CI) significantly higher than the precipitation D/H ratios (3 ± 1 ‰/°C, 95 % CI). This demonstrates significance in the evaporative D-enrichment although the CI of the slopes of MAP, root and leaf water δD values are overlapping and don't show directly significance. The goal in paleoclimatic reconstructions is the calculation of meteoric water D/H ratios, based on the leaf wax n-alkane D/H ratios by means of the apparent fractionation. The *n*-alkane δD values and ε_{app}, respectively, are controlled by the δD values of the biosynthetic water pool and the biosynthetic fractionation. The biosynthetic water pool is affected by the source water (precipitation water) as well as by the D-enrichment caused by soil and leaf water evapotranspiration. Since $\varepsilon_{leaf/root}$ and $\varepsilon_{root/p}$ were differently affected by MAT, their contribution to ε_{ET} and the biosynthetic water pool, respectively, change over the transect. At 4 °C MAT ε_{ET} is 14 ‰ with a $\varepsilon_{root/p}$ contribution of approximately 90 %, at 12 °C MAT ε_{ET} is 54 ‰ with a $\varepsilon_{root/p}$ contribution of approximately 50 %, caused by the higher slope of $\varepsilon_{leaf/root}$ compared to $\varepsilon_{root/p}$. In combination with the slightly increasing ε_{bio} an increase in ε_{app} of circa 6 ± 4 ‰/°C MAT (95 % CI) is the result. The individual fractionation processes are discussed in the subsequent chapters.

5.4.3 Soil water evaporative D-enrichment ($\varepsilon_{soil/p}$)

The root water was assumed to be representative for the soil water because during water uptake by roots is not known to cause an isotopic fractionation. However, different plants take up water from different soil depths. In the soil, there is an isotopic gradient because water at the surface is usually more exposed to evaporation. This is because the solar irradiation reaches mainly the soil surface and provides energy for the evaporation. Furthermore, the water vapor pressures are higher in the atmospheric air than in the soil air, and wind befits the evacuation of soil moisture. Solar energy is the main engine of soil evaporation but increasing temperatures have influence as well since they reduce the relative water vapor pressure (Blume, 2010). When precipitation is missing for a longer time, first water evaporates from a free water surface without shade. When this water is gone, water or vapour will move through the soil to the surface depending on hydraulic properties (Rosenberg et al., 1983). This causes higher D-enrichment in the soil surface compared to deeper soil depths (Kahmen et al., 2012b). It is known that grasses mainly take up superficial water whereat shrubs use water from deeper soil (Schulze et al., 1996). Hence, *n*-alkanes in sediments synthesized by different plant life forms can reflect different extends of soil evaporative D-enrichment. At many study sites both grasses and shrubs appeared together. The root length of the study plants has not been determined. However, at four study sites where samples from two species have been taken no species-specific pattern and even high fluctuations could be seen. One source of variation could be the root sampling. During sampling and before storing the roots air tight they are exposed to the air and an evaporative D-enrichment might have happened. In addition, conditions such as soil moisture and shade can vary on a small scale.

Two study sites were removed in this analysis due to a heavy rain event some days before sampling. In this semi-arid region such strong precipitation events are very rare. Therefore, the conditions at the study day were not representative for average annual conditions at all. The rainwater filled up the water store of the soil and changed the isotopic compositions a lot. The removed sites showed that the root water D/H ratios were very similar to the annual precipitation D/H ratios. This means that the roots are able to take up fresh rain water as soon as it becomes available. The root δD value was low even five days after sampling. When enough water is available the evaporation has a constant rate. Only when the water store has fallen below a certain level ET decreases linearly. This happens when precipitation is missing for a longer time (Rosenberg et al., 1983). These two or five days before sampling, respectively, were not enough to empty the fresh water storage via for soil evaporation and cause D-enrichment. One other site in the warmer part of the gradient showed a root water δD value close to the precipitation value. In this case, no rain event in the days before sampling was observed and no weather data are available. There might have been a precipitation event that was just not observed by us. The relation between precipitation δD and root water δD demonstrated with a slope of 1.8 that the root water has heavier isotopes than the precipitation. This enrichment increased with MAT although it was not significant. In the model, annual irradiation and daily humidity were the

main drivers for $\varepsilon_{soil/p}$ (Table 15). Light intensity is strongly correlated with latitude and increases soil evaporation by the energy input. Low humidity affects soil water evaporation since it raises the water vapor difference between soil pores and atmosphere. Another indication for increasing soil water evaporation is the soil moisture which was decreasing with MAT and day temperature, respectively, with constant MAP. Only at some sites in the north soil moisture was high due to the rain event before measuring. In addition, bare soil surfaces are higher affected by evaporation (Blume, 2010). Towards higher MAT the vegetation cover decreased and more and more bare soil surface was exposed to the atmosphere which increases evaporation. Sandy soil as found at most sites of the transect are highly exposed to evaporation. However, sand has a higher albedo than dark soils or vegetation, meaning that more solar radiation is reflected and less energy is available for evaporation (Blume, 2010).

5.4.4 Leaf water evaporative D-enrichment ($\varepsilon_{leaf/root}$)

Both design variables MAT and MAP were significant in the initial model. Leaf water D-enrichment depends on daily conditions but they reflect the annual conditions. For instance, the measured temperature on the study day was correlated with MAT. The raise in $\varepsilon_{leaf/root}$ with MAT is accordant to the hypothesis that higher temperatures cause higher transpiration and thus higher D-enrichment (Table 17). The positive impact of MAP can be explained with the on average higher amount of available water that can be used for the water passage through the plant. Only when water is available rising temperatures cause higher ET. The analysis of further explaining parameters revealed that the leaf water enrichment in heavy isotopes was primary influenced by the average light intensity on the sampling day. This daily parameter had more impact than all other daily and annual variables. The annual light intensity had the second highest importance. MAT was not part of the final model. It is correlated with other parameters, especially annual radiation which explains more of the variance than MAT. Hence, the results show in general that for the leaf water D-enrichment light is more important than temperature. Light intensity is known to be an important driver for transpiration. The measurements for *P. ligularis* demonstrated as well that light increased the transpiration although temperature was a more important parameter at ambient conditions. Here it has to be regarded that these measurements had circa 25 °C as highest temperature whereat samples were taken up to 36 °C. At this hot conditions *S. humilis* showed that the stomata are only little open and only little water is released. Hence, the transpiration – temperature relation is an optimum curve. The light curves showed that transpiration increases continuously with light intensity. When stomata are closed even with high light intensity as observed for *S. humilis.* This is due to the high temperatures and low humidity, respectively, not to the light. Furthermore, light intensity showed higher relative fluctuations than temperature. From the lowest to the highest light intensities was a factor of over 7, for temperature is was only a factor of 3. For these reasons the high impact of light intensity can be explained. Leaf water evaporative D-enrichment was observed for *S. humilis* at days where the temperatures were very high in the afternoon and only little transpiration was measured. However, the measurements were not representative for the entire day and days before. At other times of the day, e.g. in the morning and in

the evening when temperatures are lower the plants transpire much more. Here it can be concluded that the extend of $\varepsilon_{leaf/root}$ cannot be linked to the average measured transpiration rates. There was only a slight, non-significant trend that with higher mean transpiration rates the leaf water was higher enriched in heavy isotopes. The leaf water enrichment depends on various conditions of the whole day and probably the days before but the single "point-in-time" measurements don't reflect the transpiration rates of the entire day. The transpiration measurements followed a typical daily course but not for every time of the day data were available, thus the present data are thus not representative for the entire day. The sites where the *S. speciosa* took up fresh rainwater, the low precipitation δD values are reflected in the leaf water δD values immediately since $\varepsilon_{leaf/root}$ values are not higher compared to the other sites. They are relatively depleted in D just as the root water. The fresh water was used for transpiration during the days after the rain and got D-enriched. In addition, at these sites a large opening of the leaves was observed which provides a larger leaf surface. This demonstrates that the leaf water δD values are dependent on a small time scale. No species effect could be detected regarding $\varepsilon_{leaf/root.}$ The transpiration measurements between *P. ligularis* and *S. humilis* didn't show differences in transpiration rates either when comparing them under the same light and temperature conditions. The morphological and anatomical adaptions of *S. humilis* to heat like the small and short leaves and the high *n*-alkane concentrations, seem to protect mainly against transpiration thought the cuticle whereat the stomatal aperture is similar for the different species. Some the $\varepsilon_{leaf/root}$ values are negative, meaning a higher root water δD value than leaf water, which occurred at study sites were temperatures were low and transpiration didn't happen a lot. This could be due to unwanted evaporation of root water during sampling. The leaves were less affected by this because the leaf sampling was faster. Spatial variations in the leaf water isotope composition are another potential source of variation (Kahmen et al., 2012b; Sachse et al., 2006). In general there is an isotopic enrichment from the base to the tip and from the center to the edges of the leaf (Helliker & Ehleringer, 2002; Ogée et al., 2007). Furthermore, mature parts of the leaves are more exposed to the atmosphere and evaporative D-enrichment than leaves covered by the sheath of the next oldest leaf (Kahmen et al., 2012a). The samples were a mixture of different leaves of the tussock which minimizes a spatial effect but still some variation remains due to the sampling. Some plants were also protected by the shadow of shrubs.

5.4.5 Biosynthetic fractionation (ε_{bio})

The statistical analysis could not proof that environmental factors have effects on the biosynthetic fractionation (Table 19). However, the influence of MAT is at the border to statistical significance ($P = 0.107$) with a positive effect (Figure 24). The environmental influences on the biosynthetic fractionation are not well studied until now. However, no direct effects of temperature have been reported before. The *n*-alkanes are produced via several steps. The involved biosynthetic and $NADP^+$-reducing enzymes that cause fractionations are not temperature-controlled (Kahmen et al., 2012b, Sachse et al., 2012). The slight effect in this study needs further investigations.

The biosynthetic fractionation is considered to be constant for one species (Sessions, 2006). However, the values of the investigated species showed high variations. It can be assumed that the average *n*-alkane δD values reflect average annual δD values of the biosynthetic water pool because these grass species can grow during the entire year. Leaf water on the other hand is changing much faster than the *n*-alkanes due to high flow of water through the plants from roots to stomata. Already on the daily scale the isotopic composition of the leaf water can change a lot, as transpiration changes much depending on the weather. The leaf water δD values are derived from sampling at one day of the year. Therefore, it can be assumed that the measured leaf water isotopic composition is not representative for an annual average. Hence, the high variations in the calculated biosynthetic fractionations are most likely caused by the leaf water δD variations and are not a sign for varying biosynthetic fractionation within one species.

The mean values for *P. ligularis* (-179 ‰) and *S. humilis* (-182 ‰) and the value for *S. speciosa* (-150 ‰) lie in a typical range of biosynthetic fractionation of terrestrial plants (between -130 and -200 ‰) (Kahmen et al., 2012b). It is known that the biosynthetic fractionation can vary among species especially for species of different life forms (Sachse et al., 2012). The three studied grass species were not significantly differing in their biosynthetic fractionation. This is likely due to the fact that the species were all C_3 grasses with the same photosynthetic pathway and the same life form. Reasons for different ε_{bio} among species are for instance different leaf anatomies and morphologies and differential contributions from NADPH sources to hydrogen during biosynthesis (Kahmen et al., 2012b). The reasons for varying net biosynthetic fractionations are not well studied until now. Environmental influences have not been shown before but not many studies have been conducted either. Hence, the controlling factors of the variability of ε_{bio} within and among species must be studied in the future for better interpretation of *n*-alkanes e.g. found in lake sediments. If there is a systematic shift of ε_{bio} for different species along climatic gradients, the δD values of *n*-alkanes in plants and sedimentary record can be affected systematically. However, if *n*-alkanes with one specific carbon number are produced with different biosynthetic fractionations by different life forms, e.g. by monocotyledonous and dicotyledonous plants, the interpretation of sedimentary *n*-alkane data are complicated. Information of vegetation that grew at the respective time to reconstruct climate are important. Without knowing the plant life forms and the correct biosynthetic fractionation, reconstructions for the δD values cannot be made with high accuracy.

5.4.6 Apparent fractionation (ε_{app})

The leaf wax n-alkane D/H ratios reflect the precipitation D/H ratios which has also been shown before in other studies all over the earth (Sachse et al., 2012). The investigated species don't affect ε_{app} because they belong to the same life form. Therefore, they have the same *n*-alkane synthesis mechanism and a comparable biosynthetic fractionation and morphology, which leads to similar transpiration rates and similar leaf water evaporative D-enrichment. In addition, they have comparable

rooting depths and take up water that is similarly evaporative D-enriched. For none of these processes a species effect was detected leading to no species effect on ε_{app}. Missing differences in ε_{app} within one life form make reconstructions of precipitation D/H ratios easier due to less fluctuation. This is particularly true for semi-arid regions as southern Patagonia where C_3 grasses are the dominating life form and no other plants with different morphologies and metabolisms are contributing to the sedimentary record. However, often other life forms grow in the respective area and contribute to lake sediments as it was the case in northern Patagonia and the Monte where both grasses and shrubs were dominating. Here, the apparent fractionation of all plants has to be taken into account when one is to estimate an overall average ε_{app} or to reconstruct precipitation D/H ratios with the aid of lake sediments. The effect of temperature on ε_{app} is assumed to be higher in arid than in humid regions because temperature enhances ET more strongly when RH is lower (Kahmen et al., 2012b; Rosenberg et al., 1983). The finding of this study can be used for the interpretation of sedimentary records of arid regions. Temperature was the main driver of the apparent fractionation. It increased with about 6 ± 3 ‰ (95 % CI) per degree Celsius MAT (Figure 26). A rise from 4 °C to 12 °C MAT as found in Argentina would cause *n*-alkane D/H ratios that differ by 48 ‰. Thus, MAT has been shown to be a key driver of ε_{app}. Compared with studies that investigated a RH gradient at the same temperature MAT is a stronger influencing factor than solely RH. Hou et al. (2008) found a mere ~7 ‰ increase of ε_{app} at a change of RH from 80 % to 40 %. For the Argentinian transect no annual RH data were available but the daily RH values ranged between 12 % and 92 %. Assuming a linear effect of RH this would mean a change of ε_{app} by only ~14 ‰ if along the transect only the RH had changed and not temperature.

Globally, the *n*-alkane D/H ratios are strongly correlated with precipitation D/H ratios. The global monocot average of ε_{app} (calculated with $\delta D_{n\text{-}C29}$) is -149 ± 28 ‰ (Sachse et al., 2012). Usually the *n*-C_{29} is used for global integrations of sedimentary records. In this study a mean of *n*-C_{29} and *n*-C_{31} was used but the values of both *n*-alkanes were mostly not varying a lot. Here, the average ε_{app} is -149 ± 6 ‰. Hence, the results of this study fit well to the global general view. This classifies the semi-arid Argentinian transect into an intermediate area between humid and arid regions.

The relative importance of plant physiological and climatic factors on ε_{app} is still not well-studied and paleoclimatic reconstructions are linked with high uncertainties. Nevertheless, sedimentary *n*-alkanes are continuously established as paleoclimate proxies. For instance, Schefuss et al. (2005) and Tierney et al. (2008) made reconstructions in Africa. With an increasing number of studies that focus on environmental effects the interpretation of lake sediment *n*-alkanes will be gradually improved leading to more and more reliable reconstruction.

6 Conclusions and Outlook

The findings revealed that temperature is an important driver of transpiration and evaporative D-enrichment of soil and leaf water whereat RH had lower impact than temperature. Hence, differences of RH gradients that are derived by either changing MAP or changing MAT, respectively, cannot be directly compared. At the same RH conditions, the effects on total evaporative fractionation processes are most likely larger for higher temperatures. Light intensity was identified as another main driver of evaporative D-enrichments and thus ε_{app}. The focus in most of the other studies that investigated the variability of ε_{app} lies on RH. With an irradiation term the interspecies variability that still cannot be explained could be reduced. In addition, irradiation could be an explaining variable for locations at different latitudes since the differences in light intensity are in this case especially high.

ε_{app} of grasses was clearly affected by both soil water evaporative D-enrichment and leaf water evaporative D-enriched whereat the rising temperatures enhance $\varepsilon_{leaf/root}$ stronger than $\varepsilon_{root/P}$. ε_{ET} increased with about 5 ‰/°C MAT. The initial hypothesis that the leaf water evaporative D-enrichment increases with higher MAT can be accepted. Additionally, the assumption that *n*-alkane D/H ratios reflect leaf water D/H ratios can be confirmed. The findings are accordant to average global apparent fractionations which show a high correlation of *n*-alkane D/H ratios and the average precipitation D/H ratios. In this arid setting the apparent fractionation between leaf wax *n*-alkane δD values and precipitation δD values of C_3 plants was increasing with ~6 ‰/°C MAT. This result can support the interpretation of sedimentary records in order to reconstruct ancient precipitation δD values in semi-arid regions.

The root and leaf water δD values were gained from single "point in time" measurements and are subjected to daily fluctuation und are thus not representing an annual average. In order to acquire more reliable annual mean values it would be reasonable to sample at several times during the year. Additionally a Craig-Gordon model could be applied to estimate a mean isotope composition of leaf water and to compare it with the measured values. More accurate and precise conclusions could be made respective the relative and absolute contributions of leaf water evaporative D-enrichment to the apparent fractionation. The measurements of plant activity demonstrated that the investigated plants in the semi-arid region transpired higher amounts of water under conditions with higher temperatures and higher irradiation. However, the performed measurements have been only "point-in-time" as well. They could not be linked directly to the leaf water evaporative D-enrichment. For further insights into the transpiration behaviour of plants in arid and semi-arid settings more measurements during the course of the day and the year have to be done with constant environmental conditions, preferably in a greenhouse experiment as well as in a field experiment.

Three different C_3 grasses in semi-arid Argentina showed similar transpiration rates and $\varepsilon_{leaf/root}$. A weak indication of positive temperature effect on biosynthetic fractionation was observed. This has to be tested with more replicate samples and with controlled environmental conditions. Other plant life forms, especially shrubs, were dominant vegetation in the most arid part of the area, also contributing to sedimentary records. The influence of the temperature gradient on $\varepsilon_{leaf/root}$, $\varepsilon_{root/P}$ and ε_{bio} of other plant-forms should be investigated. In addition, the leaf wax *n*-alkane D/H ratios should be compared with lake sedimentary records of the same setting to research to what extend the *n*-alkane D/H ratios can be correlated in the youngest sediment layer.

Acknowledgement

Foremost, I would like to express my gratitude to my supervisors Prof. Gerd Gleixner and Valerie Schwab for enabling this special project including the fascinating field trip to Argentina. Their guidance and knowledge helped me during the entire progress of the thesis. I could not have imagined having better supervisors and a better Master's project. It has been a pleasure to work at Max-Planck-Institute for Biogeochemistry in Jena.

I would also like to acknowledge the second referee of this thesis, Prof. Kai Totsche.

Furthermore, I would like to thank all members of the Department of Biogeochemical Processes at the MPI who helped me with the conducting of field and lab work and data analysis. My sincere thanks goes to Heike Geilmann for performing the analysis of water and carbon isotopes, to Waldemar Ziegler for introducing me to the work with the Li-Cor, to Steffen Rühlow, Roman Witt and Andrej Thiele for their support with the GC, and to Markus Lange for the help with the statistical analysis.

Last, I would like to thank my family and my friends. I'm very grateful to have such dear and supportive persons in my life. I know I can rely on them any time.

7 References

Armas, C., Pugnaire, F. I., and Sala, O. E. (2008). Patch structure dynamics and mechanisms of cyclical succession in a Patagonian steppe (Argentina). *Journal of Arid Environments, 72*, 1552-1561.

Agata, W., Hakoyama, S. and Kawamitsu, Y. (1995). Influence of light intensity, temperature and humidity on photosynthesis and transpiration of Sasa nipponica and Arundinaria pygmaea. *The Botanical magazine*, *98*, 125-135.

Bisigato, A. J., Villagra, P. E., Ares, J. O. and Rossi, B. E. (2009). Vegetation heterogeneity in Monte Desert ecosystems: A multi-scale approach linking patterns and processes. *Journal of Arid Environments, 73*, 182-191.

Blume, H.-P., Brümmer, G. W., Horn, R., Kandeler, E., Kögel-Knabner, I., Kretzschmar, R., Stahr, K., Wilke, B.-M., Thiele-Bruhn, S., Welp, G. (2010). Scheffer/Schachtschabel. - Lehrbuch der Bodenkunde (16th ed.). Heidelberg: Spektrum Akademischer Verlag. pp. 240-241.

Bowen, G. J. (2014). The Online Isotopes in Precipitation Calculator, version 2.2. http://www.waterisotopes.org, retrieved: 12/01/2014

Bowen, G. J. and Revenaugh, J. (2003). Interpolating the isotopic composition of modern meteoric precipitation. *Water Resources Research,* 39, 1299.

Bowen, G. J., Wassenaar, L. I. and Hobson, K. A. (2005). Global application of stable hydrogen and oxygen isotopes to wildlife forensics. *Oecologia,* 143, 337-348.

Burnham, K. P. and Anderson, D. R. (2002). Model selection and multimodel inference. A practical information-theoretic approach (2nd ed.). New York: Springer. pp. 6-7, 271.

Cavagnaro, J.B. (1988). Distribution of C_3 and C_4 grasses at different altitudes in a temperate arid region of Argentina. *Oecologia 76*, 273–277.

Cialdella, A. M. (2012). Subfamilia Pooideae. Tribu Stipeae. In F. O. Zuloaga, Z. E. Rúgolo and A. M. Anton (Eds.), *Flora Argentina / flora vascular de la república Argentina ; Vol. 3. Tomo II Monocotyledoneae. Poaceae: Pooideae* (pp. 372-496). Cordoba: Graficamente Ediciones.

Clark, I. D. and Fritz, P. (1998): *Environmental Isotopes in hydrogeology*. Boca Raton: CRC Press/Lewis Publishers, pp. 21-31,64-77,119-123.

Coupland, R. T. (1992). Overview of South American Grasslands. In R. T. Coupland (Ed.), *Ecosystems of the world. Vol. 8A. Natural Grasslands. Introduction and Western Hemisphere*. Amsterdam: Elsevier.

Couso, L. L. and Fernández, R. J. (2012). Phenotypic plasticity as an index of drought tolerance in three Patagonian steppe grasses. *Annals of Botany, 110*, 849-857.

Dawson, T. E. (2007). *Stable isotopes as indicators of ecological change*. Academic Press: Amsterdam. p. xvii

Dawson, T. E. and Siegwolf, R. T. W. (2007). Using Stable Isotopes as Indicators, Tracers, and Recorders of Ecological Change: Some Context and Background. In T. E. Dawson and R. T. W. Siegwolf (Eds.), *Stable isotopes as indicators of ecological change*. Amsterdam: Academic Press.

Dlugokencky, E. and Tans, P. (2014). *Trends in Atmospheric Carbon Dioxide*. NOAA/ESRL (www.esrl.noaa.gov/gmd/ccgg/trends/), retrieved: 03/02/2014

Dugas, W. A., Polley, H. W., Mayeux, H. S. and Johnson, H. B. (2001). Acclimation of whole-plant *Acacia farnesiana* transpiration to carbon dioxide concentration. *Tree Physiology, 21*, 771-773.

Eglinton, G. and Hamilton, R. J. (1967). Leaf Epicuticular Waxes. *Science, 156*, 1322-1335.

Evenari, M. (1985a). The Desert Environment. In M. Evenari, I. Noy-Meir and D. W. Goodall (Eds.), *Ecosystems of the world. Vol. 12A. Hot deserts and arid shrublands* (pp. 1-22). Amsterdam: Elsevier.

Evenari, M. (1985b). Adaptations of Plants and Animals to the Desert Environment. In M. Evenari, I. Noy-Meir and D. W. Goodall (Eds.), *Ecosystems of the world. Vol. 12A. Hot deserts and arid shrublands* (pp. 79-92). Amsterdam: Elsevier.

Fernández, R. J., Sala, O. E. and Golluscio, R. A. (1991). Woody and herbaceous aboveground production of a Patagonian steppe. *Journal of Range Management, 44*, 434-437.

Fernández, O. A. and Busso, C. A. (1999). *Arid and semi-arid rangelands: two thirds of Argentina*: Agricultural Research Institute.

Fernández, M. E., Gyenge, J. E., Dalla Salda, G. and Schlichter, T. M. (2002). Silvopastoral systems in northwestern Patagonia I: growth and photosynthesis of *Stipa speciosa* under different levels of *Pinus ponderosa* cover. *Agroforestry Systems, 55*, 27-35.

Ficken, K. J., Li, B., Swain, D. L. and Eglinton, G. (2000). An *n*-alkane proxy for the sedimentary input of submerged/floating freshwater aquatic macrophytes. *Organic Geochemistry, 31*, 745-749.

Gates, M. G. (1973). Plants I. Plant Temperatures and Energy Budget. In H. Precht, J. Christophersen, H. Hensel & W. Larcher (Eds.), *Temperature and life.* Berlin: Springer. pp. 87-101.

Gehre, M., Geilmann, H., Richter, J., Werner, R. A. and Brand, W.A. (2004). Continuous flow ^{2}H-/^{1}H and ^{18}O/^{16}O analysis of water samples with dual inlet precision. *Rapid Communications in Mass Spectrometry*, *18*, 2650–2660.

Gleixner, G., and Mügler, I. (2007). Compounds-Specific Hydrogen Isotope Ratios of Biomarkers: Tracing Climatic Changes in the Past. In T. E. Dawson and R. T. W. Siegwolf (Eds.), *Stable Isotopes as Indicators of Ecological Change* (pp. 249-265). Amsterdam: Academic Press.

Golluscio, R. A., Oesterheld, M., and Aguiar, M. R. (2005). Relationship between phenology and life form: a test with 25 Patagonian species. *Ecography, 28*, 273-282.

Guevara, J. C., Grunwaldt, E. G., Estevez, O. R., Bisigato, A. J., Blanco, L. J., Biurrun, F. N., et al. (2009). Range and livestock production in the Monte Desert, Argentina. *Journal of Arid Environments, 73*, 228-237.

Habermann, G., Machado, E. C., Rodrigues, J. o .D. and Medina, C. L. z. (2003). CO_2 assimilation, photosynthetic light response curves, and water relations of "Pera" sweet orange plants infected with Xylella fastidiosa. *Brazilian Journal of Plant Physiology 15*, 79-87.

Helliker, B. R., and Ehleringer, J. R. (2002). Grass Blades as Tree Rings: Environmentally Induced Changes in the Oxygen Isotope Ratio of Cellulose along the Length of Grass Blades. *New Phytologist, 155*, 417-424.

Hijmans, R. J., Cameron, S. E., Parra, J. L., Jones, P. G. and Jarvis, A. (2005). Very high resolution interpolated climate surfaces for global land areas. *International Journal of Climatology* 25: 1965-1978.

Hoefs, J. (2009). *Stable isotope geochemistry* (6th ed.). Berlin: Springer. pp. 1,52,62,90-98.

Hou, J., D'Andrea, W. J. and Huang, Y. (2008). Can sedimentary leaf waxes record D/H ratios of continental precipitation? Field, model, and experimental assessments. *Geochimica et Cosmochimica Acta, 72*, 3503-3517.

Hunt, J. M. (1996). *Petroleum Geochemistry and Geology* (2nd ed.). New York: W H Freeman.

Jobbágy, E. G., Paruelo, J. M. and León, R. J. C. (1996). Vegetation Heterogeneity and Diversity in Flat and Mountain Landscapes of Patagonia (Argentina). *Journal of Vegetation Science, 7*, 599-608.

Kahmen, A., Schefuss, E. and Sachse, D. (2012a). Leaf water deuterium enrichment shapes leaf wax n-alkane delta D values of angiosperm plants I: Experimental evidence and mechanistic insights. *Geochimica Et Cosmochimica Acta, 111*, 39-49.

Kahmen, A., Hoffmann, B., Schefuss, E., Arndt, S. K., Cernusak, L. A., West, J. B., et al. (2012b). Leaf water deuterium enrichment shapes leaf wax n-alkane delta D values of angiosperm plants II: Observational evidence and global implications. *Geochimica Et Cosmochimica Acta, 111*, 50-63.

Klich, M., Brevedan, R. and Villamil, S. (1997). *Leaf anatomy and ultrastructure of Poa ligularis after defoliation and water stress.* Paper presented at the Proceedings of the 18th International Grassland Congress.

Labraga, J. C. and Villalba, R. (2009). Climate in the Monte Desert: Past trends, present conditions, and future projections. *Journal of Arid Environments, 73*, 154-163.

Lewis, J. D., Lucash, M., Olszyk, D. M., and Tingey, D. T. (2002). Stomatal responses of Douglas-fir seedlings to elevated carbon dioxide and temperature during the third and fourth years of exposure. *Plant, Cell & Environment, 25*, 1411-1421.

Liaw, A. and Wiener, M. (2002). Classification and Regression by randomForest. R News 2, 18-22.

Lüttge, U., and Kluge, M. (2012). Botanik. *Die einführende Biologie der Pflanzen* (6th ed). Weinheim: Wiley-VCH, p. 744-751.

Mares, M. A., Morello, J., and Goldstein, G. (1985). The Monte Desert and other Subtropical Semi-arid Biomes of Argentina, with Comments on their Relation to North American Arid Areas. In M. Evenari, I. Noy-Meir and D. W. Goodall (Eds.), *Ecosystems of the world. Vol. 12A. Hot deserts and arid shrublands* (pp. 203-238). Amsterdam: Elsevier.

McInerney, F. A., Helliker, B. R., and Freeman, K. H. (2011). Hydrogen isotope ratios of leaf wax *n*-alkanes in grasses are insensitive to transpiration. *Geochimica Et Cosmochimica Acta, 75*, 541-554.

McWhorter, C. G. (1993). Epicuticular wax on Johnsongrass (*Sorghum-halepense*) Leaves. *Weed Science, 41*, 475-482.

Mook, W. G. (2006). *Introduction to isotope hydrology stable and radioactive isotopes of hydrogen, oxygen and carbon*. London: Taylor & Francis. pp. 1-8.

Moreno, L., and Bertiller, M. B. (2012). Variation of morphological and chemical traits of perennial grasses in arid ecosystems. Are these patterns influenced by the relative abundance of shrubs? *Acta Oecologica-International Journal of Ecology, 41*, 39-45.

Nobel, P. S. (1991). *Physicochemical and environmental plant physiology*. San Diego: Academic Press, p. 455.

Noy-Meir, I. (1985). Desert Ecosystem Structure and Function. In M. Evenari, I. Noy-Meir & D. W. Goodall (Eds.), *Ecosystems of the world. Vol. 12A. Hot deserts and arid shrublands* (pp. 93-103). Amsterdam: Elsevier.

Paruelo, J. M., Beltran, A., Jobbagy, E., Sala, O. E. and Golluscio, R. A. (1998a). The climate of Patagonia: general patterns and controls on biotic. *Ecología Austral, 8*, 85-101.

Paruelo, J. M., Jobbágy, E. G., and Sala, O. E. (1998b). Biozones of Patagonia (Argentina). *Ecología Austral, 8*, 145-153.

Pisek, A., Larcher, W., Vegis, A. and Napp-Zinn, K. (1973). Plants II. The Normal Temperature Range. In H. Precht, J. Christophersen, H. Hensel and W. Larcher (Eds.), *Temperature and life.* Berlin: Springerpp. pp. 102-144.

Pospíšilová, J. and Čatský, J. (1999). Development of Water Stress under Increased Atmospheric CO_2 concentration. *Biologia Plantarum, 42*, 1-24.

Ristic, Z. and Cass, D. D. (1991). Leaf Anatomy of Zea mays L. in Response to Water Shortage and High Temperature: A Comparison of Drought-Resistant and Drought-Sensitive Lines. *Botanical Gazette, 152*, 173-185.

Rosenberg, N. J., Blad, B., Verma, S. (1983). *Microclimate the biological environment* (2nd ed.). New York: Wiley. p. 209-239.

Rozanski, K. and Araguás-Araguás, L. (1995). Spatial and temporal variability of stable isotope composition of precipitation over the South American continent. *Bull. Inst. fr. études andines, 24*(3), 379-390.

Sachse, D., Radke, J. and Gleixner, G. (2006). delta D values of individual n-alkanes from terrestrial plants along a climatic gradient - Implications for the sedimentary biomarker record. *Organic Geochemistry, 37*(4), 469-483.

Sachse, D., Billault, I., Bowen, G. J., Chikaraishi, Y., Dawson, T. E., Feakins, S. J., et al. (2012). Molecular Paleohydrology: Interpreting the Hydrogen- Isotopic Composition of Lipid Biomarkers from Photosynthesizing Organisms. *Annual Review of Earth and Planetary Sciences, 40*, 221-249.

Schefuss, E., Schouten, S. and Schneider, R.R. (2005). Climatic controls on central African hydrology during the past 20,000 years. *Nature,* 437,1003–6.

Schimmelmann, A., Lewan, M. D., and Wintsch, R. P. (1999). D/H isotope ratios of kerogen, bitumen, oil, and water in hydrous pyrolysis of source rocks containing kerogen types I, II, IIS, and III. *Geochimica Et Cosmochimica Acta, 63*, 3751-3766.

Schulze, E. D., Mooney, H. A., Sala, O. E., Jobbagy, E., Buchmann, N., Bauer, G., et al. (1996). Rooting depth, water availability, and vegetation cover along an aridity gradient in Patagonia. *Oecologia, 108*, 503-511.

Schwarz, G. E. (1978). Estimating the dimension of a model. *Annals of Statistics 6*, 461–464.

Sessions, A.L., Burgoyne, T.W., Schimmelmann, A., Hayes, J.M. (1999). Fractionation of hydrogen isotopes in lipid biosynthesis. *Org. Geochem*, 30, 1193–200.

Shmida, A. (1985). Biogeography of the Desert Flora. In M. Evenari, I. Noy-Meir & D. W. Goodall (Eds.), *Ecosystems of the world. Vol. 12A. Hot deserts and arid shrublands* (pp. 23-78). Elsevier: Amsterdam.

Smith, B. N. and Brown, W. V. (1973). The Kranz Syndrome in the Gramineae as Indicated by Carbon Isotopic Ratios. *American Journal of Botany, 60*, 505-513.

Smith, F. A. and Freeman, K. H. (2006). Influence of physiology and climate on delta D of leaf wax *n*-alkanes from C_{-3} and C_{-4} grasses. *Geochimica Et Cosmochimica Acta, 70*, 1172-1187.

SMN (Servicio Meterorológico Nacional) República Argentina. URL http://geohistoricos.blogspot.de/2009_08_01_archive.html (retrieved: 30/11/2013) (MAT and MAP maps of Argentina)

Soreng, R. J. (2012). Subfamilia Pooideae. Tribu Poeae. In F. O. Zuloaga, Z. E. Rúgolo & A. M. Anton (Eds.), *Flora Argentina / flora vascular de la república Argentina ; Vol. 3. Tomo II Monocotyledoneae. Poaceae: Pooideae* (pp. 97-371). Cordoba: Graficamente Ediciones.

Soriano, A. and Sala, O. (1984). Ecological strategies in a Patagonian arid steppe. *Vegetation, 56*, 9-15.

Soriano, A., Volkheimer, W., Walter, H., Box, E. O., Marcolin, A. A., Vallerini, J. A., et al. (1983). Deserts and semi-deserts of Patagonia. In N. E. West (Ed.), *Ecosystems of the world. Vol. 5. Temperate Deserts and Semi-Deserts* (pp. 423-460). Amsterdam: Elsevier. Stewart, G. R., Turnbull, M. H., Schmidt, S. and Erskine, P. D. (1995). C-13 Natural-Abundance in Plant Communities Along a Rainfall Gradient: a Biological Integrator of Water Availability. *Australian Journal of Plant Physiology, 22*, 51-55.

Stewart, G. R., Turnbull, M. H., Schmidt, S. and Erskine, P. D. (1995). C-13 Natural-Abundance in Plant Communities Along a Rainfall Gradient: a Biological Integrator of Water Availability. *Australian Journal of Plant Physiology, 22*, 51-55.

Tierney, J.E., Russell, J.M., Huang, Y.S., Damste, J.S.S., Hopmans, E.C., Cohen, A.S. (2008). Northern hemisphere controls on tropical southeast African climate during the past 60,000 years. *Science,* 322, 252–55.

Walter, H. and Box, E. (1976). Global classification of natural terrestrial ecosystems. *Vegetation, 32*, 75-81.

Wang, X., Zhang, W. and Liu, X. (2013). Daily variations in transpiration rate and water potential of Robinia pseudoacacia. *Journal of Food, Agriculture & Environment, 11*, 999-1005.

Welander, N. T. and Ottosson, B. (2000). The influence of low light, drought and fertilization on transpiration and growth in young seedlings of *Quercus robur* L. *Forest Ecology and Management, 127*, 139-151.

West, N. E. (1983). Approach. In N. E. West (Ed.), *Ecosystems of the world. Vol. 5. Temperate deserts and semi-deserts.* Amsterdam: Elsevier. pp. 1-2.

Willmer, C. M. (1996). *Stomata* (2nd ed.), Chapman & Hal: London, pp. 1, 126-177.

Winkler, F. J., Schmidt, H.-L. (1980). Einsatzmöglichkeiten der ^{13}C Isotopen-Massenspektroskopie in der Lebensmitteluntersuchung. *Z Lebensm Unters Forsch* 171, 85-94

Worldclim (2013): http://www.worldclim.org (Retrieved: 13/05/2013)

Wullschleger, S. D., Gunderson, C. A., Hanson, P. J., Wilson, K. B. and Norby, R. J. (2002). Sensitivity of stomatal and canopy conductance to elevated CO2 concentration – interacting variables and perspectives of scale. *New Phytologist, 153*, 485-496.

8 Appendix

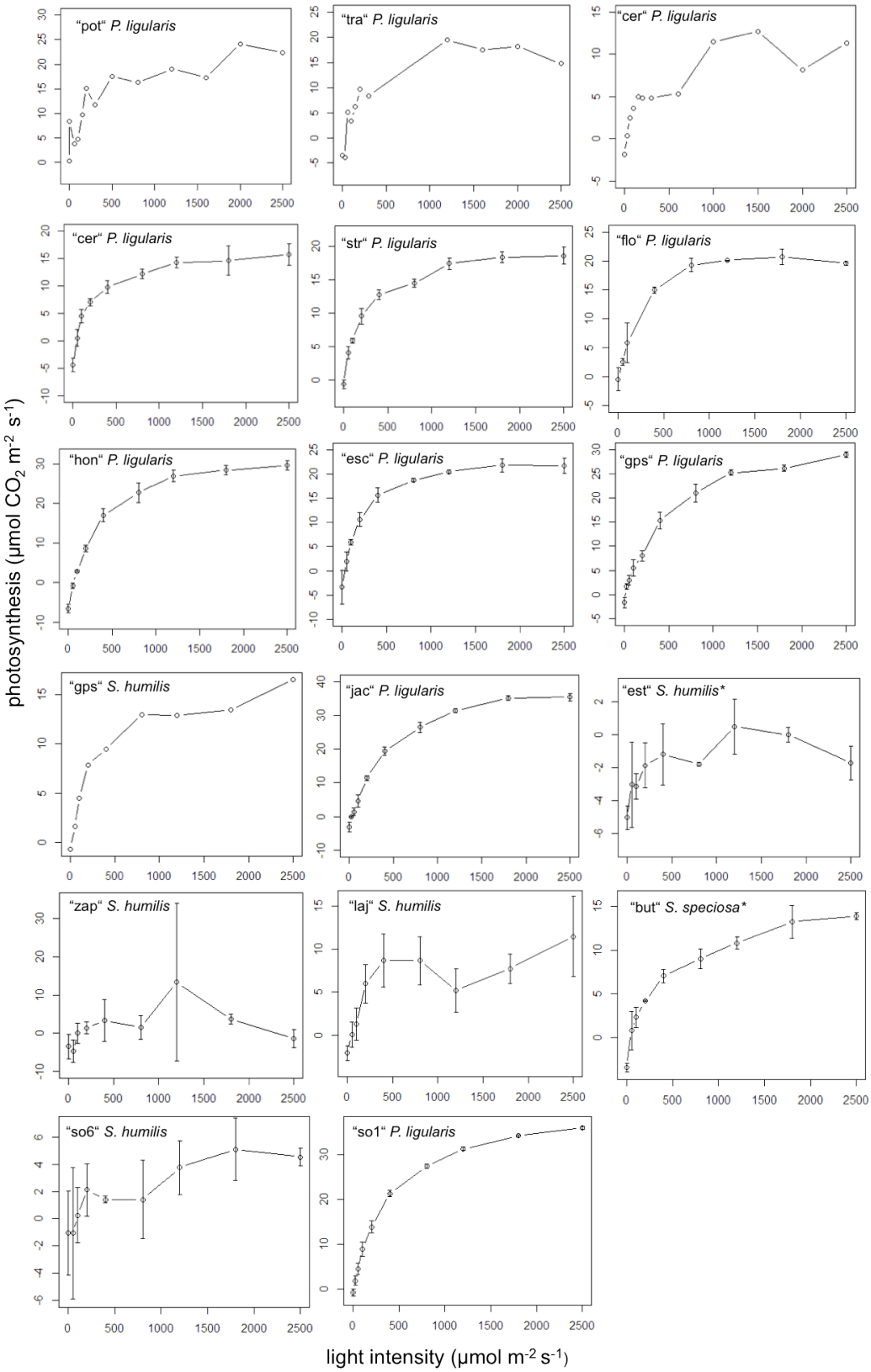

Figure A1. Light response curves with photosynthesis as response variable. Error bars are SD of the mean. *Curves were removed for statistical analyses.

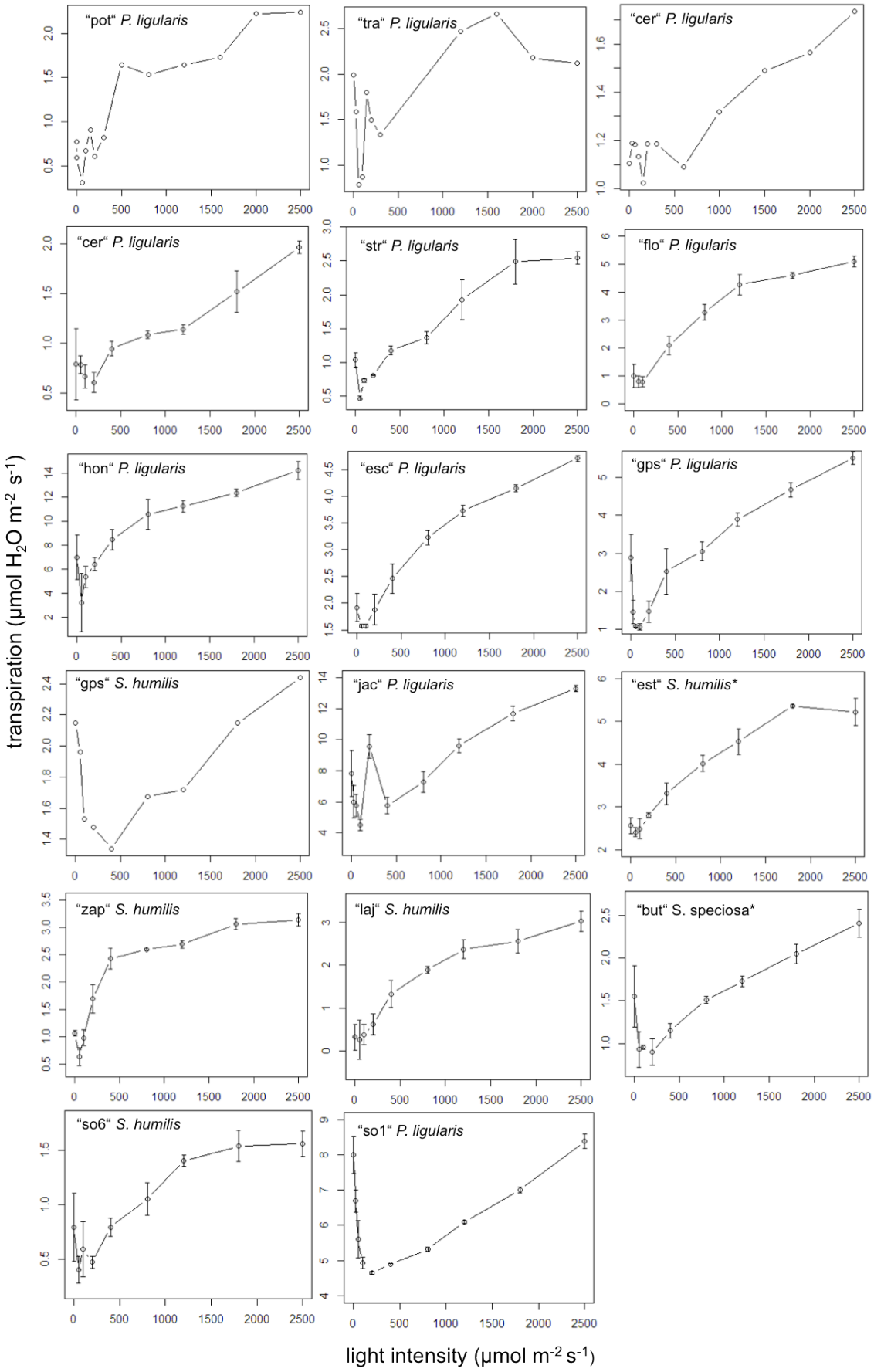

Figure A2. Light response curves with transpiration as response variable. Error bars are SD of the mean. *Curves were removed for statistical analyses.

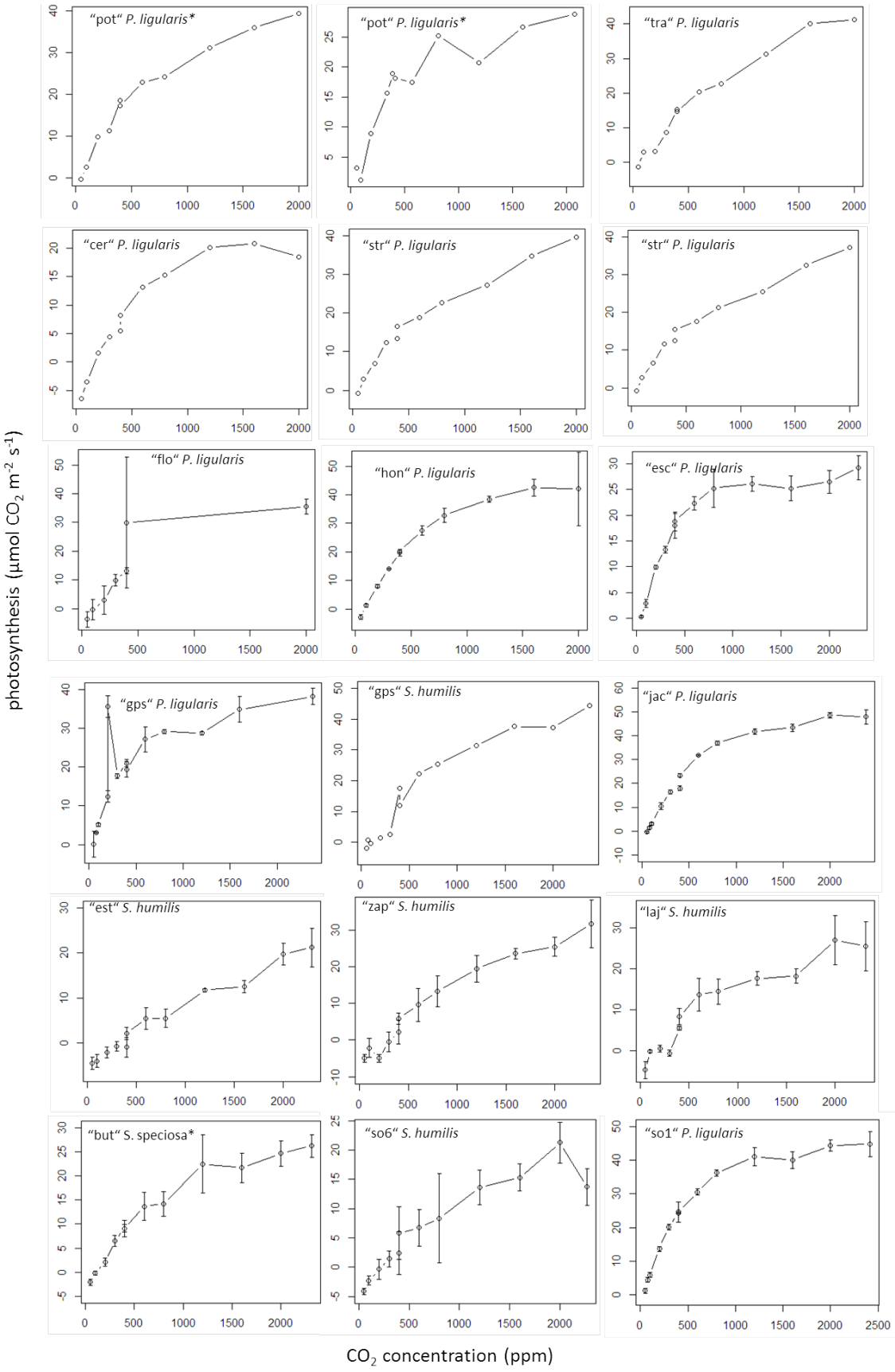

Figure A3. CO_2 response curves with photosynthesis as response variable. Error bars are SD of the mean. *Curves were removed for statistical analyses.

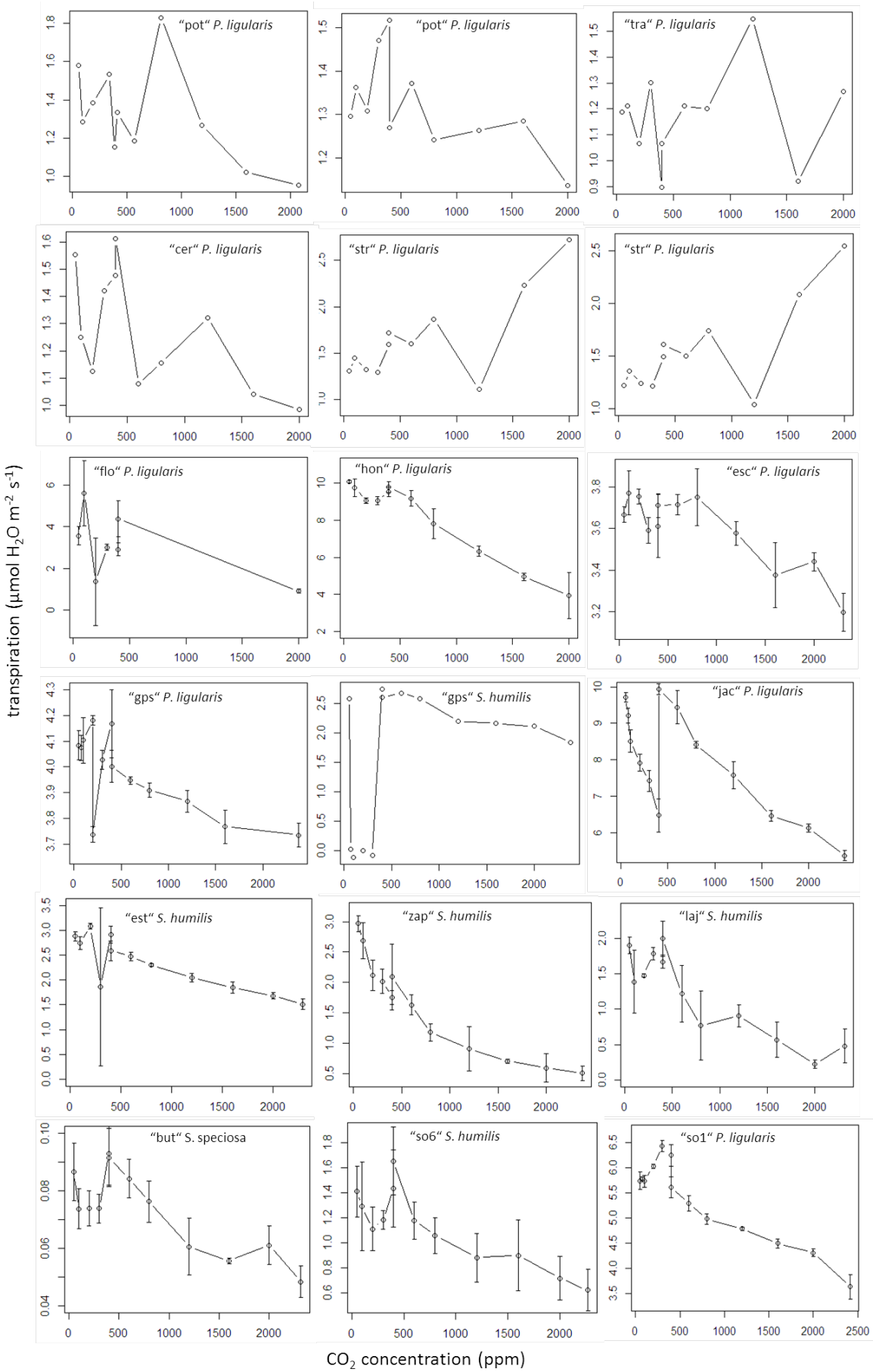

Figure A4. CO_2 response curves with transpiration as response variable. Error bars are SD of the mean.

Table A1. Random forest for variables explaining light compensation point. Bold variables were used for stepwise backward selection.

variable	Mean Decrease in Accuracy
air temperature	32.7
RH (reference air)	31.6
species	16.9
soil moisture	-6.3

Table A2. Random forest for variables explaining CO_2 compensation point. Bold variables were used for stepwise backward selection.

variable	Mean Decrease in Accuracy
species	57.6
air temperature	28.5
RH (reference air)	22.7
soil moisture	1.2

Table A3. Random forest for variables explaining total *n*-alkane concentration. Bold variables were used for stepwise backward selection.

variable	Mean Decrease in Accuracy
species	47.6
day mean RH	25.3
day temperature	18.9
annual radiation	11.6
soil moisture	-4.2
day light intensity	-7.8
CO2 concentration	-8.4
wind strength	-8.4

Table A4. Random forest for variables explaining $\varepsilon_{root/p}$. Bold variables were used for stepwise backward selection.

variable	Mean Decrease in Accuracy
annual irradiation	29.0
daily temperature	15.7
mean RH	14.3
daily light intensity	9.0
CO_2	7.6
species	6.0
wind	-3.1
soil moisture	-5.1

Table A5. Random forest for variables explaining $\varepsilon_{leaf/root}$. Bold variables were used for stepwise backward selection.

variable	Mean Decrease in Accuracy
day light intensity	41.1
annual light intensity	24.3
day temperature	14.6
day mean RH	12.8
measured photosynthesis	11.2
time	-1.5
CO_2 concentration	-2.3
soil moisture	-2.5
measured stomatal conductance	-4.9
longitude	-5.5
measured transpiration	-5.8
wind speed	-7.0
altitude	-9.1

Table A6. Random forest for variables explaining ε_{bio}. Bold variables were used for stepwise backward selection.

variable	Mean Decrease in Accuracy
daily temperature	4,6
annual irradiation	-5,8
daily RH	-8,4
species	-12,1
CO_2 concentration	-18,2
daily light intensity	-18,8
soil moisture	-32,0

Table A7. Random forest for variables explaining ε_{app}. Bold variables were used for stepwise backward selection.

variable	Mean Decrease in Accuracy
annual irraditation	57.8
daily temperature	26.1
daily light intensity	11.6
daily RH	1.6
CO_2 concentation	-10.1
soil moisture	-20.5

Declaration

Herewith I affirm that I have written this thesis on my own. I did not enlist unlawful assistance of someone else. Cited sources of literature are perceptibly marked and listed at the end of this thesis. The work was not submitted previously in same or similar form to another examination committee and was not yet published.

Jena, 3rd February 2014